Calcium signaling in glomerular cells in health and disease

INAUGURAL-DISSERTATION

zur Erlangung des Doktorgrades
der Mathematisch-Naturwissenschaftlichen Fakultät
der Universität zu Köln

vorgelegt von

Julia Binz-Lotter

Calcium signaling in glomerular cells in health and disease

INAUGURAL-DISSERTATION

zur Erlangung des Doktorgrades
der Mathematisch-Naturwissenschaftlichen Fakultät
der Universität zu Köln

vorgelegt von

Julia Binz-Lotter

aus Köln

Köln 2019

Berichterstatter	Prof. Dr. Thomas Benzing
(Gutachter)	Prof. Dr. Peter Kloppenburg

Tag der mündlichen Prüfung: 23. September 2019

Table of Contents

List of Tables

List of Figures

List of abbreviations

Abbreviation	
% v/v	Volume concentration
% w/v	Mass concentration
μl	Microliter
μm	Micrometer
μM	Micromolar
°C	Degree celsius
ADR	Adriamycin
AngII	Angiotensin II
AT1R	Angiotensin II type 1 receptor
AT2R	Angiotensin II type receptor
BSA	Bovine serum albumin
bp	Base pair
Ca^{2+}	positive charged calcium ion
$CaCl_2$	Calcium chloride
cm	Centimeter
CNO	Clozapine-N-oxide
ddH_2O	Double distilled water
DMSO	Dimethyl sulfoxide
DNA	Deoxyribonucleic acid
dNTP	Deoxyribonucleotide triphosphate
DREADD	Designer receptor exclusively activated by designer drugs
DTT	Dithiothreitol
EDTA	Ethylenediaminetetraacetic acid
fp	Forward primer
GFP	Green fluorescent protein
h	Hour
H_2O	Water
HBSS	Hank's balanced salt solution
HE	Haemotoxylin and eosin
hM_3D	human muscarinic type 3 receptor
Hz	Hertz
KCl	Potassium chloride
kDa	Kilodalton
l	Liter
mA	Milliampere
mg	Milligram

Continued on next page

$MgCl_2$	Magnesium chloride
$MgSO_4$	Magnesium sulphate
min	Minutes
ml	Milliliter
mM	Millimolar
MP	Multiphoton
MPM	Multiphoton microscopy
NaCl	Sodium chloride
ng	Nanogramm
nm	Nanometer
nM	Nanomolar
OPO	Optical parametric oscillator
pM	Picomolar
p Value	Probability
PAS	Periodic acidic schiff
PBS	Phosphate-buffered saline
PCR	Polymerase chain reaction
PFA	Paraformaldehyde
ROSA26	(Gt(ROSA)26Sor)
rp	Reverse primer
s	Seconds
SP	Spectral photometric
TAE	TRIS-Acetat-EDTA-Buffer
TCS	True Confocal Scanner
TEMED	N,N,N',N'-tetramethylethylenediamine
tg	Transgenic
U	Units
USP	United states pharmacopeia
V	Volt
wt	Wild type

1 Abstract

Intracellular calcium levels are tightly regulated and control many biological functions through direct interactions with proteins or indirectly by modifying calcium-binding proteins. In the glomerulus, the filtration unit of the kidney, podocytes form a crucial part of the filtration barrier and podocyte injury is strongly associated with loss of kidney function. Patient mutations in the podocyte calcium channel TRPC6 demonstrated that both loss-of-function or gain-of-function mutations can induce kidney disease indicating that a regulated calcium homeostasis is needed to prevent podocyte damage.

The at hand thesis aimed to understand calcium dynamics in healthy and injured podocytes *in vivo*. Previous studies in mice have demonstrated that activity of the Angiotensin II (AngII) receptors, predominately AngII type 1 receptor (AT1R), is associated with podocyte injury and increased intracellular calcium levels. Using intravital microscopy of the kidney we can show that podocytes maintain a low intracellular calcium level at baseline while stimulation with AngII results in calcium transients in a minor fraction of podocytes and glomeruli. Next, we caused podocyte injury by either inducing Adriamycin nephropathy or deleting the slit diaphragm component podocin resulting in proteinuria and FSGS-lesions in the kidney. Strikingly, AngII treatment of mice with preexisting glomerular disease resulted in increased responsiveness to AngII with a significant higher percentage of glomeruli and podocytes showing a calcium transient.

Furthermore, we wanted to investigate the role of ATP-mediated calcium signals in different cell types of the nephron. Therefore, we generated mouse lines expressing the calcium indicator GCaMP3 specifically in endothelial cells, proximal tubular cells or podocytes. We can demonstrate that endothelial cells and proximal tubular cells display a strong calcium response to ATP *in vivo*, while this is absent in

podocytes at the same dose. This is in line with our *ex vivo* data obtained from isolated glomeruli. Here, podocytes show a response to ATP only at higher doses.

In summary, our *in vivo* data challenge the current concepts of receptor mediated calcium signaling in healthy podocytes while revealing a more pronounced role of calcium signaling in podocyte's pathophysiology.

2 Zusammenfassung

Die intrazelluläre Kalziumkonzentration wird streng reguliert und kontrolliert viele biologische Funktionen durch direkte Wechselwirkungen mit Proteinen oder indirekt durch die Modifikation von Kalzium-bindenden Proteinen. Im Glomerulus, der Filtrationseinheit der Niere, bilden Podozyten einen entscheidenden Teil der Filtrationsbarriere und Podozytenverletzungen resultieren in einem Verlust der Nierenfunktion. Patientenmutationen im Podozytenkalziumkanal TRPC6 zeigen, dass sowohl eine "Gain-of-function" als auch eine "Loss-of-function" Mutation des Kalziumkanals eine Nierenerkrankung auslösen kann. Dies weist darauf hin, dass eine regulierte Kalziumhomöostase erforderlich ist, um eine Schädigung der Podozyten zu verhindern.

Der Schwerpunkt dieser Arbeit lag auf der Untersuchung der Kalziumdynamik in gesunden und kranken Podozyten *in vivo*. Frühere Studien an Mäusen haben gezeigt, dass die Aktivität der Angiotensin-II (AngII) Rezeptoren, vorwiegend des AngII-Typ-1-Rezeptors (AT1R), mit einer Podozytenverletzung und einer Erhöhung des intrazellulären Kalziumspiegels verbunden ist. Mithilfe der intravitalen Nierenmikroskopie können wir zeigen, dass Podozyten basal einen niedrigen intrazellulären Kalziumspiegel beibehalten, während die Stimulation mit AngII nur zu Kalziumtransienten in einem geringen Teil von Podozyten und Glomeruli führt. Als nächstes verursachten wir eine Schädigung der Podozyten, indem wir entweder eine Adriamycin-Nephropathie induzierten oder die Schlitzmembrankomponente Podocin deletierten. Bemerkenswerterweise führte die Stimulation mit AngII bei Mäusen mit vorbestehender glomerulärer Erkrankung zu einer erhöhten Kalziumantwort, wobei ein signifikant höherer Prozentsatz an Glomeruli und Podozyten einen Kalziumtransienten aufwies.

Zudem wollten wir die Rolle von ATP-vermittelten Kalziumsignalen in verschiedenen Zelltypen des Nephrons untersuchen. Hierzu haben wir verschiedene

Mauslinien generiert, welche den Kalziumindikator GCaMP3 spezifisch in Endothelzellen, proximalen Tubuluszellen oder Podozyten exprimieren. Wir können *in vivo* zeigen, dass Endothelzellen und proximale tubuläre Zellen eine starke Kalziumantwort auf ATP zeigen, während diese in Podozyten bei gleicher Dosis ausbleibt. Dies steht im Einklang mit unseren *ex vivo* Daten, welche mit isolierten Glomeruli generiert wurden. Hier zeigen Podozyten nur bei hohen Dosen eine Reaktion auf ATP.

Zusammenfassend stellen unsere *in vivo* Daten die gegenwärtigen Konzepte der Rezeptor-vermittelten Kalziumsignalübertragung in gesunden Podozyten in Frage, während sie eine bedeutendere Rolle der Kalziumsignalübertragung in der Pathophysiologie von Podozyten aufdecken.

3 Introduction

3.1 Podocyte biology & pathobiology

Kidneys generate approximately 180 liter of ultrafiltrate per day consisting of electrolytes, low molecular weight waste and water. A complex reabsorbtion and concentration mechanism of the tubular system results in a final urine volume of about 1 liter per day [1]. The primary filtrate is generated in the glomerulus, the filtration unit of the kidney. Blood enters the glomerulus via the afferent arteriole and exits it via the efferent arteriole. In between, the blood is passing through the capillary loops where filtration occurs. The primary filtrate is collected in the Bowman's space, from where it enters the proximal tubule. Filtration is achieved by a highly developed filtration barrier, whose size and charge selectively retains proteins and molecules of more than $\sim$ 70 kDa in the blood (Figure 1).

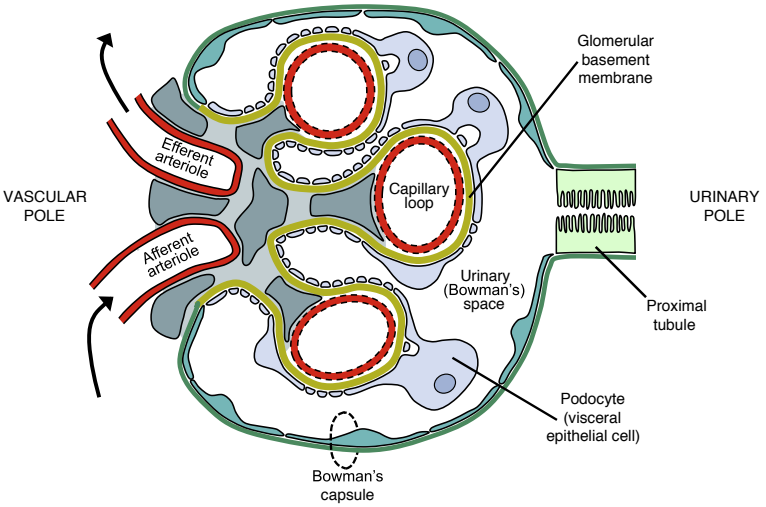

Figure 1: Schematic representation of the glomerular filtration unit. The blood enters the glomerulus via the afferent arteriole at the vascular pole and passes through the capillary loops, where filtration occurs and exits via the efferent arteriole. The generated primary urine is excreted into the Bowman's space where it passed on to the proximal tubule. (adapted from Leeuwis et al. 2010, [2])

The filtration barrier is formed by a complex spatial arrangement of three layers: a fenestrated endothelial cell layer, the glomerular basement membrane and the podocyte slit diaphragm [3, 4] (Figure 2). Thereby podocytes play a critical role in maintaining the function of the filtration barrier. Podocytes are terminally differentiated epithelial cells, which sit on the glomerular basement membrane (GBM) and wrap around the capillaries. Podocytes originate from mesenchymal cells during kidney development. In the course of nephrogenesis podocytes lose their mitotic activity and start to express distinctive proteins responsible for the formation of specialized cell-cell contacts, termed slit diaphragm, and adapt a highly sophisticated cell shape [3, 5, 6]. Each podocyte can be structurally subdivided into a large cell body, primary processes and small finger like extensions called foot processes. Foot processes of neighboring podocytes are interdigitating and are connected by the slit diaphragm establishing a filtration slit with of $\sim$ 40 nm [7].

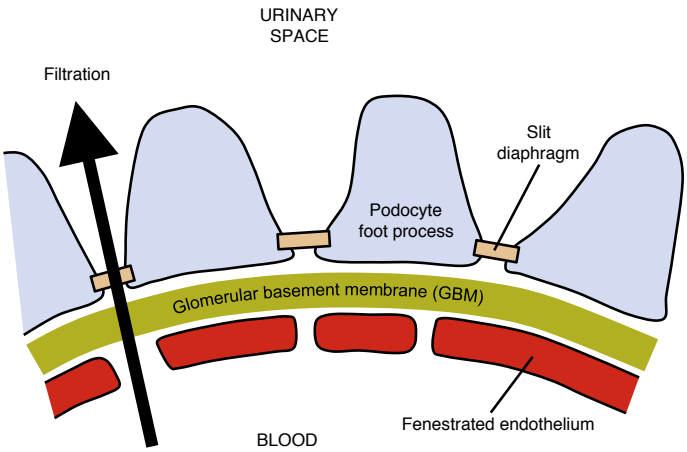

Figure 2: Detailed schematic view of the filtration barrier. Composition of the filtration barrier: fenestrated endothelial cells, the glomerular basement membrane and the slit diaphragm in between podocyte foot processes. (adapted from Leeuwis et al. 2010, [2])

The consequence of incorrect slit diaphragm formation for kidney diseases was identified in children with mutations of nephrin, encoded by the *NPHS1* gene. Mu-

tation of *NPHS1* results in congenital nephrotic syndrome of the Finnish type [8, 9]. Since then a number of slit diaphragm protein complex including Zonula Occludens-1 (ZO-1), podocin, Neph1 and 2, CD2AP and many more have been identified as crucial slit diaphragm components [10, 11, 12]. Nephrin is a transmembrane protein with an extracellular domain and a short intracellular tail. The extracellular domain interacts with Nephrin and Neph1 expressed on the cell membrane of neighboring podocytes thereby spanning the filtration slit. Its intracellular domain allows interaction with signaling proteins and can be phosphorylated at conserved tyrosine and threonine residues [13, 14]. Thus important cellular functions and programs including cell polarity, actin organization, cell survival and membrane trafficking are tightly connected to the slit diaphragm and the maintenance of the filtration barrier [13]. Since podocytes lose their ability to divide during nephrogenesis, any podocytes lost due to disease or acute injury cannot be replaced. Podocyte injury goes in hand with loss of their complex foot process structure resulting in the so-called "foot process effacement". Thereby, foot processes apparently fuse and flatten, completely abrogating the formation of a functional kidney filter. Finally, podocytes can detach from the basement membrane, resulting in hypertrophy of the remaining podocytes and ultimately in scarring of the glomeruli. Disruption of the slit diaphragm results in loss of proteins into the urine, termed proteinuria [5]. Kidney diseases presenting with a large proteinuria (>4 g/day) lead to the clinical picture of nephrotic syndrome, consisting of edema, proteinuria and hyperlipidemia. Causes of podocyte injury can be classified into three main categories: congenital, hereditary and acquired. Podocyte disease with congenital presentation are for example the Finnish nephropathy [8, 9]. Lack of proteins essential for podocyte architecture lead to an immediate phenotype even before birth. Hereditary causes are commonly found as mutations in genes encoding for podocyte specific proteins such as podocin, α-actinin-4 and TRPC6 [15, 16, 17, 18] with clinical disease

onset during childhood or adolescence. Podocyte injury produced by acquired factors can be separated into immune-mediated and non-immune causes. The first comprises diseases involving dysregulation of the immune system, such as membranous nephropathy and minimal change disease. Non-immune causes of podocyte injury represent the most common cause of nephrotic syndrome often caused by chronic hypertension, diabetes or infections [19, 20]. In most cases podocyte injury ends in a common pathological glomerular phenotype called focal segmental glomerulosclerosis (FSGS). Patients presenting with FSGS show sclerotic glomerular lesions in the kidney but not all glomeruli and not all regions of a glomerulus are affected. Therefore, the remaining functional glomeruli encounter increased filtration resulting in increased cell stress and ultimately loss of nephron function [21].

3.2 Calcium signaling

Calcium is a mediator of many different molecular processes in a cell. In general, intracellular calcium levels are maintained at a low level of ∼100 nM while extracellular calcium levels can be up to 20,000 fold higher [22]. Calcium can either exert its effects by directly binding to a target protein or indirectly by binding to calcium-sensing proteins, where it induces conformational changes which enable the sensing protein to bind its target proteins to induce signaling. Thus, calcium is able to influence many different cellular functions like cell motility, regulated cell death, proliferation and metabolism [23]. The consequences of calcium on cytoskeletal organization have been elegantly presented by the group of Roland Wedlich-Söldner. They defined a mechanism of calcium-mediated actin reset (CaAR), in which stimulation of Ca^{2+} induced actin rearrangement in many different mammalian cell types, including podocytes [24]. Furthermore, dysregulation of intracellular calcium levels have profound effects on cell viability. Many signaling pathways activate calcium

release from intracellular stores like the endoplasmatic reticulum (ER) and/or direct influx from the extracellular space to transmit their information. Therefore, tight regulation of cytosolic calcium levels is required for cell homeostasis.

3.2.1 Calcium signaling in podocytes

In 2005 Winn and colleagues reported that a gain-of-function mutation of the transient potential receptor cation channel 6 (Trpc6) causes focal segmental glomerulosclerosis (FSGS) in patients [16, 17], a phenotype which could by recapitulated in mice by overexpressing mutant Trpc6 channels [25]. On the other hand, loss-of-function mutations found in humans have been associated with FSGS as well [26], which further emphasizes the importance of maintenance of a calcium homeostasis. The Trpc channel family comprises a large number of ion channels in different mammalian species. Trpc1 and Trpc3-6 have been shown to be expressed in podocytes [27]. They form ion channels out of four subunits with each subunit containing six transmembrane domains with the C- and N-terminus facing the cytoplasm. Trpc6 harbors four ankyrin repeats on his N-terminus responsible for protein-protein interactions [28]. The $Trpc6^{P112Q}$ mutation resulting in overactivation is located on the first ankyrin repeat [16, 29, 30]. Trpc6 is an unselective cation channel, permeable for monovalent cations and calcium ions (Ca^{2+}). Studies demonstrated that it localizes in podocytes within the cell body and at the foot processes to the slit diaphragm. There it interacts directly with CD2AP, nephrin and podocin [17]. Opening of Trpc6 channels can be induced by different factors including diacylglycerol (DAG), Ca^{2+} itself and agonists of phospholipase-C-(PLC)-linked receptors [31, 30, 32]. DAG is a product of PLC activation which results in cleavage of the membrane lipid phosphatidylinositol-4,5-biphosphate (PIP_2) to diacylglycerol (DAG) and inositol-1,4,5-triphosphate (IP_3). DAG remains at the plasma membrane due to its hydrophobic tail and can activate Trpc6 while IP_3 can activate

calcium channels on the ER resulting in release of Ca^{2+} into the cytoplasm. PLC itself is activated by ligands binding to G-protein coupled receptors (GPCRs) on the plasma membrane [32] (Figure 3).

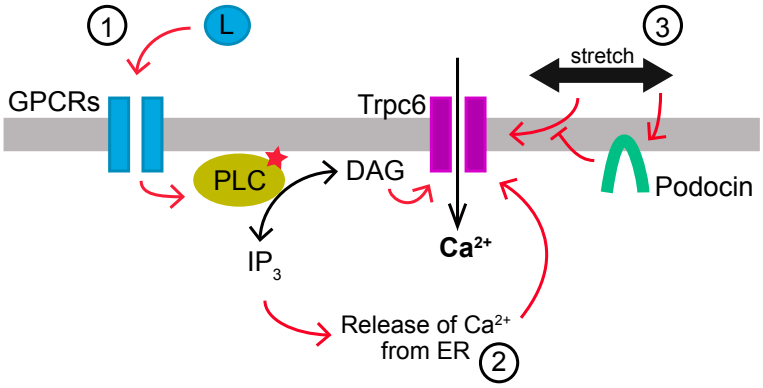

Figure 3: Simplified overview of Trpc6 activation in podocytes. Activation of Trpc6 can be mediated by different stimuli. Ligands can bind to G-protein coupled receptors (GPCRs) on the plasma membrane triggering activation of phospholipase-C (PLC) and subsequently production of Diacylglyerol (DAG) which directly activates Trpc6 (1). Simultaneous generation of inositol-1,4,5-triphosphate (IP_3) can induce Ca^{2+} efflux from the endoplasmatic reticulum (ER) inducing activation of Trpc6 (2). Finally, mechanical stretch on the plasma membrane which can be modulated by podocin can activate Trpc6 (3).

Additional, studies indicate that Trpc6 is part of a mechanosensitive complex including nephrin, podocin, CD2AP and α-actinin-4 [27]. In *C. elegans* the podocin homologue Mec2 interacts with Trpc6 in a cholesterol dependent manner and thereby changes Ca^{2+} conductivity (Figure 3) [33]. And *in vitro* studies have established that mutant $Trpc6^{N143S}$ shows loss of Ca^{2+} channel activity upon osmotic stretch [34]. Taken together there is evidence that Trpc6 activity is regulated by mechanical strain on podocytes, but the published data is insufficient to draw a conclusion whether this is a direct or indirect effect [35, 36]. Despite general effects of calcium on various signaling pathways it has been shown that activation of Trpc6 directly effects the elaborate actin cytoskeleton of podocytes and therefore plays a role in disease [37]. Tian et al. (2010) demonstrated that activation of Trpc6 activated

Rac1, a small GTPase, resulting in loss of stress fibers while activation of the Trpc5 activated RhoA and thereby preserving cytoskeletal organization [38]. The effects of Rac1 on podocyte morphology have been also presented *in vivo* [39]. Physiological factors such as Angiotensin II (AngII) and adenosine-triphosphate (ATP) and have been linked to Trpc6 activation.

3.3 The renin-angiotensin-aldosterone system in the kidney

The renin-angiotensin-aldosterone system, short RAAS, is the main signaling pathway regulating systemic blood pressure and salt balance. Renin is an aspartyl protease which is primarly synthesized and secreted in the kidney from the juxtaglomerular (JG) apparatus, situated at the branching point of the afferent arteriole leading to the glomerular vascular bed [40]. Renin levels are regulated either by signaling of baroreceptors located on endothelial cells and on JG cells or by sodium chloride levels in the filtrate of distal tubules sensed by macula densa cells. Drops in renal perfusion pressure as well as reduced sodium chloride levels increase expression and secretion of renin. The hormone aldosterone is produced by the adrenal gland plays and important role in electrolyte homeostasis [41]. The main active compound of RAAS is angiotensin II (AngII). AngII is synthesized in two steps: first renin cleaves a 10 amino acid long peptide from the N-terminus of angiontensinogen (Agt) resulting in AngI. The main source of Agt are liver cells. In a second step AngII is generated by removal of 2 amino acids from the C-terminus of AngI by the angiotensin-converting-enzyme (ACE). ACE is a dicarboxydasepeptidase, which is expressed as a membrane bound form on the surface of endothelial cells or is present as a soluble form in the plasma. The hormone AngII binds either angiotensin II type 1 (AT_1) or type 2 (AT_2) membrane receptors. In humans a single gene on chromosome 3 encodes for AT_1 (*Atrg1*) while mice and rats harbor two genes (*Atrg1a* and *Atrg1b*) on two chromosomes resulting in two subtypes

of the AT_1 receptor: AT_{1A} and AT_{1B} [42, 43]. Studies using overexpression and knock-out mouse models indicate that AT_{1A} has a predominant role in the kidney mediating vasoconstriction and regulation of blood pressure [44, 45]. Still, both receptor subtypes have been found to be expressed in podocytes [46].

3.3.1 AngII signaling as a mediator of podocyte injury

Blockade of AngII signaling in chronic kidney disease using ACE-inhibitors or AT1 receptor blockers (ARBs) such as Losartan is a mainstay of treatment in patients suffering from diabetic and non-diabetic nephropathy. However, the mechanisms of how RAAS inhibition prevents kidney disease progression are not fully understood.

In the kidney AngII regulates glomerular perfusion by increasing resistance at the exit of the glomerular vascular bed. Thus local AngII physiologically counteracts drops in renal perfusion pressure to keep the glomerular filtration pressure constant. Upon RAAS overactivation the AngII levels are increased, which results in swelling of the capillary loops due to increased filtration pressure as AngII induces vasoconstriction of the efferent arteriole [1]. Furthermore, it has been validated that overexpression of the AT1R in podocytes of rats is sufficient to induce glomerulusclerosis [47]. Thus the effects of AngII can be separated into hemodynamic and non-hemodynamic effects.

Prolonged activation of the AngII pathway occurs during hypertension or diabetic nephropathy resulting in glomerular injury [48, 49]. Glomerular hypertension has been modeled in rats and mice by either feeding desoxycorticosterone acetate (DOCA) or by reduction of kidney mass by 5/6 nephrectomy [50, 51, 52]. In both models administration of ARBs or ACE inhibitors resulted in ameliorating effects which are not solemnly accounted for by decreasing systemic blood pressure [53, 54].

Numerous *in vitro* and *in vivo* studies suggested that AngII can directly stimulate podocytes. Using cell culture and isolated glomeruli it has been presented that

administration of AngII results in a robust increase of calcium levels of podocytes [55, 56, 57, 27, 58]. AngII receptors belong to the group of G-protein coupled receptors and their activation has been associated with elevated calcium levels in podocytes via Trpc6 [16, 59]. Furthermore, experiments identified that AT1 activation relates to levels of nephrin expression and thereby influences slit diaphragm stability while administration of ACE or AT1 blockers restores nephrin protein levels [60, 61, 62]. Furthermore, AngII signaling has been shown to induce accumulation of reactive oxygen species (ROS) in mice [63, 64]. In the past years AngII-mediated calcium signaling has been in the focus of podocyte research. Still there is an on-going debate on whether the effects on calcium signaling are due to direct binding of AngII to its receptor expressed on the podocyte cell membrane or whether the induced mechanical stress activates calcium signaling in podocytes.

3.4 Purinergic signaling and podocytes

Podocytes have been demonstrated to express adenosine-triphosphate (ATP) receptors and upregulation of these receptors occurs during disease [65, 66]. Purinergic signaling plays a role in mediating intracellular and extracellular signals. Release of purinergic nucleotides such as ATP into the extracellular space is often associated with a pathological cell state. Two families of receptors are activated by purinergic nucleotides: P2X and P2Y. P2X receptors are cation channels activated by ATP, while P2Y receptors belong to the group of G-protein coupled receptors (GPCRs) and can be activated by different nucleotides such as adenosine-diphosphate (ADP), uridine-diphosphate (UDP), uridine-triphosphate (UTP) and ATP. In context of the kidney, activation of both receptors plays a role in regulating tubular function and vasoconstriction [67, 68, 69]. In general these nucleotides have a short half-life due to a fast degradation by ectonucleases present in almost all compartments of the nephron including the glomerulus [70]. There is evidence that $P2X_7$ and $P2Y_1$ play a role in kidney disease [65, 71, 72]. Data from hypertensive and diabetic nephropathy models in rats suggest an upregulation of $P2X_7$ in podocytes during disease [65] while whole-body deletion of $P2X_7$ ameliorates experimental glomerulonephritis [72]. Experiments using podocyte cell culture identified a role of P2Y receptors in mediating calcium signaling via Trpc6. Thereby it is proposed that ATP induces calcium transients in a fashion similar to AngII by binding to its receptor, since both receptor types belong to the family of GPCRs [66]. Using isolated glomeruli, the $P2Y_1$ receptor has been identified as the most abundantly expressed P2Y receptor on podocytes [73]. However, podocyte cell culture data suggest that $P2Y_2$ and $P2Y_6$ play a predominant role in ATP mediated calcium increases [74]. The controversy regarding receptor type and subtype might be based on the model system used and differences in experimental set up [74, 35]. Additionally, it has been shown that podocytes themselves are able to release ATP upon mechanical

stretch which can then again activate $P2X_4$ channels. Further, activation of $P2X_4$ induces actin reorganization and thus might contribute to podocyte injury [35]. Besides podocytes themselves, endothelial cells, erythrocytes, mast cells as well as sympathic and parasympathic nerve endings have been identified as sources of extracellular ATP [67]. ATP also plays a role in mediating calcium transients in the tubuloglomerular feedback (TGF) as studies revealed propagation of calcium signal from the juxtaglomerular cells to endothelial cells and finally to podocytes [75]. Finally, there is evidence for a role of in mediating a calcium wave from one podocyte to the next upon acute podocyte laser-induced injury using intravital microscopy, which could be slowed down by inhibition of purinergic receptors and deletion of $P2Y_2$ [75]. Taken together, purinergic signaling influences podocyte biology, even though the detailed effects of the different receptors involved and the downstream signaling molecules remain elusive.

3.5 *In vivo* imaging of the kidney using multiphoton microscopy

3.5.1 Characteristics of multiphoton microscopy

Technical advances over the last years have made it possible to visualize cells in the living functioning kidney. The main breakthrough was the development and application of multiphoton lasers in intravital imaging. Multiphoton lasers generate a pulsed laser beam at wavelengths between 700 and 1100 nm in contrast to conventional laser lines used in confocal microscopy which employ non-pulsed lasers of defined wavelengths such as 405 nm, 448 nm or 488 nm. Applying a longer wavelength has several benefits in contrast to short wavelengths: the light is scattered less by the tissue and thereby allows for deeper tissue penetration and imaging. Additionally,it is less phototoxic compared to short wavelengths since it contains less energy. One photon of 800 nm wavelengths has half the energy compared to one photon of 400 nm wavelengths. To excite a fluorophore such as the green fluorescent protein (GFP) two photons of 800 nm wavelengths need to reach the fluorophore simultaneously so that the combined energy is able to excite the fluorophore. Consequently, the process of excitation itself is already confocal and therefore no pin hole is needed as in conventional microscopy. Thus, all of the emitted light can be gathered. The use of ultra-sensitive detectors allows for a close to maximum collection of the emitted light (see 5.2.7).

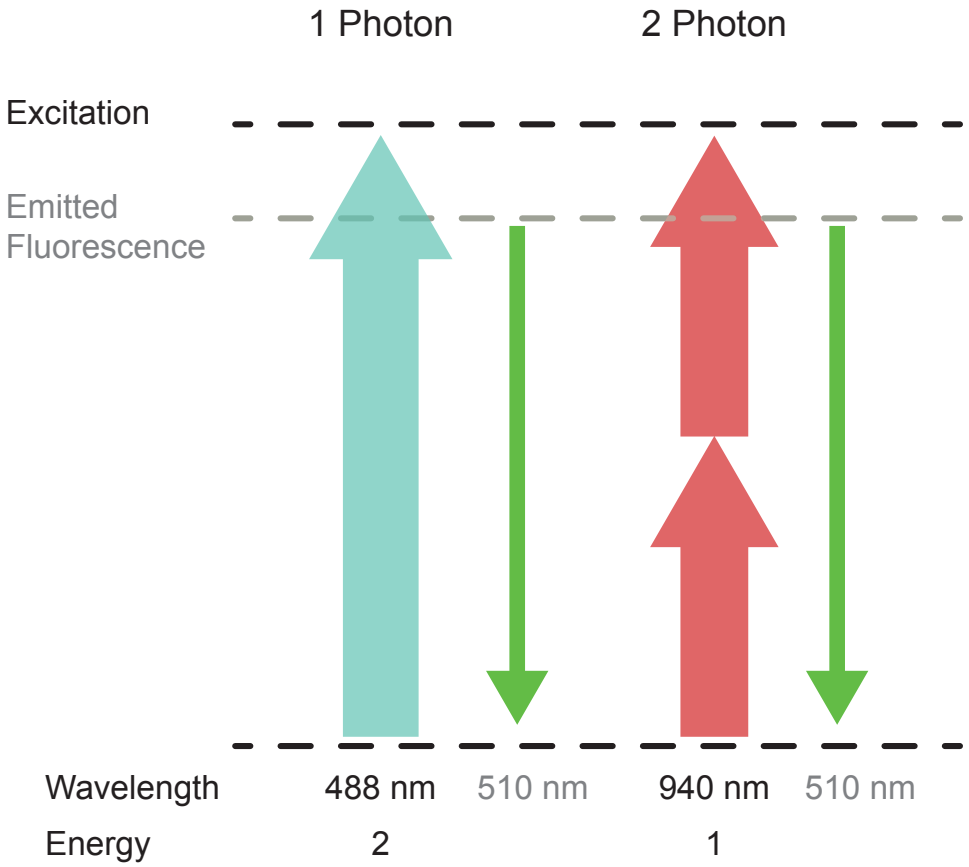

Figure 4: Physical aspects of 2-photon imaging. In 2-photon imaging a pulsed laser is tuned to a long wavelength of light (800-1000 nm). In contrast to conventional microscopy (400-600 nm) two photons are needed to excite a fluorophore as the long wavelength light contains less enegery. This makes the excitation process itself confocal.

3.5.2 *In vivo* imaging of the kidney

In contrast to the groups of Molitoris [76], Peti-Peterdi [75] and others we use an upright microscope instead of an inverted model. Therefore, we designed a novel kidney mounting (Fig. 5a) in collaboration with the on-campus company *Medres* which allows stabilization and adjustment of the kidney position in the x-, y- and z-axis. Furthermore, a mouth piece for anaesthesia gas and a heating system to maintain the body temperature are integrated into the animal mount. For imaging a cover slip is placed on top of the kidney with slight pressure to facilitate contact of the water immersion objective with the kidney (Fig 5b).

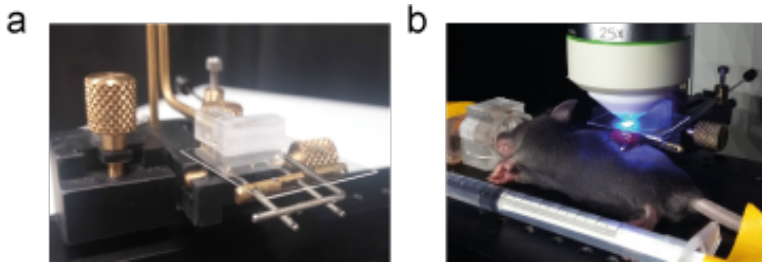

Figure 5: Equipment for *in vivo* imaging. **a**, custom-designed kidney holder. **b**, anesthetized mouse with an exteriorized kidney under the microscope.

In vivo imaging of the kidney allows for visualization of tubular structures of the superficial layers of the kidney cortex, consisting mainly of proximal tubular sections and some distal tubular sections which can be distinguished by the degree of auto-fluorescence and structure [77]. Visualization of peritubular structures and blood flow is achieved by injecting a fluorescently labeled 70 kDa dextran (Texas Red, tab. 2) (Fig. 6a) which is not filtered, retained in the circulation and thus labels the vasculature red. In order to visualize glomerular structures, we used mice in a C57Bl6 background of three to four weeks of age. Due to the young age and genetic background of the mice glomeruli were situated superficially enough which is a prerequisite for imaging [78]. In contrast to proximal tubular cells, the glomerular cells display no auto-fluorescence (Fig. 6b). Injection of 70 kDa dextran

Texas Red visualizes the capillary loops of the glomerulus (Fig. 6b) and blood flow of single glomeruli can be monitored during imaging.

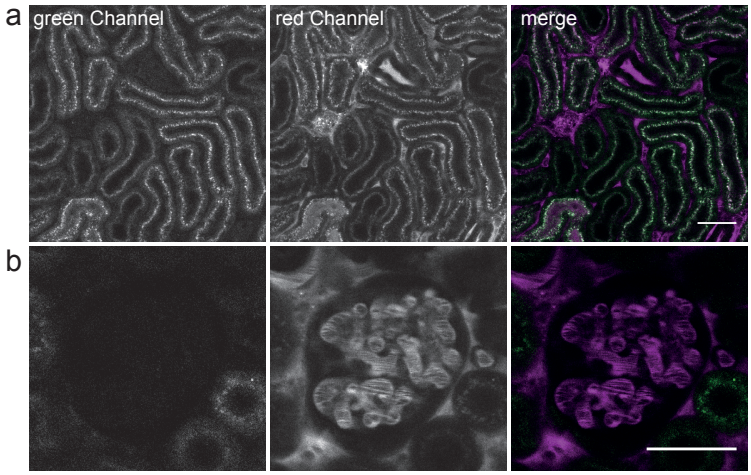

Figure 6: *In vivo* imaging of kidney structures. a, cortical tubular structures. Left: auto-fluorescence of the tubules in the green channel. middle: autofluorescence of the tubules and labeling of the peritubular bed with Texas Red shown in magenta. right: merge. **b**, glomerular structures. left: autofluorecence. middle: labeling of the glomerular capillary loops using Texas Red (magenta). right: merge. Scale bars: 40 μm.

Using *in vivo* imaging, functional aspects of the kidney such as filtration can be observed. Injection of low molecular fluorescent molecules allows monitoring of the filtration and calculation of the glomerular filtration rate (GFR) of a single glomerulus. A number of different compounds can be applied to label kidney structures and cells in the kidney. Injection of fluorescently labeled compounds such as Lectin-FITC allows *in vivo* detection of the capillary walls without the necessity for a transgenic mouse line. Compounds such as propidium iodide (PI) or AnnexinV can be used to label necrotic or apoptotic cells.

4 Objectives

4.1 Calcium signaling in podocytes upon Angiotensin II stimulation

Studies using podocyte cell culture and isolated glomeruli revealed that podocytes respond to AngII stimulation with calcium transients [56, 79] and overactivation of RAAS has been associated with kidney damage [41]. We therefore aimed to investigate the role of AngII-mediated calcium transients *in vivo* using intravital microscopy. To answer the fundamental question of how podocytes react upon stimulation with AngII in their specific environment *in vivo*, we employed mice expressing GCaMP3 exclusively in podocytes and stimulated them with AngII to induce calcium signaling.

To expand our experiments towards glomerular disease, we used two established disease models, Adriamycin nephropathy and deletion of podocin, to understand the pathophysiological role of AngII-mediated calcium signaling. Additionally, we used a *Trpc6* knock out mouse line to assess its role in AngII-mediated calcium transients. Finally, we conducted quantitative proteomic analyses to reveal the underlying mechanisms responsible for the observed increase in responsiveness to AngII.

4.2 Purineric calcium signaling in podocytes

Studies using cell culture and isolated glomeruli suggested that ATP triggers calcium transients in podocytes [27]. Furthermore, Burford et al. [75] demonstrated that ATP plays a role in mediating podocyte injury signals between podocytes. We aimed to investigate the contribution of ATP signaling in various cell populations in the kidney. We therefore used mice expressing GCaMP3 in endothelial cells, proximal tubular cells and podocytes to validate the role of ATP in calcium signaling in the nephron. We performed bolus injection of ATP at different doses and recorded

and analysed the induced calcium transients. Additionally we performed *ex vivo* experiments to unravel differences between *in vivo* and *ex vivo* models.

5 Material and methods

5.1 Material

Table 2: Chemicals and reagents

Chemicals/Reagents	Provider	Catalog Number
4 % Para Formaldehyde (PFA)	Sigma	P6148
37 % Formaldehyde	Th. Geyer	4979.1
Acetic Acid	Sigma	49199
Adriamycin (ADR)	Teva	45963-0733-55
Agarose	Sigma	A9539
Ammonium persulfate (APS)	Applichem	A1142,0250
Ammonium sulfate	Carl Roth	3746
Angiotensin II	Sigma	A9525
Bovine Serum Albumin (BSA)	Sigma	A9418
Bromophenol blue	Carl Roth	A512
Collagenase Type 1A	Sigma	C-9891
Coomassie Brilliant Blue	BioRad	161-0400
Dimethyl sulfoxide (DMSO)	AppliChem	A3672,0100
Dithiothreitol (DTT)	Thermo Fisher	R0862
dNTPs (100 mM)	Thermo Fisher	R0182
Dynabeads M-450 Tosylactivated	Thermo Scientific	14203
Ethanol 99 %	Applichem	A5007
Ethanol absolute	Carl Roth	9065
Ethidiumbromide solution (1 %)	Carl Roth	2218
Ethylenediaminetetraacetic acid disodium salt dihydrate (EDTA)	Sigma	60-00-4

Continued on next page

Fluo-4, AM	Thermo Fisher	F14217
FuraRed, AM	Thermo Fisher	F3021
GeneRuler 50bp DNA Ladder	Thermo Fisher	SM0372
Glycerol	Carl Roth	3783
Isoflurane	Piramal Healthcare	103058
Isopropanol	Carl Roth	5752.3
KCl	Sigma	P5405
Ketavet® (100 mg/ml)	Pfizer	
KH_2PO_4	Sigma	P5655
Loading Dye Solution (6X)	Thermo Fisher	R0611
Losartan	Sigma	124750-99-8
Mayer's hematoxylin	AppliChem	A0884
Methanol	Carl Roth	4627
$MgCl_2$	Merck	1.05833.0250
N,N,N',N'-tetramethylethylenediamine (TEMED)	Carl Roth 2367	
Normal Saline (0.9 %)	Fresenius Kabi	
Ortho-phosphoric acid (85 %)	Roth	6366.1
Paraformaldehyde (PFA)	Sigma	P6148
PD123319	Cayman Chemicals/ Bertin Pharma	136676-91-0
Polyacrylamide	Carl Roth	T802
RNase-free water Ultra Pure	Thermo Fisher	10977-035
Rompun® 2%	Bayer	102596
Sesame oil	Sigma	S3547

Continued on next page

Sodium dodecyl sulfate SDS (For transfer buffer)	AppliChem	A2263, 0500
Sodium acetate	Merck	6268
Sodium chloride (NaCl)	Sigma	S5886
Sodium deoxycholate	Sigma	D6750
Tamoxifen	Sigma	T5648
Temgesic (1 ml zu 0,3 mg)	RB Pharmaceuticals Limited	
Texas Red	Thermo Scientific	D-1830
Triton X-100	Applichem	A4975,1000
Trypsin	Sigma	T6567
Urea	Sigma	U1250
Water PCR Reagent	Sigma	R2523

Table 3: Solutions and buffers

Solution	Composition	
Anesthetic and analgetic Solution	6.8 ml	0.9 % NaCl
	1 ml	Ketavet (100 mg/ml)
	0.4 ml	Rompun 2 %
Base Solution (50X)	12.5 ml	NaOH (5N)
	1 ml	EDTA (0.5 M)
	36.5 ml	ddH_2O
Base Solution (1X)	0.5 ml	Base solution (50X)
	24.5 ml	ddH_2O

Continued on next page

		pH 12
Coomassie staining solution	756.14 mM	$H_8N_2O_4S$
	520.4 mM	ortho-phorphoric acid
	117.09 mM	Coomassie brilliant
	970ml	H_2O
	activate with	20 % (v/v) Ethanol
Fixing solution	250 ml	Isopropanol
	100 ml	Acetic acid (100%)
	1 L	H_2O
HBSS Buffer 1 (10X)	53 mM	KCl
	4.4 mM	KH_2PO4
	1.36 M	NaCl
	41.6 mM	NaHCO3
	5.6 mM	Na_2HPO_4
	55.5. mM	Glucose
HBSS Buffer 2 (10X)	13 mM	$CaCl_2$ x 2H2O
	4.9 mM	$MgCl_2$ x 6H2O
	4.3 mM	$MgSO_4$ x 6H2O
HBSS Buffer (1X)	100 ml	HBBS Buffer 1 (10 X)
	100 ml	HBSS Buffer 2 (10 X)
	800 ml	H_2O
Lysis Buffer	8 M	Urea
	50 mM	Ammonium bicarbonate
Neutralization Solution (50X)	100 mM	Tris-HCl
	in 50 ml	H_2O
Neutralization Solution (1X)	0.5 ml	stock sol. 50X

Continued on next page

	24.5 ml	H_20
		pH 5
Resolving Gel	750 mM	Tris
	10% (v/v)	PAA
	0.2% (w/v)	SDS
Running Buffer	25 mM	Tris
	192 mM	Glycine
	0.1% (w/v)	SDS
Stacking Gel	250 mM	Tris
	5% (v/v)	PAA
	0.2% (w/v)	SDS
		pH 6.8
TAE (1X)	40 mM	Tris
	20 mM	Acetic Acid
	1 mM	EDTA
		pH 8.5
Bath Solution	145 mM	NaCl
	2 mM	$CaCl_2$
	4.5 mM	KCl
	2 mM	$MgCl_2$
	10 mM	HEPES
	$\rightarrow$ pH 7.35	(adjusted with NaOH)
Calcium Recording Solution	125 mM	NaCl
	2 mM	$CaCl_2$
	4.5 mM	KCl
	2 mM	$MgCl_2$

Continued on next page

20 mM	HEPES
10 mM	Glucose
→ pH 7.4	(adjusted with NaOH)

Table 4: List of materials

Material	Company	Catalog Number
1.5 ml Epis	Sarstedt	72.706.201
2 ml Epis	Sarstedt	72.691
Biosphere Filter Tip 10 μl, sterile	Sarstedt	70.1116.210
Biosphere Filter Tip 1000 μl, sterile	Sarstedt	70.762.211
Biosphere Filter Tip 200 μl , sterile	Sarstedt	70.760.211
Combs (10 well, 1 mm) for acrylamide gels	Thermo Fisher	NC3010
Combs (12well, 1 mm) for acrylamide gels	Thermo Fisher	NC3012
Coverslip (18 x 18 mm)	LH22.1	Roth
Dyna Mag 2 (Magnet)	Thermo Scientific	12321D
Gel cassette (1 mm)	Thermo Fisher	NC2010
Hamilton Pipette 50 μl	Hamilton	705
Hypodermic needle (30 gauge)	BD	AN-3013R
Needle (27 gauge)	BD	ND635
Nitrile gloves S	Abena	224685
PCR Soft-lids ml 8 Tubes/Flat Caps	Sarstedt	65989002

Continued on next page

PCR Soft-tubes 0.2 ml 8 Tubes/Flat Caps, clear	Sarstedt	72985002
Polyethylene tubing (PE10)	Braintree Scientific	B-PE-10-100FT
Pipetboy	Integra Bio-sciences	1550
Pipettes	GILSON	P2, P10, P20, P200, P1000
Polypropylene conical tube (15 ml)	Greiner	227261
Polypropylene conical tube (50 ml)	Greiner	188271
Syringe (PlastipakTM 1 ml)	BD	7392/2007
Syringe (10 ml)	BD	309110
TipOne (0.1-10 μl XL), sterile	Starlab	S1110-3810
TipOne (101-1000 μl graduated), sterile	Starlab	S1111-6811
TipOne (1-200 μl beveled), sterile	Starlab	S1111-1816
TipOne Pipette Tip 10μl, refill	Starlab	S1111-3700
TipOne Pipette Tip 1000μl, refill	Starlab	S1111-6700
TipOne Pipette Tip 200μl, refill	Starlab	S1111-1700
Suture material(6-0 USP)	Resorba	88153
Surgical suture (5-0-USP)	Resorba	H2F

Table 5: Equipment

Equipment	Company
Bandpass filter 525/50	Leica Microsystems
Detectors (NDD HyD)	Leica Microsystems

Continued on next page

Heating system (water) (KS 92-1)	Medres, medical research company GmbH
Kidney Holder (custom made)	Medres, medical research company GmbH
Knock out box	Medres, medical research company GmbH
Multiphoton laser (Chameleon Vision II)	Coherent
Infusion Pump (AL-1000)	World Precision Instruments (WPI)
Isoflurane Vapor	Dräger
Hair Trimmer Contura (HS61)	Wella
Scale Imaging Room	OHAUS
Scale Hood	Kern PCB
Stereo Microscope M80	Leica Microsystems
TCS SP8 MP-OPO	Leica Microsystems

Table 6: Software

Software	Company
Excel	Microsoft
Imaris	Bitplane
ImageJ	National Institute of Health (NIH)
LasX	Leica Software
LaTeX	LaTeX Program Team
Prism	GraphPad
Illustrator	Adobe

Table 7: Genotyping primers

Primer name	Sequence (5' to 3')
Beta globin fp	TGCTCACACAGGATAGAGAGGGCAGG
Beta globin rp	GGCTGTCCAAGTGATTCAGGCCATCG
Cre fp	GCATAACCAGTGAAACAGCATTGCTG
Cre rp	GGACATGTTCAGGGATCGCCAGGCG
mTmG wt fp	CTCTGCTGCCTCCTGGCTTCT
mTmG wt rp	CGAGGCGGATCACAAGCAATA
mTmG tg rp	TCAATGGGCGGGGGTCGTT
Nphs2 lox2 fp	CCAGCATCCCATTAGATAGATGAGG
Nphs2 lox2 rp	GCATCCAAATGATCAGAGTTCCCAGG
TRPC6 E7 fp	CAGATCATCTCTGAAGGTCTTTATGC
TRPC6 E7 rp	TGTGAATGCTTCATTCTGTTTTGCGCC
TRPC6 IF fp	GGGTTTAATGTCTGTATCACTAAAGCCTCC
Pgk rp	ACGAGACTAGTGAGACGTGCTACTTCC

Table 8: Kits

Kit	Company	Catalog Number
Go Taq Flexi DNA Polymerase 5U/μl	Promega	M7808
REDTaq® ReadyMix^{TM} PCR Reaction Mix	Sigma	R2523

5.2 Methods

5.2.1 Genetic mouse models

In order to visualize cytosolic calcium levels in different cell types of the kidney, calcium reporter mouse lines (Tab. 9) were crossed to different cell specific Cre lines (Tab. 10). GCaMP3 is a calcium sensor protein in which the green fluorescent protein (GFP) is fused to the Ca^{2+}-binding protein calmodulin [80]. Podocyte specific expression was achieved by crossing GCaMP3$^{fl/fl}$ with Pod:cre mice [81], generating Pod:cre GCaMP3$^{fl/fl}$ mice. To delete the transient receptor potential cation channel 6 (Trpc6) these mice were crossed with a conventional Trpc6 knockout line [82] generating a Pod:cre GCaMP3$^{fl/fl}$ Trpc6$^{KO/KO}$ line. The generated mouse lines were maintained in a C57BL6 background. Further, Pod:cre GCaMP3$^{fl/fl}$ mice were bred with Podocin$^{fl/fl}$ mice carrying floxed podocin alleles [18] resulting in the generation of Pod:cre GCaMP3$^{fl/fl}$ Podocin$^{fl/wt}$ or Pod:cre GCaMP3$^{tfl/fl}$ Podocin$^{fl/fl}$ mice. These mice were kept in a mixed Sv129/C57BL6 background. To express GCaMP3 in endothelial cells, GCaMP3$^{fl/fl}$ mice were crossed with Tie2:cre animals [83] resulting in Tie2:cre GCaMP3$^{fl/fl}$ animals respectively. To achieve GCaMP3 expression in the entire nephron the Pax8:cre mouse line [84] was used, genereating Pax8:cre GCaMP3$^{fl/fl}$. Table 9 and 10 list all mouse lines used in this thesis.

Table 9: Mouse lines

Mouse line	use	Publication
GCaMP3$^{fl/fl}$	visualization of cytosolic Ca^{2+} levels	Zariwala et al. (2012)
Trpc6^{KO}	whole body deletion of the Trpc6 ion channel	Dietrich et al. (2005)

Continued on next page

Podocin$^{fl/fl}$	cell-type specific deletion of podocin	Mollet et al. (2009)

Table 10: Cre mouse lines

Mouse line	use	Publication
Pod:cre	Cre expressed in podocytes	Moeller et al. (2003)
Pax8:cre	Cre expressed in the entire nephron	Bouchard et al. (2002)
Tie2:cre	Cre expressed in endothelial cells	Kisanuki et al. (2001)

5.2.2 Sample preparation of DNA for genotyping

DNA samples of mice (ear tags) were provided by the in house animal facility. Samples were frozen at -20 °C until DNA preparation. For DNA extraction 75 μl of Base solution (1 X) (Tab. 3) were added to the ear tag and boiled at 95 °C for 25 minutes, followed by five minutes on ice. Then, 75 μl of neutralization solution (1 X) (Tab. 3) were added [85]. Samples were run on a 2 % agarose gel and stored at 4 °C until the genotyping was conclusively finished.

5.2.3 Polymerase chain reaction for genotyping

For genotyping the Go Taq Flexi DNA Polymerase 5U μl or the REDTaq® ReadyMix^{TM} PCR Reaction (Tab. 8) were used following the companies protocols.

Table 7 lists all primers used for genotyping. Table 11 lists the specific reaction composition and table 12 list the specific cycling conditions for each genotyping. For all PCRs 2.5 μl ($\sim$ 50 ng) of DNA were used (see 5.2.2).

Table 11: Reaction composition

Gene	Reaction Mix	
Cre	5 μl	ddH_2O
	1.25 pM	Beta globin fp
	1.25 pM	Beta globin rp
	1.25 pM	Cre fp
	1.25 pM	Cre rp
	12.5 μl	REDTaq® ReadyMix™
	~ 50 ng	DNA
GCaMP3	6.8 μl	ddH_2O
	25 pM	mTmG wt fp
	17 pM	mTmG wt rv
	33 pM	mTmG tg rv
	12.5 μl	REDTaq® ReadyMix™
	~ 50 ng	DNA
Podocin	13.1 μl	ddH_2O
	1.25 pM	Nphs2 lox2 fp
	1.25 pM	Nphs2 lox2 rp
	1.5 mM	$MgCl_2$ (25 mM)
	0.2 mM	dNTP (25 mM)
	2 Units	Go Taq Flexi DNA Polymerase
	~ 50 ng	DNA
$Trpc6^{KO}$	9.6 μl	ddH_2O

Continued on next page

1.5 pM	TRPC6KO E7 fp
1.5 pM	TRPC6KO E7 rp
1.5 pM	TRPC6KO IF rp
1.5 pM	Pgk rp
1.5 mM	$MgCl_2$ (25 mM)
0.2 mM	dNTP (25 mM)
2 Units	Go Taq Flexi DNA Polymerase
~ 50 ng	DNA

Table 12: Genotyping cycler conditions

Gene	Step	Temperatur [°C]	Duration [s]	Number of cycles
Pod:cre				
	1	94	180	
	2	94	45	
	3	59	60	
	4	72	45	goto step 2, 30 repeats
	5	72	600	
	6	15	∞	
mtmg				
	1	94	180	
	2	94	30	
	3	61	60	
	4	72	60	goto step 2, 35 repeats
	5	72	120	
	6	15	∞	

Continued on next page

Podocin			
1	94	300	
2	94	30	
3	62	45	
4	72	30	goto step 2, 40 repeats
5	72	420	
6	15	∞	
$Trpc6^{KO}$			
1	94	180	
2	94	30	
3	56	45	
4	72	90	goto step 2, 45 repeats
5	72	600	
6	15	∞	

5.2.4 Perfusion of mice

The animal was anesthetized using the anesthetic solution (Tab. 3) with a dose of 10 μl/g body weight (i.p.). After complete loss reflexes (negative paw pinch) the mouse was fixated on a Styrofoam surface. The chest cavity was opened and the heart was exposed. A 30 gauge needle was carefully inserted into the left ventricle and a the right ventricle was cut using a scissor. Manual perfusion with PBS from a 20 ml syringe was started. As soon as the liver became pale the syringe was changed to one containing 10 ml of 4 % para formaldehyde. Afterwards the kidneys were removed and processed for histological staining.

5.2.5 Induction of Adriamycin nephropathy

Kidney disease was induced in 4 weeks old mice using Adriamycin (ADR) [86] [87]. Prior to injection of Adriamycin a urine sample was collected. Anesthesia/ analgesia was performed with Isoflurane/ Buprenorphine (0.05 mg/kg). The mouse was transferred to a warmed surgery stage and the right jugular vein was dissected via a longitudinal incision of $\sim$ 1 cm to the right next to the mid line of the neck. 25 mg/kg ADR or normal saline in control animals was administered via a catheter (PE10) placed into the jugular vein. Positioning of the catheter was checked by injecting a small volume of normal saline. After injection of ADR, the incision was closed with simple interrupted stitches and the animal was allowed to recover. The day of injection was counted as day 1 of the treatment. On the following days the mice were monitored for weight changes and urine was collected. Successful induction of Adriamycin nephropathy was confirmed by detection of proteinuria on commassie gels (Tab. 5.2.13). On day 5 mice underwent *in vivo* imaging.

5.2.6 Preparation for *in vivo* imaging

Anesthesia/ analgesia was performed with Isoflurane/ Buprenorphine (0.05 mg/ kg). The mouse was shaved on the left flank using a hair trimmer (Tab. 5). The mouse was then transferred to a warmed surgery stage and the right carotid artery was dissected via a longitudinal incision under the chin. The tissue above the trachea was prepped and the right carotid artery isolated. The carotid artery was closed at the cranial end by a knot (6-0 USP, silk) and a second knot was prepared for fixation of the catheter (Tab. 4). The artery was clamped caudally creating an approximately 0.8-1 cm long section without blood flow. Now a small incision into the artery was made using a scissor. The catheter was inserted into the carotid artery and fixed with two threads. The incision was closed with 2 to 3 interrupted stitches. The mouse was now positioned on its right side. Then the left kidney was

exteriorized by an approximately 4-8 mm long incision at the left flank cutting through the skin and the peritoneal wall. The mouse was placed on the heated imaging stage and the kidney was immobilized with a custom-build kidney holder (Tab. 5). A cover slip (Tab. 4) was placed on the kidney with minimal pressure and the animal was transferred to the microscope. A 70 kDa dextrane Texas Red (Tab. 2) was administered to label the blood circulation in red.

5.2.7 *In vivo* imaging

In vivo imaging was carried out using an upright multiphoton microscope (MPM) (Tab. 5) with a 25x water immersion objective with a numerical aperture of 0.95. The multiphoton laser was tuned to a wavelength of 940 nm and the signal was recorded using non descanned hybrid detectors and a bandpass filter 525/50 (Tab. 5). The following image settings were used: bi-directional scanning mode, speed of 600 Hz and a line average of two. As resolution 512x512 pixels were used. Time series were recorded with a frame rate of 1 image/second. Z-Stacks were recorded with 2 μm per plane.

5.2.8 Laser induced injury

Laser induced injury was done similarly as previously described by Burford et al. in 2014 [75]. In brief, the Live Data Mode provided by the Leica software was used. First, a 10 second time series was defined before the laser induced injury, which serves as a baseline measurement of the GCaMP3 fluorescence. Then, a second time series was defined during which the laser zoomed in to a pre-defined position in the glomerulus causing the laser injury. The degree of induced laser injury was monitored and stopped manually. Subsequently the image zoomed out again and the resulting calcium wave was recorded.

5.2.9 Infusion of AngII/ Losartan/ PD123319

In order to administer different compounds during imaging the vascular access via the arterial catheter was used. To ensure steady infusion an infusion pump was used for administration. All infusion were done with a rate of 10 μl/min. The used doses for different substances are shown in table 13. Infusion of AngII was stopped as soon as a signal was recorded or 80 seconds elapsed without a signal. Between two infusions a 10 minute time interval was included, to ensure circulating AngII to be degraded. In order to test the effects of the AT1R inhibitor PD123319 and the AT2R inhibitor Losartan the same glomerulus was imaged before and after administration of an inhibitor.

Table 13: Substances and doses for infusion

Substance	Dose
Angiotensin II	10 or 100ng/g
Losartan	10 mg/kg BW
PD123319	10 mg/kg BW

5.2.10 Isolation of glomeruli

Prior to glomerular preparation the animal was killed by cervical dislocation and the kidneys were removed together with the connecting vessels and the aorta. Kidneys were transferred to a dish filled with ice-cold HBSS buffer (Tab. 3). The aorta was prepped, cut longitudinally and a 27 gauge needle was inserted into the arteria renialis. The kidneys were perfused with tosylactivated magnetic beads (20 μl beads/ml/kidney) (Tab. 4). After successful perfusion the kidneys were either processed for calcium imaging experiments (see 5.2.11) or for mass spectrometry (see 5.2.12).

5.2.11 Calcium Imaging of isolated glomeruli

After successful perfusion, kidneys were decapsulated and minced using a scalpel. The tissue was incubated with collagenase 1A (1 mg/ml) for 20 minutes at 37 °C. Subsequently, the tissue was homogenized by gently pipetting up and down with a 1000 μl pipet tip with the tip cut off. The generated kidney solution was transferred onto a 100 μm sieve and the solution was gently pushed through using the cone of a 5 ml syringe. The sieve was washed with 3-4 ml of cold HBSS. The flow-through was poured on top of a fresh 100 μm sieve. After passive passage of the solution, the sieve was washed with 3-4 ml of cold HBSS. The resulting solution (10 - 12 ml) containing the glomeruli was transferred into 2 ml eppis which were put in a magnetic holder. This allowed for the glomeruli, containing magnetic beads, to concentrate at the magnet. The liquid was removed leaving the isolated glomeruli on the magnet. The glomeruli were washed of the magnet with 1 ml HBSS and collected from the different tubes. Finally the glomeruli were washed in 1 ml of HBSS using the magnet and finally dissolved in 1 ml of RPMI medium containing 5 % bovine serum albumin (BSA). In order to load the cells with a calcium sensitive dye we incubated the glomeruli with Fluo4. 1 μl of Fluo4 (dissolved in DMSO, Stock: 5 μM) was added to the glomeruli solution. The eppi was covered with aluminum foil and the glomeruli were incubated at room temperature for 30 minutes on a shaker. After incubation, the medium containing the calcium dye was removed by using the magnet, and the isolated glomeruli were dissolved in 150-200 μl of RPMI medium containing 5 % BSA.

5.2.12 Preparation of isolated glomeruli for mass spectrometry

These experiments were done in cooperation with Dr. Markus Rinschen. In brief, isolated glomeruli were snap-frozen in liquid nitrogen and stored at -80 °C. Pelleted glomeruli were lysed in 8M urea, reduced and alkylated as previously described

[88]. Then, 25 μg of protein lysates were digested using trypsin. After acidification using 4 % formic acid, peptides were cleaned up using stop and go extraction tips (STAGEtips) as described previously [89].

5.2.13 Coomassie proteinuria gel

In order to check for albuminuria/ proteinuria in spot urine of mice injected with Adriamycin (Section 5.2.5) or carrying a knock out of podocin the following sample was prepared: 2 μl urine, 8 μl H_2O, 10 μl 2x loading buffer.

For gel electrophoresis a 10 % poly acrylamide gel was used. As a control a bovine serum albumin (BSA) in defined amounts (1 and 10 μg) were loaded. The gel was run first at 70 V for 30 minutes followed by 35 mA for 1 h 45 minutes. The gel was then transferred into the fixing solution (tab. 3) for 30 minutes at RT on a shaker. The gel was rinsed with water and then transferred into the coomassie staining solution (tab. 3) and stained over night at RT on the shaker. Destaining was done by transferring the gel into water and destaining it until only the protein bands remained blue.

5.3 Data analysis

5.3.1 Percentage of podocyte area showing a calcium signal

For data analysis, only glomeruli showing a calcium signal were analyzed. Data analysis was conducted using FIJI (Table 6). The FIJI PlugIn "Correct 3D Drift" was used for motion correction to minimize shifting in the time series due to breathing, changes in blood flow and effects of systemic AngII administration. After successful motion correction a new registered image file is generated. Measurements where the registration failed were not analyzed. Subsequently a Z-projection with average intensity was done reducing the frames of the time series to one frame

allowing the measurement the total podocyte area. In a next step a maximum Z-Projection was done to measure podocyte area showing a calcium signal.

5.3.2 Measurement of signal duration

After motion correction with the FIJI PlugIn "Correct 3D Drift" the duration of single podocyte calcium signals was determined. The signal duration as determined by the time between GCaMP3 baseline fluorescence to a rapid increase in GFP fluorescence and back to GCaMP3 baseline fluorescence. The baseline fluorescence was thereby defined as the average GCaMP3 fluorescence before AngII infusion.

5.3.3 Counting of Podocytes showing a calcium signal

Podocyte number was determined by manual podocyte counting using the FIJI (Tab. 6). First the FIJI PlugIn "Correct 3 D Drift" was used reducing the shifting caused by breathing artifacts. Then a maximum Z-Projection was carried out which reduced the 180 frames of the time series to a single frame, thus excluding any podocyte from being counted twice.

5.3.4 Analysis of nLC-MS/MS and bioinformatics analysis

Analysis of the mass spectrometry data was done by Dr. Markus Rinschen. In brief, peptides were separated using nanoflow liquid chromatography (nLC) followed by a tandem mass spectrometry (MS/MS) approach. After nLC the peptides were sprayed into a Quadrupole-Orbitrap hybrid mass spectrometer (QExactive plus, Thermo) using a 1 h gradient and mass spectrometer configurations as previously described [89]. Bioinformatic analysis was performed using MaxQuant 5 and Perseus v 1.5.5.3 6 essentially as previously described [90]: A complete database from mouse without isoforms was used (uniprot, downloaded January 2017) and the label-free quantification (LFQ) option was enabled. LFQ values were log2 transformed and

samples with less than 50 % expression in the global protein expression matrix were removed. The significance analysis of microarray (SAM) approach initially developed by Tusher et al. [91] was used to define significantly altered proteins and correct for multiple testing between treated and untreated samples. False discovery rate (FDR) was 0.05, s0 was 0.1. Proteins were annotated with gene ontology (GO) terms and uniprot keywords using the Perseus annotation package. The mass spectrometry proteomics data have been deposited to the ProteomeXchange Consortium via the PRIDE [92] partner repository (http://www.ebi.ac.uk/pride) with the dataset identifier PXD007717. Submission details: Project Name: Doxorubicin treated mouse and glomerular proteome; Project accession: PXD007717; Username: reviewer84945@ebi.ac.uk; Password: 0dOrZwNh.

5.4 Statistics

Statistical calculations were done using Graph Pad PRISM. Comparison of two groups was done by two-tailed student's t-test with a confidence interval of 95 %. Comparison of more than two groups was done with One-Way ANOVA with Tukey's Multiple Comparison Test with a significance level alpha of 0.05.

6 Results

6.1 AngII mediated calcium signaling in podocytes

6.1.1 Expression of GCaMP3 in podocytes.

In order to study calcium signals in podocytes we made use of a transgenic mouse line expressing GCaMP3 from the Rosa26 locus upon excision of a lox-stop-lox casette by Cre recombination. GCaMP3 is a fusion protein consisting of the calcium binding protein calmodulin and the Green Fluorescent Protein (GFP), whose fluorescence increases upon elevation of intracellular cytosolic calcium levels [80]. In order to achieve podocyte specific expression we crossed GCaMP3$^{fl/fl}$ mice with Pod:cre (*Nphp2*:cre) mice (see 5.2.1). Expression of GCaMP3 was visualized *in vivo* using intravital imaging of the kidney. Since we used an adjustable Titanium-Sapphire laser for two-photon microscopy to enable deep tissue imaging of the living kidney, we performed a lambda scan and determined a laser wavelength of 940 nm as best compromise between penetration depth and brightness of the calcium indicator GCaMP3. Figure 7 shows the expression of GCaMP3 in podocytes. To monitor blood flow and perfusion of the imaged glomerulus we injected a 70 kDa dextrane coupled to a red fluorescent probe (Texas Red). Due to its size the fluorescently labelled dextrane is retained in the blood circulation and is not filtered.

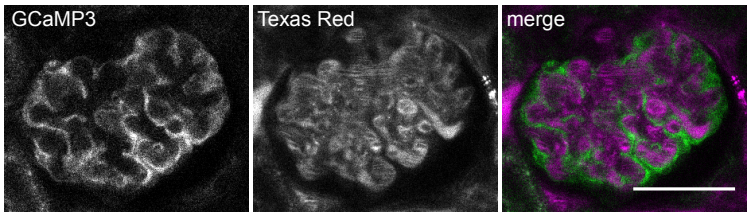

Figure 7: Expression of GCaMP3 in podocytes *in vivo*. left: GCaMP3 florescence, middle: labelling of the vasculature using 70 kDa dextrane Texas Red, right: merge. Scale bar: 40 μm.

6.1.2 Calcium signaling in podocytes upon Angiotensin II stimulation

Dysregulation of calcium signaling pathways has been associated with podocyte injury [16]. Podocyte cell culture studies and experiments using isolated glomeruli have shown that stimulation with Angiotensin II (AngII) can elict calcium transients podocytes [93, 55, 56]. However, calcium signaling in podocytes upon AngII treatment has not been shown *in vivo*. In order to induce calcium signals *in vivo*, we infused Angiotensin II (AngII) using an infusion pump with a speed of 10 μl per minute (see 5.2.9). Out of 29 imaged glomeruli only one showed a calcium signal at a dose of 10 ng/g/min AngII (Figure 8 a). Infusion of normal saline alone (vehicle), did not induce any calcium transients. An increase of the AngII dose to 100 ng/g/min (10 μl/minute) triggered a calcium signal in 21 % of the imaged glomeruli (Figure 8 b). One of the main physiological functions of AngII is regulation of the single nephron glomerular filtration rate (GFR). Thereby AngII acts on the efferent arteriole mediating constriction of the capillary to maintain filtration pressure in the event of drops of the systemic blood pressure. In higher doses it results in reduced blood flow and a swelling of the glomerular capillary network. During administration of AngII we observed this described effect indicating that the chosen dose of AngII was sufficient even though it induced unstable imaging acquisition.

In order quantify the number of podocytes showing a calcium signal in an unbiased fashion we chose to calculate the percentage of the area of GCaMP3 fluorescence showing an increase upon stimulation with AngII and thus indirectly representing the number of podocytes showing a calcium signal (see 5.3.1). Therefore only measurements showing a calcium signal were analyzed, completely excluding the groups with infusion of normal saline since they did not show a signal in any measurement. The quantification showed that a mean of 12 % area of GCaMP3 fluorescence showed calcium signal at the dose of 100 ng/g/min. Figure 8c shows

a representative time series of an animal infused with AngII (100 ng/g/min). Podocytes showing a calcium signal are indicated by arrow heads.

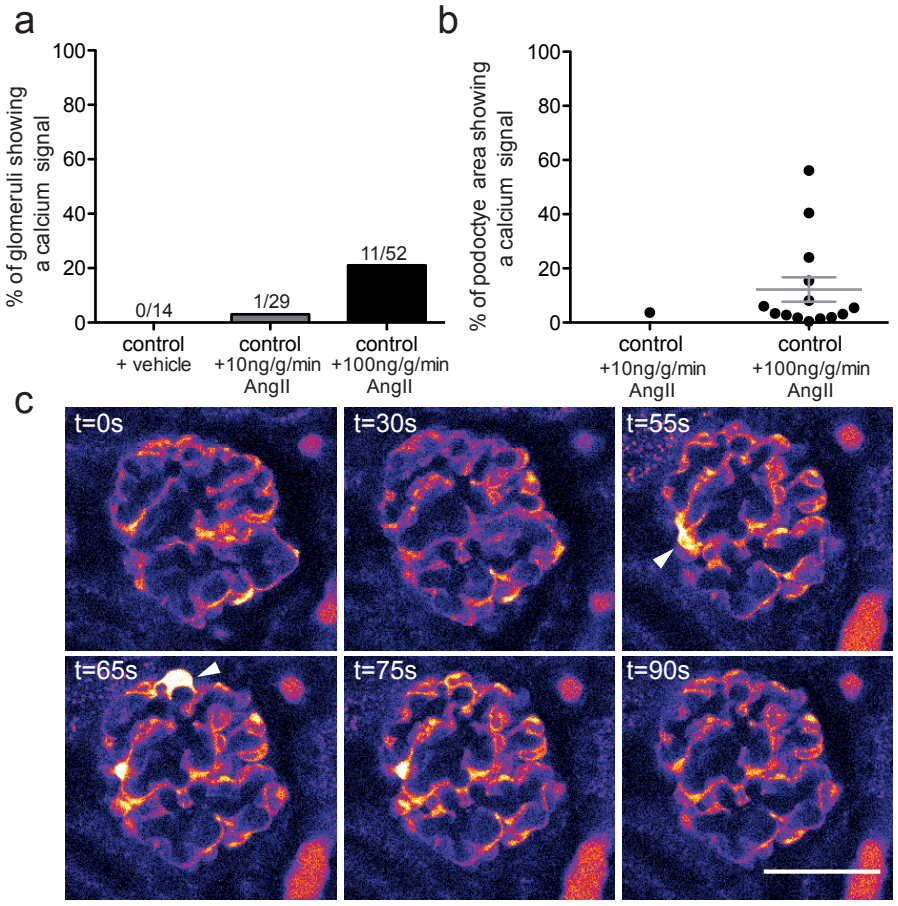

Figure 8: Angiotensin II induces calcium transients in only a small fraction of podocytes *in vivo*. **a**, Percentage of glomeruli of Pod:cre GCaMP3$^{fl/fl}$ (control) animals showing a calcium signal in at least one podocyte upon infusion of normal saline (normal saline) (n=3), AngII (10 ng/g/min, n=5) or AngII (100 ng/g/min, n=13). Numbers above bars indicate: glomeruli showing a calcium signal / total number of glomeruli imaged. **b**, Percentage of podocyte area responding with a calcium signal upon AngII stimulation is depicted for the same animal groups as in (a). control + 10ng/g/min AngII (3.7 %, signal in only one glomerulus analyzed), control + 100 ng/g/min AngII (mean=12±4.5 %, signal in 14 glomeruli analyzed). **c**, Representative time series of a glomerulus (green channel shown in false color code) during infusion of AngII (100 ng/g/min, infusion time: 43 seconds). t=1 s shows the glomerulus before infusion. Arrow heads indicate podocytes showing a calcium signal. mean=SEM, n=number of mice, Scale bar: 40 μm.

6.1.3 *Ex vivo* stimulation of podocytes with AngII

Additionally we performed *ex vivo* experiments using isolated glomeruli in an effort to analyze the observed calcium transients in more detail. Unfortunately we could not use our transgenic mice expressing GCaMP3 selectively in podocytes (Pod:cre GCaMP3$^{fl/fl}$) since the fluorescence of the calcium indicator was completely diminished after the isolation process (data not shown). We therefore loaded glomeruli with Fluo4, a commercially available calcium indicator (see 5.2.11). Similar to GCaMP3, the fluorescence of Fluo4 increases upon elevation of intracellular calcium levels. We then stimulated isolated glomeruli with either 10 or 100 μM AngII using a perfusion system and measured changes in fluorescence intensity over time. Comparable experiments have previously been published using rat and mouse glomeruli [56, 57, 79]. Figure 9a shows representative images of a glomerulus loaded with Fluo4 and stimulated with 100 μM AngII. An increase in fluorescence can be observed in a small fraction of labelled cells as indicated by the arrow heads.

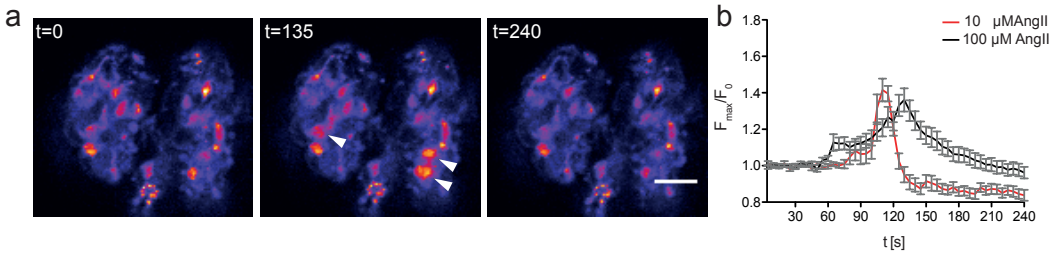

Figure 9: Isolated glomeruli show a low responsiveness to AngII *ex vivo* **a**, Representative images of a glomerulus loaded with Fluo4 and stimulated with 100 μM AngII (1 ml/min). Arrow heads indicate cells with increased fluorescence. Green channel is shown in false colors. **b**, Relative changes in fluorescence (F_{max}/ F_0) measured in response to 10 μM (n=31) (red line) or 100 μM (black line) (n=66) AngII. Start of infusion at t=50 s) n=number of cells analyzed, scale bar: 20 μm.

Quantification of the changes in fluorescence intensity over time (F_{max}/ F_0) as depicted in Figure 9b indicates that both doses of AngII (10 or 100 μM) induced an increase in intracellular calcium while the effect lasted longer with the higher

dose. In our hands the elicited calcium transients did not prove themselves as reproducible as previously published [56, 57, 79].

Since the isolation protocol involves digestion of the *ex vivo* perfused kidney by collagenase and several sieving and washing steps we checked the viability of the isolated glomeruli by performing Propidium iodide (PI) staining (Figure 10 a). Therefore, the isolated glomeruli were incubated for 5 minutes with 5 μM PI solution. Finally, the PI positive nuclei were counted and revealed a mean of 29 positive nuclei per glomerulus (Figure 10 b).

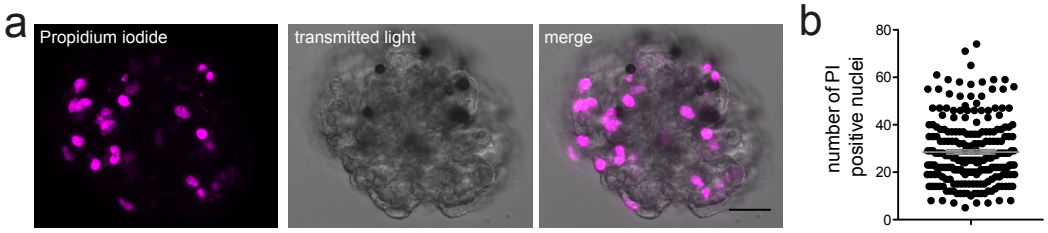

Figure 10: Isolated glomeruli show a high number of propidium iodide positive nuclei. a, Representative images of a glomerulus stained with Propidium ioddide (magenta). **b**, Quantification of the number of PI positive nuclei with a mean of 29 nuclei per glomerulus. n=219, scale bar: 40 μm.

Since some nuclei stained positive are located at positions usually occupied by podocytes in the glomerular architecture it can be speculated that podocytes undergo some kind of damage during the isolation process process resulting in nuclear uptake of Propidium iodide.

6.1.4 Adriamycin nephropathy as model of kidney disease

Since misregulation of intracellular calcium levels has been shown to play a role in kidney disease we utilized a chemically induced kidney disease model to induce podocyte injury (see 5.2.5). Adriamycin (ADR) nephropathy was induced by intravenous injection of 25 mg/kg ADR which induces acute podocyte injury [86]. Successful induction of kidney disease was controlled by the analysis of spot urine for the presence of proteinuria (Figure 11 a). Of note, the animals did not show equal amounts of protein in the urine. This could be due to the spot urine sample collected or to the degree of disease induction. Furthermore we performed histological analysis using Periodic acid Schiff (PAS) staining to check for glomerulosclerosis. Figure 11b shows representative images for control and ADR treated mice. The latter shows pronounced extra cellular matrix depositions in the glomerulus and proteinuria in the Bowman's capsule indicated by the asterisk (*). The arrow heads indicate positions of abnormal contact between podocytes and the Bowman's capsule [5, 94].

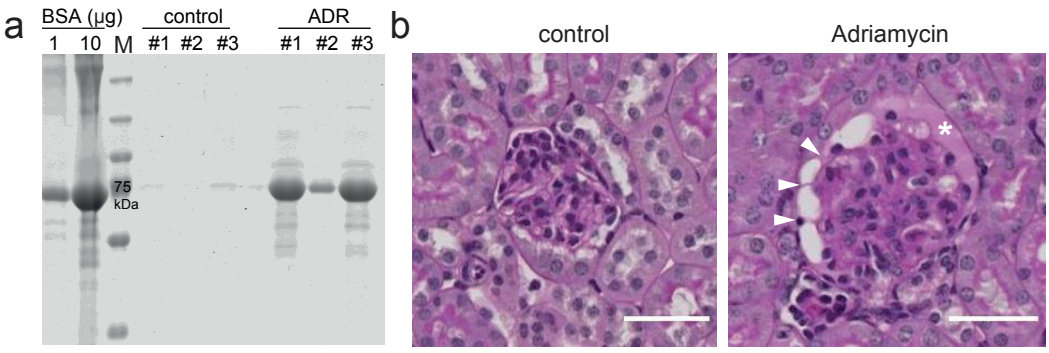

Figure 11: Adriamycin induced nephropathy as a model for podocyte injury. a, Identification of proteinuria in spot urine (2 μl) of 3 control and 3 ADR treated animals 5 days after disease induction on a coomassie gel. Bovine serum albumin (BSA) was used as standard (1 μg, 10 μg). **b**, Periodic acid–Schiff (PAS) staining of paraffin embedded kidney sections of control and ADR treated animals. Arrowhead indicates contacts between podocytes and the Bowman's capsule. Asteriks (*) indicates proteinuria. Scale bar: 40 μm.

6.1.5 Injury renders podocytes responsive to Angiotensin II

In order to investigate the role of AngII induced calcium transients in injured podocytes we challenged ADR treated animals with AngII to check if the responsiveness is altered in disease. As in untreated animals the AngII response to 10 ng/g/min AngII (10 μl/min) was low as only 7 % of the imaged glomeruli showed any calcium response (Figure 12 a). Nevertheless, healthy control animals showed even less signal with only 3 % of glomeruli showing a calcium signal (Figure 8 a). Upon increase of the dose to 100 ng/g/min 41 % of the imaged glomeruli in the group of ADR showed a calcium signal (Figure 12 a), which is a two-fold increase compared to control (Figure 8 a). Analysis of podocyte area showed, that on average 26 % of podocyte area was involved in the calcium transient (Figure 12 b) which is also increased compared to controls (Figure 8 b). Figure 12c shows representative images of a glomerulus with a strong calcium signal involving almost all of podocytes of the imaged plane. In summary, podocyte injury leads to an increase in calcium response upon AngII stimulation and a greater percentage of podocyte area contributes to the observed calcium signal.

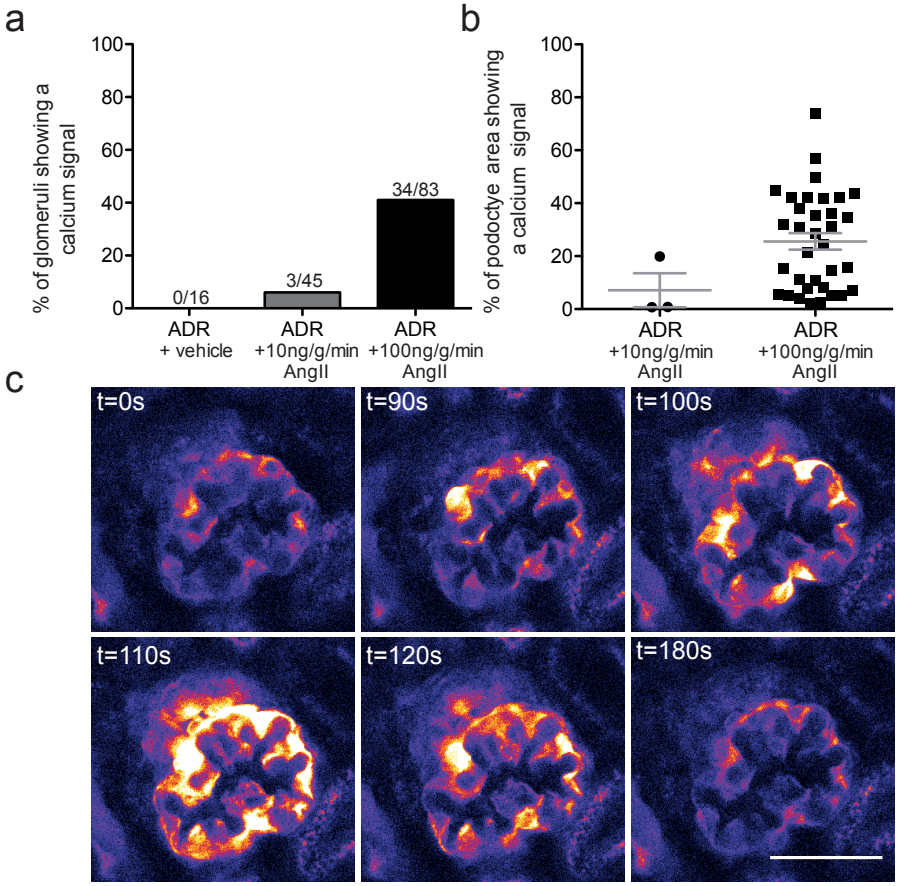

Figure 12: Angiotensin II-induced calcium signals in podocytes increase after induction of Adriamycin nephropathy. **a**, Percentage of glomeruli of Pod:cre GCaMP3$^{fl/fl}$ animals pre-treated with Adriamycin (ADR) infused with vehicle (n=3), AngII (10 ng/g/min, n=6) or AngII (100 ng/g/min, n=24). Numbers above bars indicate: glomeruli showing a calcium signal / total number of glomeruli imaged. **b**, Percentage of podocyte area responding with a calcium signal upon AngII stimulation is depicted for the same animal groups as in (a). ADR + 10 ng/g/min AngII (mean=7±6.4 %, signal in 3 glomeruli analyzed), ADR + 100 ng/g/min AngII (mean=26±3.1 %, signal in 34 glomeruli analyzed). **c**, Representative time series of a glomerulus (green channel shown in false color code) during infusion of AngII (100 ng/g/min, infusion time: 82 seconds). t=0 s shows the glomerulus before infusion. mean=SEM, n=number of mice. Scale bar: 40 μm.

To utilize a second approach to quantify the AngII induced changes in intracellular calcium levels, we counted the number of podocytes showing a calcium signal in control and ADR treated animals. To do so, we generated a t-projection of time series measurements, which showed a calcium signal upon AngII infusion, thereby combining 180 frames into a single image. This allowed us to count the number of podocytes more accurately, since infusion of AngII in most cases resulted in shifting during image acquisition. In control animals on average only two podocytes displayed a calcium transient upon stimulation with 100 ng/g/min, while in diseased animals this number increased significantly to seven podocytes (Figure 13). The number of podocytes counted is in accordance with measurements of podocyte area as shown in Figure 8b and Figure 12b. Since the response to Angiotensin II was consistently more pronounced to 100 ng/g/min in healthy and diseased animals we chose this dose for all further experiments.

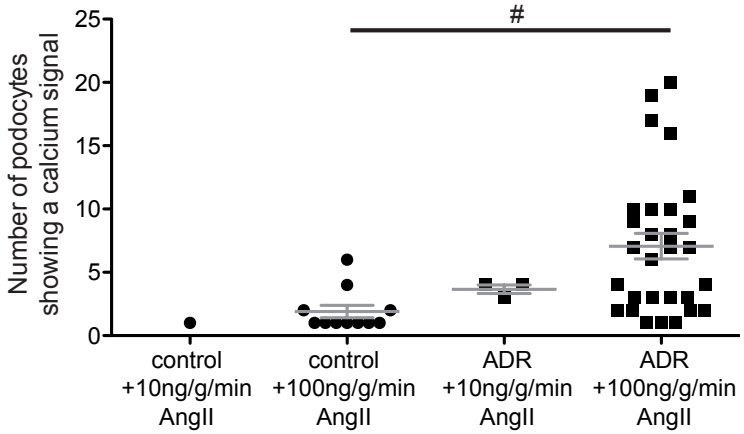

Figure 13: Number of podocytes showing a calcium signal upon Angiotensin II infusion. Control + 10 ng/g/min (n=1 with one podocytes reacting to AngII with a calcium signal in a single measurement). Control + 100 ng/g/min (n=11, mean=2±0.5). ADR + 10 ng/g/min (n=3, mean=3.7±0.3) and ADR + 100 ng/g/min (n=29, mean=7±1). n=number of glomeruli analyzed. mean=SEM, statistics: One-way ANOVA Tukey's Multiple Comparison Test: #p=0.01.

6.1.6 Deletion of *Trpc6* reduces the reponsiveness to AngII

As previous studies have shown that the transient receptor potential channel 6 (*Trpc6*) plays a role in elevating intracellular calcium levels in podocytes we made use of a whole-body knock-out mouse model. We crossed $Trpc6^{KO/KO}$ mice with our podocyte specific calcium reporter mouse line Pod:cre $GCaMP3^{fl/fl}$ to generate Pod:Cre $GCaMP3^{fl/fl}$ $Trpc6^{KO}$ ($Trpc6^{KO}$) animals (Table 9). As published previously the loss of Trpc6 did not induces a kidney phenotype in healthy mice [82].

Upon stimulation of $Trpc6^{KO}$ mice with AngII (100 ng/g/min) we observed that 10 % of the imaged glomeruli showed a calcium signal (Figure 14 a), which is slightly less than in control animals with 13 % (Figure 8 a). Induction of albuminuria by pre-treatment of $Trpc6^{KO}$ animals with ADR resulted in an increase of this number to 25 % (Figure 14 a), which is a reduction compared to $Trpc6^{wt}$ animals treated with ADR which showed a signal in 41 % of glomeruli (Figure 8 a). $Trpc6^{KO}$ animals treated with Adriamycin developed comparable levels of proteinuria to control animals (data not shown). Comparison of podocyte area of untreated $Trpc6^{KO}$ and $Trpc6^{KO}$ animals pretreated with ADR shows a clear increase (Figure 14 b) which is also represented by the number of podocytes showing a calcium signal as shown in Figure 14c. Taken together, in our model Trpc6 is partially involved in mediating Angiotensin II induced calcium currents in podocytes in health and disease, as we observed a decrease in number of glomeruli showing a calcium signal and less podocyte area was involved in the calcium signal as compared to ADR and control animals.

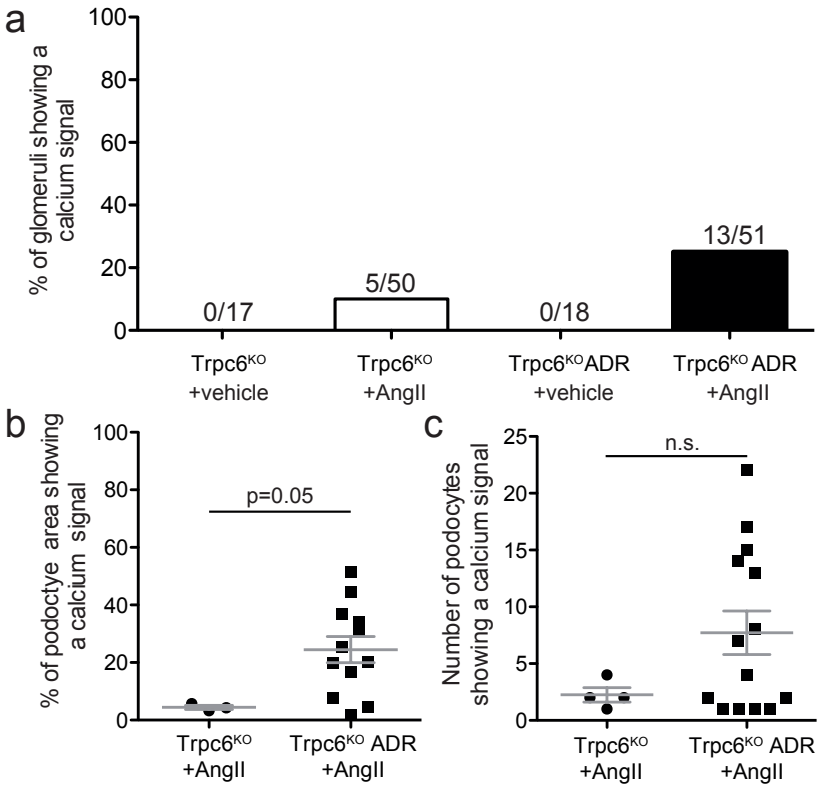

Figure 14: Loss of *Trpc6* reduces calcium transients in podocytes upon AngII stimulation. a, Percentage of glomeruli showing a calcium signal upon stimulation with with 100 ng/g/min AngII. Pod:cre GCaMP3$^{fl/fl}$ Trpc6$^{KO/KO}$ (Trpc6^{KO}) + vehicle (normal saline) (n=4), Trpc6^{KO} animals treated with AngII (n=9). Trpc6^{KO} animals pre-treated with Adriamycin (ADR) and infused with vehicle (n=4) or stimulated with AngII (n=16). Numbers above bars indicate: glomeruli showing a calcium signal / total number of glomeruli imaged. **b**, Podocyte area showing a calcium signal for the same groups as in (a). Trpc6^{KO} (mean=8±3.5 %, signal in 5 glomeruli analyzed), Trpc6^{KO} ADR (mean=21±4.3 %, signal in 24 glomeruli analyzed). **c**, Podocyte number showing a calcium signal. Trpc6^{KO} mean=2.2±0.6 (n=4), Trpc6^{KO} ADR mean=7.7±2 (n=14). n=number of glomeruli analyzed, student's t-test: p=0.05, mean=SEM.

6.1.7 Loss of *Nphp2* induces nephrotic syndrome with an early onset

To investigate if the increased responsiveness of podocytes to AngII after injury is a general mechanism we used a second disease model. In this model the slit diaphragm component podocin (*Nphp2*) is deleted specifically in podocytes. To study the impact of loss of podocin on calcium signaling we generated the following mouse line: Pod:cre GCaMP3$^{fl/fl}$ Podocin$^{fl/fl}$ (Pod^{pKO}) and Pod:cre GCaMP3$^{fl/fl}$ Podocin$^{fl/wt}$ (Pod^{pHet}) (Table 9). Heterozygous loss of podocin did not result in a phenotype, while homozygous loss resulted in severe glomerular damage. Figure 15a shows that Pod^{pKO} mice developed strong proteinuria already at the age of 3-4 weeks while Pod^{pHet} mice are healthy. In the histological analysis of paraffin embedded kidney sections using PAS staining control and Pod^{pHet} animals did not exhibit any glomerulusclerosis, while Pod^{pKO} animals showed severe glomerular sclerosis (Figure 15 b).

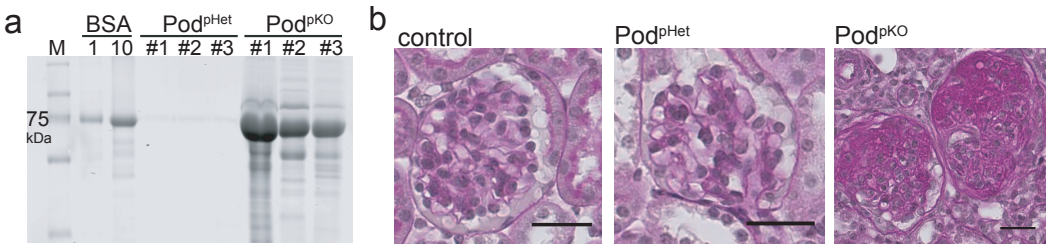

Figure 15: Loss of podocin results in severe glomerular damage. a, Analysis of proteinuria in spot urine of 3 Pod^{pHet} and 3 Pod^{pKO} animals using a Coomassie gel. Bovine serum albumin (BSA) was used as standard (1 μg, 10 μg). **b**, PAS staining on paraffin embedded kidney sections (2 μm) of control, Pod^{pHet} and Pod^{pKO}. Scale bar: 40 μm.

In vivo imaging of Pod^{pKO} animals expressing GCaMP3 in many cases showed sclerotic glomeruli correlating with impaired glomerular blood flow. Figure 16 shows four glomeruli imaged in a single animal, with each of them showing some degree of abnormalities as a dilated Bowman's capsule (Figure 16 a), pathological changes in podocyte structure, enlarged cell body as indicated by the asterisk (*)

and elevated calcium levels in podocytes (Figure 16 b-d). Therefore, the observed pathological changes in Pod^{pKO} animals observed by histological analysis (Figure 15 b) can be recapitulated by intravital imaging, while Pod^{pHet} animals did not show any alterations (data not shown).

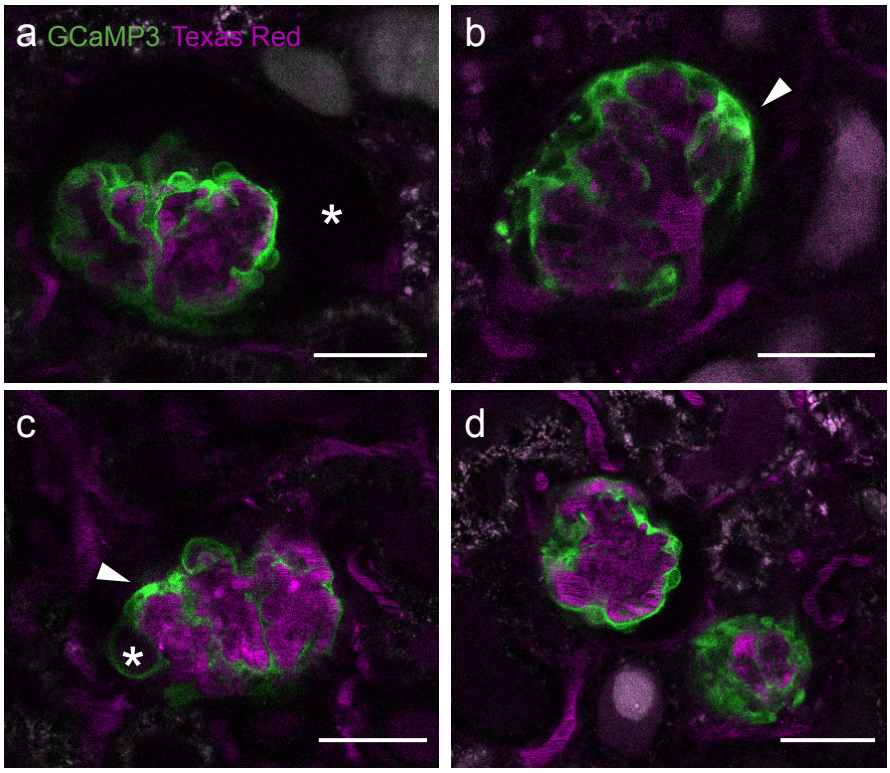

Figure 16: Podocin knock out animals show a severe glomerular phenotype *in vivo*. Representative images of glomeruli using intravital microscopy. **a**, Podocytes expressing GCaMP3 show normal morphology and normal perfusion (Texas Red in magenta) but the Bowman's capsule is dilated as indicated by the asterisk (*). **b**, the shown glomerulus is highly sclerotic with podocytes filling Bowman's space. The arrow head indicates a cell with increased calcium levels compared to neighbouring cells. **c**, Glomerulus shows a dilated cell body indicated by the asterisk (*) and cells with elevated calcium levels indicated by the arrow head. **d**. Two glomeruli shown next to each other. One (left) shows partly normal morphology and blood flow, while the second one (right) is completely sclerotic and has almost no blood flow. Scale bar: 40 μm.

6.1.8 Increased responsiveness to AngII is a common characteristic of podocyte injury

In order to validate if the observed effect of disease on the responsiveness to acute AngII treatment is a general mechanism we stimulated Pod^{pKO} mice with a dose of 100 ng/g/min AngII. The homozygous deletion of podocin rendered the cells responsive to AngII as 59% of the imaged glomeruli in the group of Pod^{pKO} showed a calcium transient (Figure 17 a). This number is even higher than in the model of Adriamycin nephropathy as shown in Figure 12a. Surprisingly, stimulation of Pod^{pHet} animals resulted in a calcium signal in 36 % of the imaged glomeruli, which is less than in Pod^{pKO} (Figure 17 a). but substantially higher than the observed response in control animals, even though the Pod^{pHet} do not show any phenotype (Figure 8 a). Measurement of podocyte area showed that in the group of Pod^{pKO} animals a mean of 21 % of podocyte area showed a calcium signal. In Pod^{pHet} animals a mean area of 28 % was measured, the highest percentage of all studied groups. Figure 17c shows representative images of AngII stimulated glomeruli of Pod^{pHet} and Pod^{pKO} mice. In summary, loss of podocin resulted in a strong responsiveness of podocytes to AngII stimulation. Furthermore, the loss of one podocin allele already increased the sensitivity to AngII comparable to the investigated disease models.

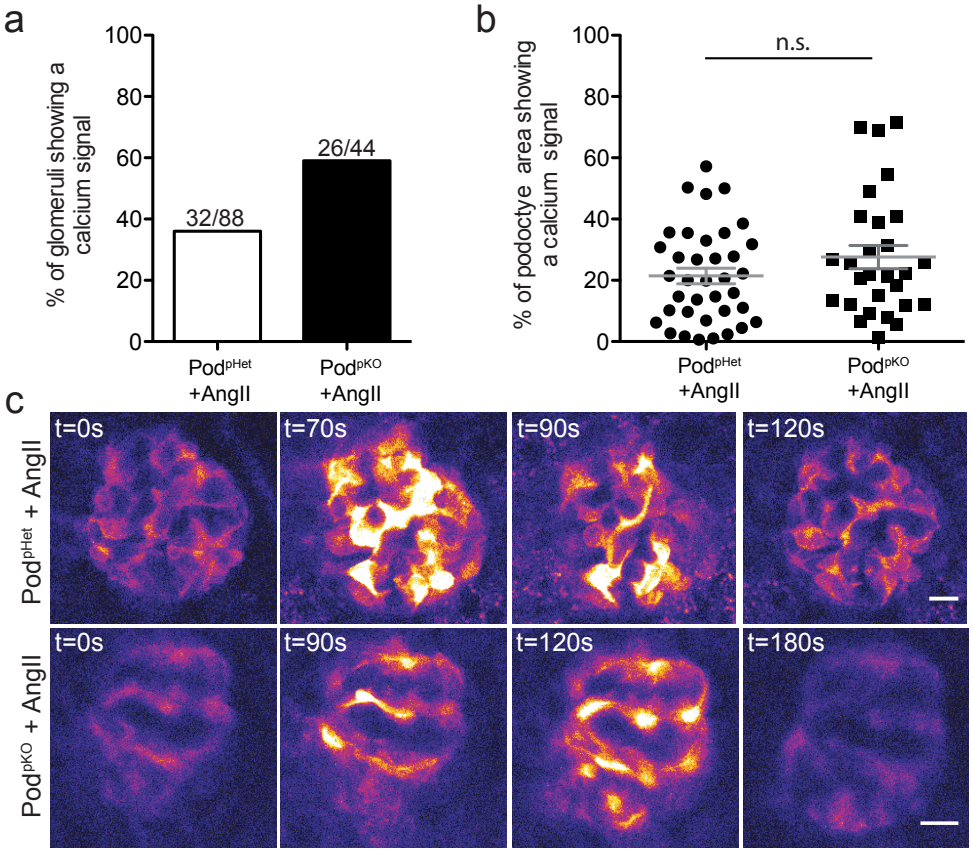

Figure 17: Loss of podocin renders podocytes responsive to AngII *in vivo*. **a**, Percentage of glomeruli showing a calcium signal upon stimulation with 100 ng/g/min AngII in Pod:cre GCaMP3$^{fl/fl}$ Podicin$^{fl/wt}$ (Pod^{pHet}) (n=31) and Pod:cre GCaMP3$^{fl/fl}$ Podicin$^{fl/fl}$ (Pod^{pKO}) (n=10) mice. Numbers above bars indicate: glomeruli showing a calcium signal / total number of glomeruli imaged. **b**, Percentage of podocyte area reacting with a calcium signal upon AngII (100 ng/g/min) stimulation is depicted for the same animal groups as in (a). Pod^{pHet} (mean=21±2.5, glomeruli analyzed=37) and Pod^{pKO} (mean=28±3.8, glomeruli analyzed=28). **c**, Representative images of Pod^{pHet} and Pod^{pKO} animals stimulated with AngII. Green channel is shown in false color code. mean=SEM, student's t-test: p=0.1649, Scale bar: 20 μm.

6.1.9 AngII-induced signals are mediated by the Angiotensin II Type 1 Receptor

It has been shown that podocytes express two Angiotensin II receptors, AngII type 1 receptor (AT1R) and type 2 receptor (AT2R) [95]. To clarify which receptor is responsible for mediating the observed calcium transients in podocytes *in vivo* we aimed at pharmacological inhibition of both receptors. To verify the role of AT1R, we imaged the same glomerulus before and after administration of losartan, a clinically used AT1R blocker. Podocyte area reacting with a calcium signal measured before and after administration of losartan is shown in Figure 18a. After administration of losartan no signal could be induced by AngII infusion indicating that losartan completely blocks AngII-mediated calcium transients. Representative images of a glomerulus before and after treatment of losartan is shown in Figure 18b.

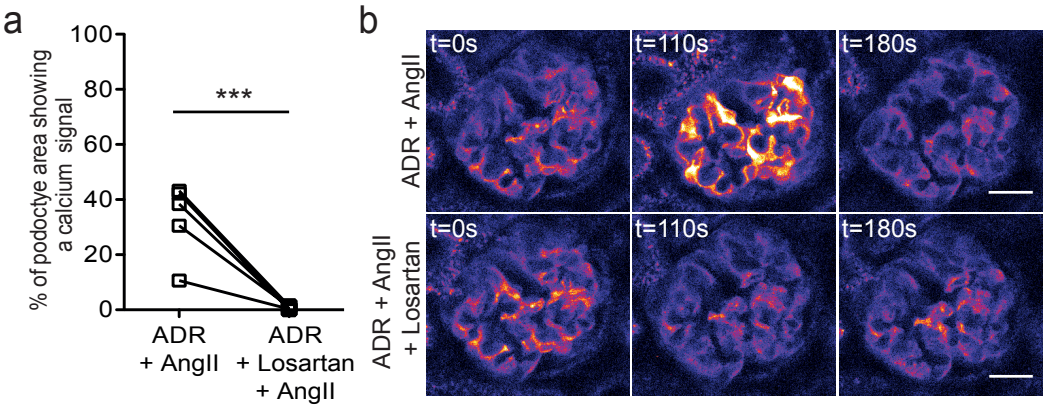

Figure 18: Losartan, an inhibitor of the AT1R, completely inhibits AngII mediated calcium signaling *in vivo*. **a**, Percentage of podocyte area reacting with a calcium signal upon AngII (100 ng/g/min) before and after treatment with Losartan (10 mg/kg). **b**, Representative images of the same glomerulus stimulated with AngII before (top row) and after treatment with Losartan (bottom row). Green channel is shown in false color code. student's t-test: ***p=0007. Scale bar: 20 μm.

To understand the role of AT2R we administered PD123319, a compound which has been shown to selectively and effectively inhibit signaling mediated by

the AT2R [96]. Inhibition of AT2R had no consistent effect on AngII induced calcium transients in podocytes. In some measurements the signal is decreased after PD123319 while in other measurements the signal is further increased concluding that PD123319 is not able to inhibit AngII-mediated calcium transients in podocytes. The measured podocyte area showing a calcium signal in response to AngII infusion before and after administration of PD123319 is shown in Figure 19a. Figure 19b shows representative images of a glomerulus stimulated with AngII before and after administration of PD123319.

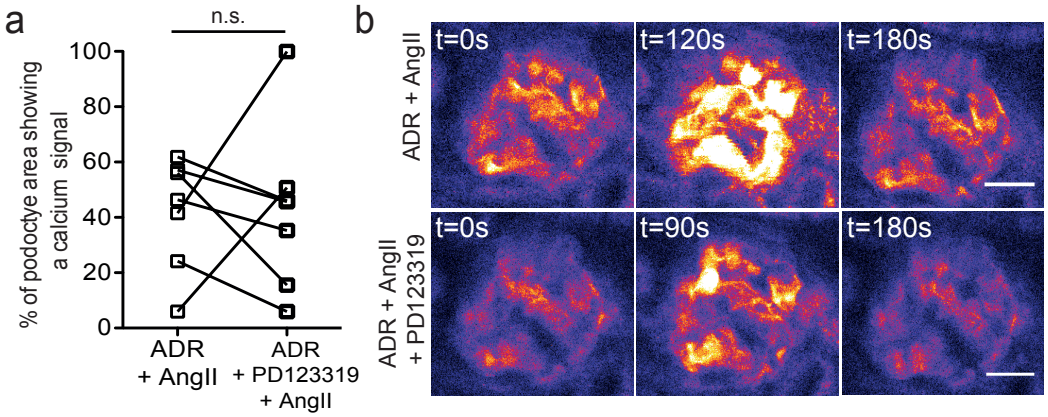

Figure 19: PD123319, an inhibitor of the AT2R, does not inhibit AngII-mediated calcium transients *in vivo*. **a**, Percentage of podocyte area reacting with a calcium signal upon AngII (100 ng/g/min) before and after treatment with PD123319 (10 mg/kg). **b**, Representative images of the same glomerulus stimulated with AngII before (top row) and after treatment with PD123319 (bottom row). Green channel is shown in false color code. student's t-test: p=0.9496. Scale bar: 20 μm.

6.1.10 Characterization of the AngII mediated calcium signal

In a next step we aimed at characterizing possible differences between the AngII-mediated calcium signaling measured in healthy and injured podocytes. Therefore we measured single podocyte fluorescence dynamics in healthy controls and mice pre-treated with Adriamycin. Figure 20 shows representative images of a glomerulus of a control animal infused with AngII (100 ng/g/min) (Figure 20 a) and for ADR treated animals (Figure 20 c). In the initial images (t=0s) two regions of interest (ROIs) are defined. The relative fluorescence changes measured in these ROIs over time are shown in b and d, respectively. In these measurements both animals were infused the same dose of Angiotensin II (infusion time: 80 s). In the control animal two podocytes showed a calcium signal while in the ADR treated animals almost all podocytes in the plane of imaging showed a calcium signal. The relative change in GCaMP3 fluorescence is comparable between both groups with a maximum increase between three and four fold (Figure 20 b, d). Therefore we could not verify a difference in the calcium increase between healthy and disease state on a single podocyte level, if a calcium transient is triggered.

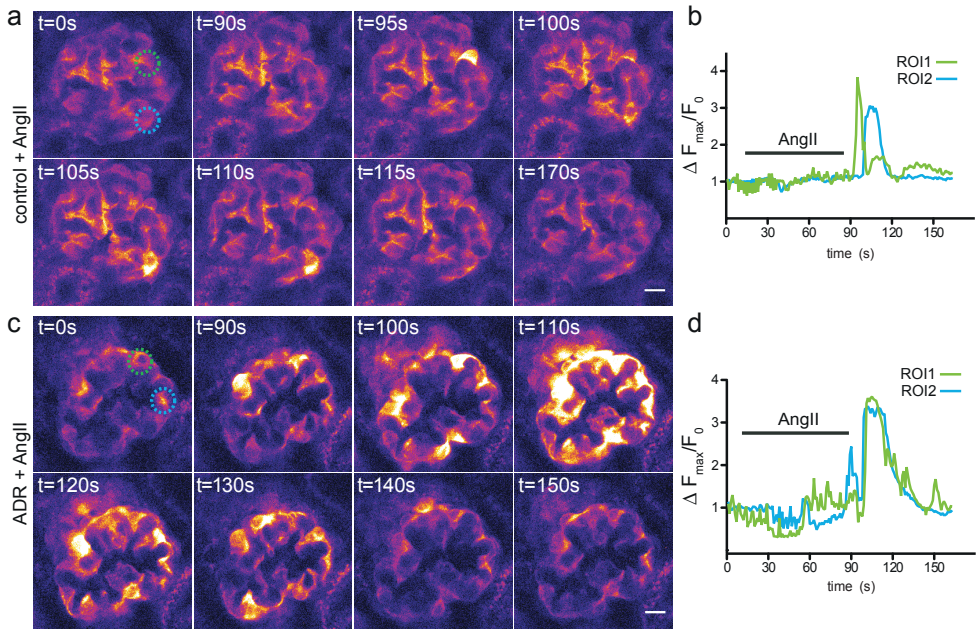

Figure 20: Analysis relative GCaMP3 fluorescence over time in single podocytes. a, Time lapse images of a glomerulus of a Pod:cre GCaMP3$^{fl/fl}$ (control) animal during infusion of 100 ng/g/min AngII (depicted by a bar in (b)). Green channel is shown in false color code. Two regions of interest (ROIs) (green and blue) for single podocytes are defined in the first image. **b**, Relative changes in fluorescence (F_{max}/ F_{F0}) in the ROIs shown in (a) are plotted over time. **c**, Time lapse images of a glomerulus of a Pod:cre GCaMP3$^{fl/fl}$ animal pretreated with Adriamycin (ADR) and stimulated with 100 ng/g/min AngII (depicted by a bar in(d)). Two regions of interest (ROIs) (green and blue) for single podocytes are defined in the first image of the time series. **d**, Relative changes in fluorescence (F_{max}/F_0) for the ROIs shown in (c) are plotted over time. Scale bar: 20 μm.

Furthermore, we wanted to investigate if the AngII induced calcium signals differ in duration of the signal in the different animal groups, specifically between healthy and diseased animals (ADR treated and Pod^{pKO} animals) and whether loss of Trpc6 (Trpc6^{KO} and Trpc6^{KO} ADR) had an effect on the signal duration. Signal duration of a single podocyte was defined by the time between the start of increased fluorescence intensity during AngII infusion and the decrease of fluorescence intensity back to its baseline level. The baseline level was defined as the measured fluorescence intensity before AngII.

Additionally, we compared our results to two published ways to trigger calcium signals in podocytes. Podocyte injury by laser damage has been demonstrated by Burford et al. [75]. The heat damage caused by the laser results in a calcium increase around the burning site and triggers a calcium wave across the glomerulus. And in 2016 Koehler et al. [97] showed that calcium transients can be induced in podocytes expressing a designer receptor, which can be exclusively activated by designer drug (DREADD). In this set up clozapine-N-oxide (CNO) was used as stimulating compound.

Analysis of signal duration of single podocytes for animals stimulated with 100 ng/g/min and laser induced unjury showed a mean signal duration of 10 to 19 s, while DREADD + CNO stimulation showed a significant longer signal of 32 seconds (Figure 21 a). Furthermore, we analyzed the relative fluorescence increase (F_{max}/F_0) in all groups. As shown in Figure 21b all groups showed an increase in fluorescence between 3- to 4 fold. Taken together, the AngII treated groups show a comparable increase in fluorescence intensity and signal duration, indicating that podocytes respond with a uniform calcium transient if a certain threshold has been passed and have a mechanism to quickly revert back to baseline.

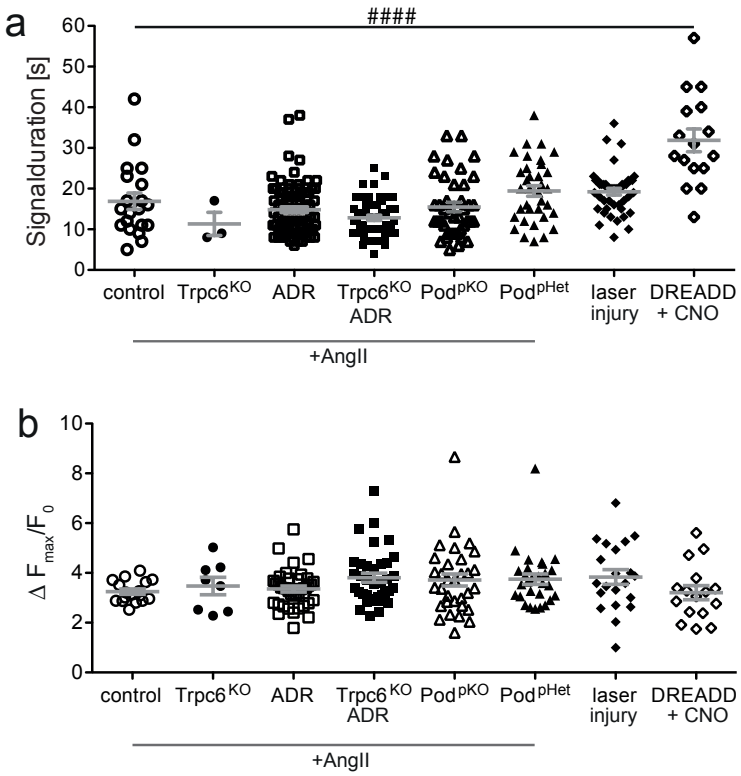

Figure 21: Characterization of Angiotensin-II induced calcium transients. **a**, Signal duration of calcium signals measured in single podocytes triggered by stimulation with 100 ng/g/min AngII, laser induced damage and designer drug-designer receptor (DREADD) interaction. Pod:cre GCaMP3$^{fl/fl}$ (control) (mean=17±1 s, n=20), Pod:cre GCaMP3$^{fl/fl}$ Trpc6$^{ko/ko}$ (Trpc6^{KO}) (mean=11±2.8 s, n=3), Pod:cre GCaMP3$^{fl/fl}$ treated with Adriamycin (ADR) (mean=15±0.7 s, n=81), Trpc6^{KO} treated with Adriamycin (Trpc6^{KO} ADR) (mean=13±0.6 s, n=52), Pod:cre GCaMP3$^{fl/fl}$ Podocin$^{fl/fl}$ (Podp^{pKO}) (mean=15±1.1 s, n=41), Pod:cre GCaMP3$^{fl/fl}$ Podocin$^{fl/wt}$ (Podp^{pHet}) (mean=19±1.2 s, n=35), laser injury in Pod:cre GCaMP3$^{fl/fl}$ mice (mean=19±0.8 s, n=45) and a designer receptors exclusively activated by designer drug (DREADD+CNO) in Pod:cre GCaMP3$^{fl/wt}$ R26hM3D$^{tg/wt}$ mice (mean=32±2.8 s, n=16). **b**, Changes in relative GCaMP3 fluorescence (F_{max}/F_0) are shown for the same groups as in (a). Control (mean=3.2±0.1, n=6, m=17), Trpc6^{KO} (mean=3.4±0.3, n=8, m=3), ADR (mean=3.4±0.1, n=39, m=9), Trpc6^{KO} ADR (mean=3.8±0.2, n=36, m=6), Pod^{pKO} (mean=3.7±0.2, n=32, m=5), Pod^{pHet} (mean=3.7±0.2, n=28, m=7), laser injury (mean=3.8±0.3, n=20, m=4) and DREADD (mean=3.2±0.3, n=16, m=3). n=number of podocytes analyzed, m=number of mice. mean=SEM, One-way ANOVA Tukey's multiple comparison Test: #p<0.0001.

6.1.11 Proteomic analysis of adriamycin treated mice

To understand the underlying mechanisms resulting in the observed increase in responsiveness to AngII stimulation upon podocyte injury we performed quantitative proteomic analysis to investigate dynamic changes of protein expression in mice treated with ADR or NaCl (vehicle) at day 3 after treatment. To this end, we isolated glomeruli as described in 5.2.10 and 5.2.12 from mice and performed nLC-MS/MS. We identified a total of 3207 proteins and quantified 1847 of them (see 5.2.12). Differential analysis as described in 5.3.4 demonstrated a significantly increased expression of 127 proteins, whereas 150 proteins were decreased. Among the increased proteins associated with calcium signaling were glutathione S-transferase omega-1 (Gsto1), ankryin-3 (Ank3), citrin (solute carrier family 25 member 13, Slc25a13), Bax and demantin (Dmtn) (Figure 22). Table 14 lists the top 10 of proteins upregulated in Adriamycin nephropathy and table 15 lists the top 10 proteins down regulated compared to control. We were not able to detect any angiotensin II receptor (AT1R and AT2R) or the Trpc6 channel.

Table 14: Top 10 of upregulated proteins in Adriamycin nephropathy

P-value	Protein name	Gene name
5,494169681	Glutathione S-transferase omega-1	Gsto1
3,902950498	Pleckstrin homology-like domain family A member 3	Phlda3
2,974969838	Cystatin-C	Cst3
2,781908504	28S ribosomal protein S22, mitochondrial	Mrps22
2,53533579	Plastin-1	Pls1

Continued on next page

2,529581351	NADH dehydrogenase [ubiquinone] iron-sulfur protein 7, mitochondrial	Ndufs7
2,473646713	NADH dehydrogenase [ubiquinone] iron-sulfur protein 7, mitochondrial	Por
2,374697773	L-xylulose reductase	Dcxr
2,207090917	NFU1 iron-sulfur cluster scaffold homolog, mitochondrial	Nfu1
2,195622915	Cathepsin-D	Ctsd

Table 15: Top 10 of downregulated proteins in Adriamycin nephropathy

P-value	Protein name	Gene name
3,108866222	Sorting nexin-27	Snx27
2,871112004	Ras-related protein Ral-B	Ralb
2,737441072	Target of Myb protein 1	Tom1
2,591391439	Fryl	
2,509630694	Protein BUD31 homolog	Bud31
2,387389673	Importin subunit alpha-4	Kpna3
2,332024744	26S proteasome non-ATPase regulatory subunit 11	Psmd11
2,32021624	Serine/threonine-protein kinase PAK 1	Pak1
2,313692403	Phosphoribosylformylglycinamidine synthase	Pfas
2,292647546	Engulfment and cell motility protein 2	Elmo2

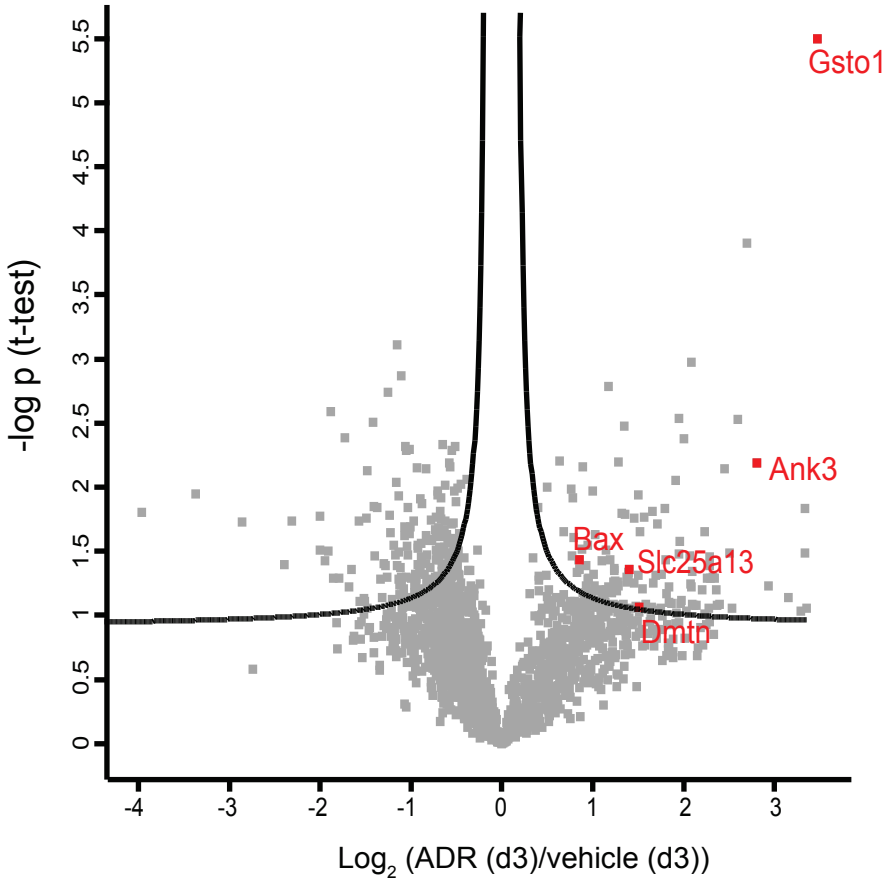

Figure 22: Quantitative proteomic analysis of protein expression of Adriamycin treated C57BL6 wildtype mice at day 3 after injection compared to vehicle treated mice (d3). volcano-Blot representing the differentially regulated proteins in control vs Adriamycin (ADR) treated animals (day 3). The negative decadic logarithm of each protein is plotted against the log2 Difference (control (day 3)/ADR (day 3)) of each protein. Proteins beyond the line represent proteins largely different between both samples (s0 = 1 and FDR >0.01). Proteins upregulated and associated with calcium signaling are labeled in red and with their respective gene symbol.

6.2 Puringeric calcium signaling in glomerular cells

6.2.1 Expression of GCaMP3 in endothelial cells

Purinergic signaling, especially signaling mediated by adenosine-triphosphate (ATP), has shown to play a crucial role in regulating renal hemodynamics and is a potent activator of calcium signaling in endothelial cells [98, 99]. In order to observe calcium signaling in glomerular endothelial cells we crossed our GCaMP3$^{fl/fl}$ mice to a Tie2:cre mouse line, which expresses Cre under an endothelial cell specific promoter. Figure 23a shows the overall expression pattern of GCaMP3 in glomerular endothelial cells. Fluorescence is visible in a thin cell layer enclosing the capillary lumen (Figure 23 b). The vasculature was labelled by injection of 70 kDa Texas Red.

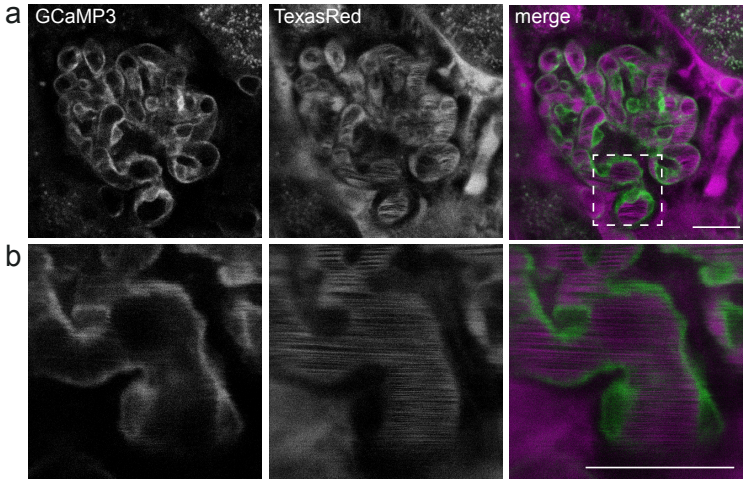

Figure 23: Expression of GCaMP3 in glomerular endothelial cells *in vivo* **a**, Representative image of a glomerulus with endothelial cells expressing GCaMP3. Vasculature was labelled by injection of 70 kDa dextrane Texas Red (magenta). **b**, Higher zoom onto a part of a calpillary indicated by the dashed box in (a). Scale bar: 20 μm.

6.2.2 Glomerular endothelial cells show a strong response to ATP *in vivo*

Stimulation of endothelial cells was accomplished by bolus injection of 0.5 μg ATP. During bolus injection a minor part of the administered dose remains in the catheter, therefore a manual flush of the catheter is necessary to ensure that the entire dose is administered. Due to handling there is always a short pause between bolus injection and flushing of the catheter.

Upon injection of ATP endothelial cells showed a strong calcium signal in all glomerular cells expressing GCaMP3 (Figure 24 a). Bolus injection was carried out at t=10s (not shown) and the calcium signal was recorded $\sim$ 3s later (t=13s). Interestingly, the endothelial cells of the efferent arteriole, indicated by dashed lines, also showed a calcium signal. The efferent arteriole was localized by comparing the Z-Stack acquired before administration of ATP with the time series acquired during ATP injection. The signal shown here lasted approximately 4 to 5 seconds. Analysis of changes in the relative fluorescence of GCaMP3 in single endothelial cells, marked in (a) at t=0s, shows a 3 to 4 fold increase in relative fluorescence (Figure 24 b). The relative fluorescence increase of the total glomerular area (black line trace) is less, which is accounted for by additionally averaging areas in the glomerulus not expressing GCaMP3 like the capillary lumen. We conclude, that ATP is a potent activator of calcium signaling in glomerular endothelial cells.

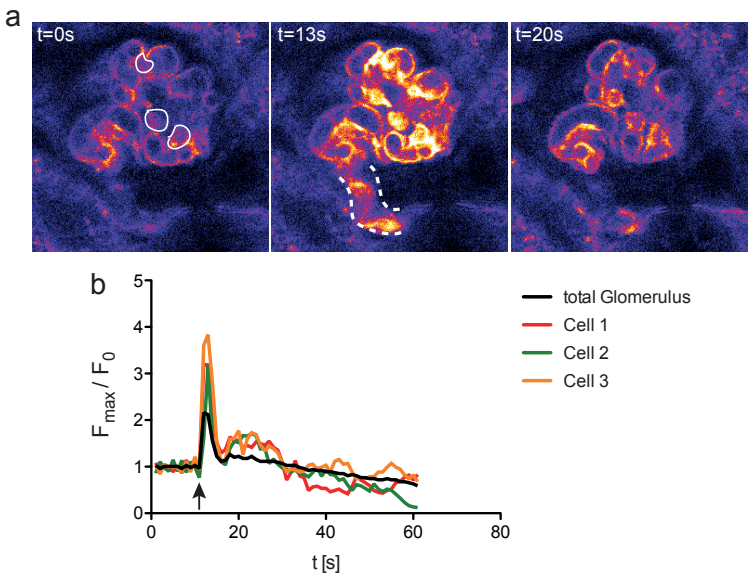

Figure 24: ATP induces a strong calcium signal in glomerular endothelial cells *in vivo*. **a**, Representative images of a glomerulus expressing GCaMP3 in endothelial cells injected with 0.5 μg ATP. Green channel is shown in false color code. t=0 s shows the glomerulus before injection of ATP, t=13 s shows the calcium signal immediately after injection (t=10 s, no shown), t=20 s calcium levels back at baseline. In the first image (t=0 s) three cells are marked, corresponding to b. **b**, Relative fluorescence changes for three single cells marked in a (first image) and the entire glomerulus. Arrow indicates time point of injection. Scale bar: 40 μm.

Upon increasing the ATP dose by 10-fold to 5 μg we were able to stimulate the peritubular capillary bed, as post-glomerular endothelial cells showed a calcium signal as indicated by the arrow heads and asterisks (*) (Figure 25). This indicates that ATP is not completely consumed by binding to its receptors or is degraded by enzymes called ectonucleotidases which can be found in the entire nephron [70]. Meaning, that a sufficient amount of the injected ATP reaches the glomerulus and capillaries downstream of the glomerular capillary bed. Taken together, endothelial cells show a strong calcium response to ATP and to target endothelial cells downstream of the glomerulus higher doses are necessary.

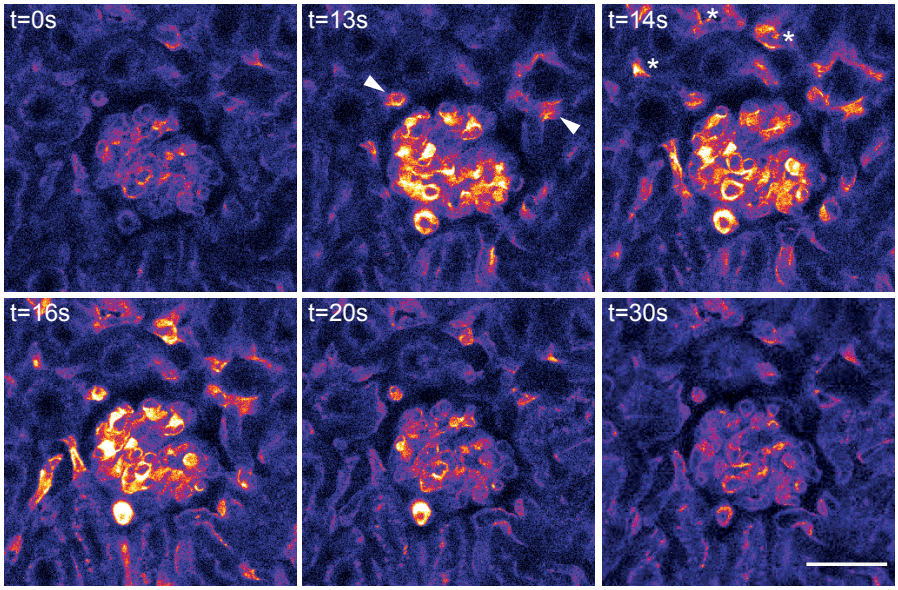

Figure 25: High doses of ATP reaches endothelial cells downstream of the glomerulus. Representative images of a mouse expressing GCaMP3 in endothelial cells injected with 5 μg ATP. Green channel is shown in false color code. t=0 s shows the glomerulus before injection of ATP. t=13 s shows the calcium signal immediately after injection (t=10 s, not shown). Arrow heads indicate peritubular endothelial cells showing a calcium signal together with the glomerular endothelial cells. t=14 s shows that more distant endothelial cells (*, asteriskses) now are stimulated by ATP and react with a calcium signal. t=30 s , the calcium level is back at baseline. Scale bar: 40 μm.

6.2.3 ATP-mediated calcium transients can be blocked by high-dose Suramin

In a next step we administered Suramin, an unspecific purinergic receptor inhibitor to block the ATP-mediated calcium signals. In order to achieve complete inhibition we injected a total dose of 2.5 mg. At lower doses Suramin was not potent to achieve inhibition (not shown). Representative images show the same glomerulus stimulated with 0.5 μg ATP before and after administration of Suramin (Figure 26 a, b). One can notice that in b the injection of ATP induced a strong shift which resulted in an increase in fluorescence. This increase is also represented in the graph (Figure 26 c) and correlates with the time point of ATP injection (grey arrow). The observed shift is due to the endogenous function of ATP on vascular hemodynamics resulting in vasoconstriction. Concluding, that blocking of purinergic receptors is possible but requires high doses and that the observed signal is based on the direct effect of ATP binding to its receptor and not by a heamodynamic effect on endothelial cells.

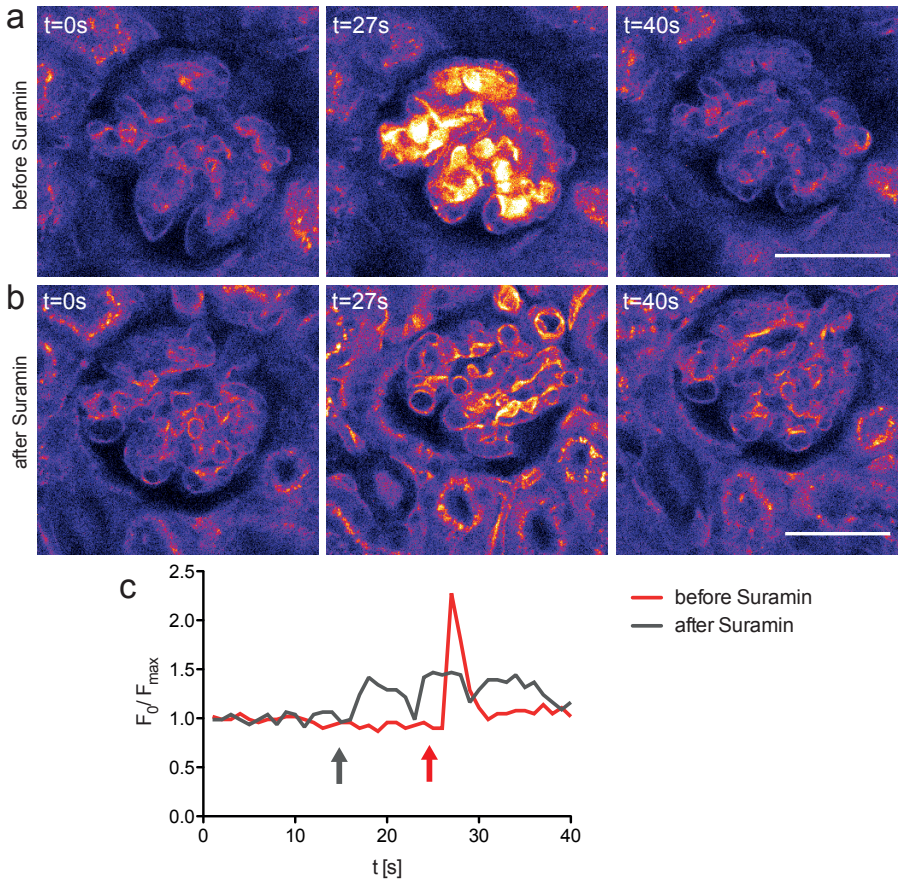

Figure 26: High dose of Suramin completely inhibits ATP-mediated calcium signals in endothelial cells. a, b, Representative images of a glomerulus expressing GCaMP3 in endothelial cells injected with 0.5 μg ATP before (a) and after (b) adminstration of Suramin (2.5 mg). t=0 s shows the glomerulus before injection of ATP, t=27 s shows the glomerulus shortly after administration of ATP and t=40 s shows the glomerulus with the fluorescence back at baseline. Baseline is defined as the fluorescence intensity before administration of ATP. Green channel is shown in false color code. **c**, Relative changes in GCaMP3 fluorescence over time upon injection of 0.5 μg ATP. The red arrow indicates the time point of ATP injection before administration of Suramin, and the grey arrow indicated the time point of ATP injection after administration of Suramin. Scale bar: 40 μm.

6.2.4 Proximal tubular cells respond with a calcium signal upon stimulation with ATP

To this point, we were able to show that ATP induces dose-dependent calcium transients in endothelial cells which can be blocked by inhibition of ATP receptors. Since it has been shown that enzymes, termed ectonucleotidases, capable to degrade ATP to adenosine diphosphate (ADP), are present in the glomerulus [70] we wanted to investigate if ATP is filtered into the primary ultrafiltrate and could therefore directly act on podocytes *in vivo*. To clarify this question we set out to investigate the calcium response to ATP in proximal tubular cells. To be able to monitor calcium transients in proximal tubular cells we crossed GCaMP3$^{fl/fl}$ with Pax8:cre mice to achieve GCaMP3 expression. Pax8:cre shows expression in the entire nephron, whereby the expression is higher in proximal and distal tubular cells compared to podocytes as shown in Figure 27. Again the vasculature was labelled by injection of 70 kDa Texas Red. The left panel shows the expression of GCaMP3 mainly in proximal cells with a pronounced apical localization but also in a distal tubule indicated by the dashed lines (right panel) and in podocytes.

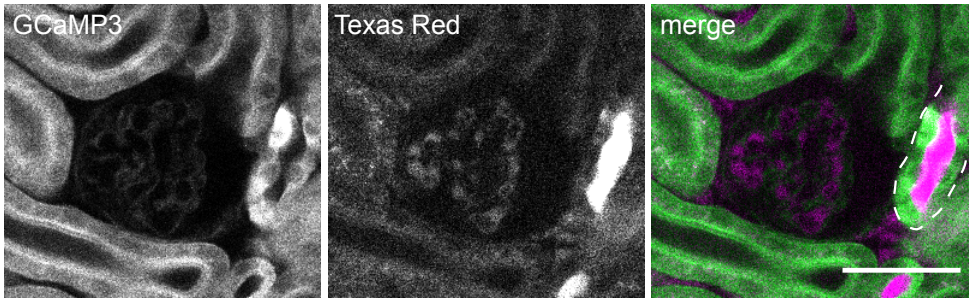

Figure 27: Expression of GCaMP3 in proximal tubular cells Left: GCaMP3 expression in proximal and distal tubular segments and in podocytes. Arrow head indicates a cell of a distal tubular segment with an increased calcium level. Middle: Red channel, fluorescence of 70 kDa Texas Red labelling the vasculature. Right: merged channels. Dashed line indicates a distal tubular segment. Scale bar: 40 μm.

Interestingly, tubular cells show spontaneous intracellular calcium oscillations represented by changing levels of GCaMP3 fluorescence as shown in Figure 28.

The images depicts the same tubular region within a time frame of 60 seconds without any intervention during this time. Arrowheads indicate cells with increased GCaMP3 fluorescence. This observation has been also made been made previously using transgenic rats [100].

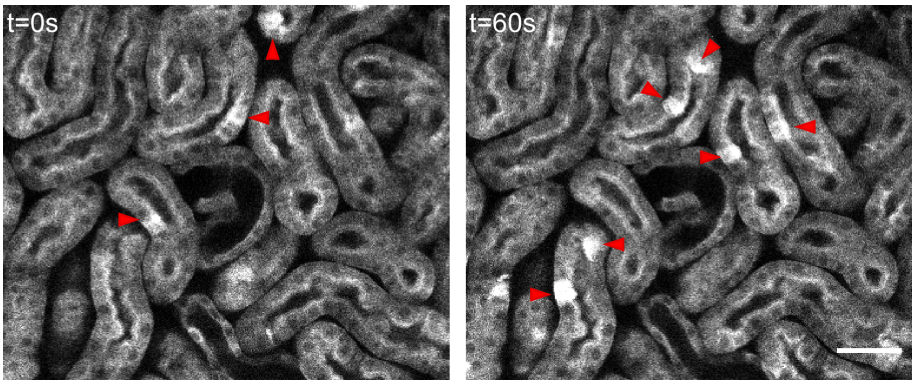

Figure 28: Tubular cells show spontaneous calcium oscillations at baseline Green channel is shown in grey. Arrowheads point to cells with increased GCaMP3 fluorescence. Scale bar: 40 μm.

6.2.5 Proximal tubular cells show a strong response to ATP

To verify if the injected dose of ATP is filtered and thus present in Bowman's space where it could potentially bind to ATP receptors expressed by podocytes we injected mice expressing GCaMP3 in tubular cells with 1 μg ATP (Figure 27). Figure 29 shows the calcium transients induced by ATP in proximal tubular cells. For clarification t=0s, i) shows the imaged region with the GCaMP3 fluorescence shown in green and Texas Red shown in red with the glomerulus indicated by the dashed line. Image t=0s, ii) and subsequent images only show the green channel in false color code. t=25s shows the area just after injection of ATP. Within a few seconds a bright GCaMP3 signal can be observed, reflective of high intracellular calcium levels. The signal increases further over time with its maximum at t=35s where almost all tubular segments show a strong calcium signal. At t=50s the signal is approximately back at baseline (t=0s). Taken together, 1 μg was sufficient to induce a strong signal in proximal tubular segments but no signal could be detected in podocytes. The observed calcium transients in proximal tubular cells could be possible induced by either stimulation through the peritubular capillary system or by ATP being present in the primary ultrafiltrate.

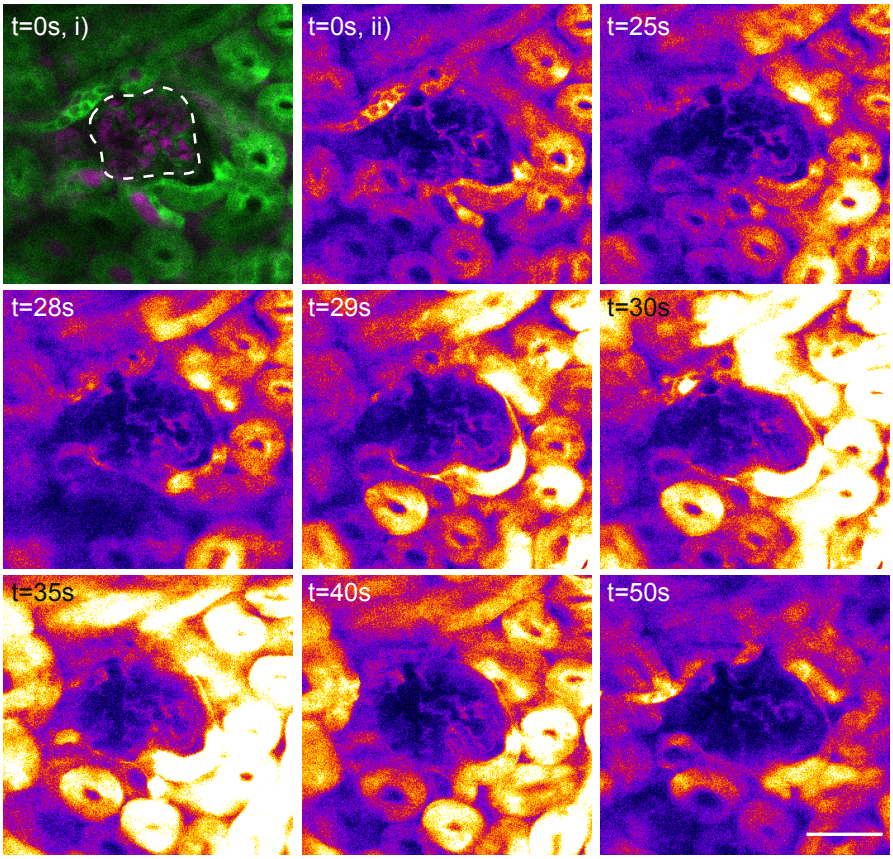

Figure 29: Tubular cells show a strong calcium signal upon injection of ATP. Representative images of a glomerulus and tubular region during injection of 1 μg ATP. t=0 s, i) show the GCaMP3 fluorescence in green and Texas Red fluorescence in magenta. Dashed line indicates the glomerulus. Image t=0 s, ii) and subsequent images shows the GCaMP3 fluorescence only in false color code, the red channel (magenta) is not shown. Image t=0 s shows the region before injection of ATP. t=25 s show the region immediately after injection of ATP. Scale bar: 40 μm.

6.2.6 Calcium wave in podocytes induced by laser injury

To this point, we have shown that endothelial and proximal tubular cells can be stimulated by ATP resulting in intracellular calcium transients. Furthermore, purinergic signaling has been shown to induce calcium transients in podocyte cell culture experiments and using isolated glomeruli. Also, Burford et al. (2014) have shown that purinergic signaling could play a role in mediating calcium transients in podocytes using intravital microscopy [75]. In their publication they induced elevated calcium levels in podocytes by causing a laser-induced injury. To achieve this, the laser is focused on one podocyte in a glomerulus which leads to a heat damage at that point due to high laser power focused on a small area (see 5.2.8). We recapitulated their findings using our *in vivo* imaging settings. Figure 30a depicts how the calcium wave spreads from the point of injury (marked by an X) to podocytes further away. At t=1s a calcium signal can be observed directly adjacent to the injury site (Fig. 30 a, red circle). In this region the fluorescence decreases over time but does not go back to the baseline level, indicating sustained podocyte damage [75]. This is in contrast to the other podocytes showing a calcium signal. Here, the intracellular calcium levels rises and goes back to baseline levels (Figure 30 b). The spreading of the calcium signal has been termed "calcium wave" [75].

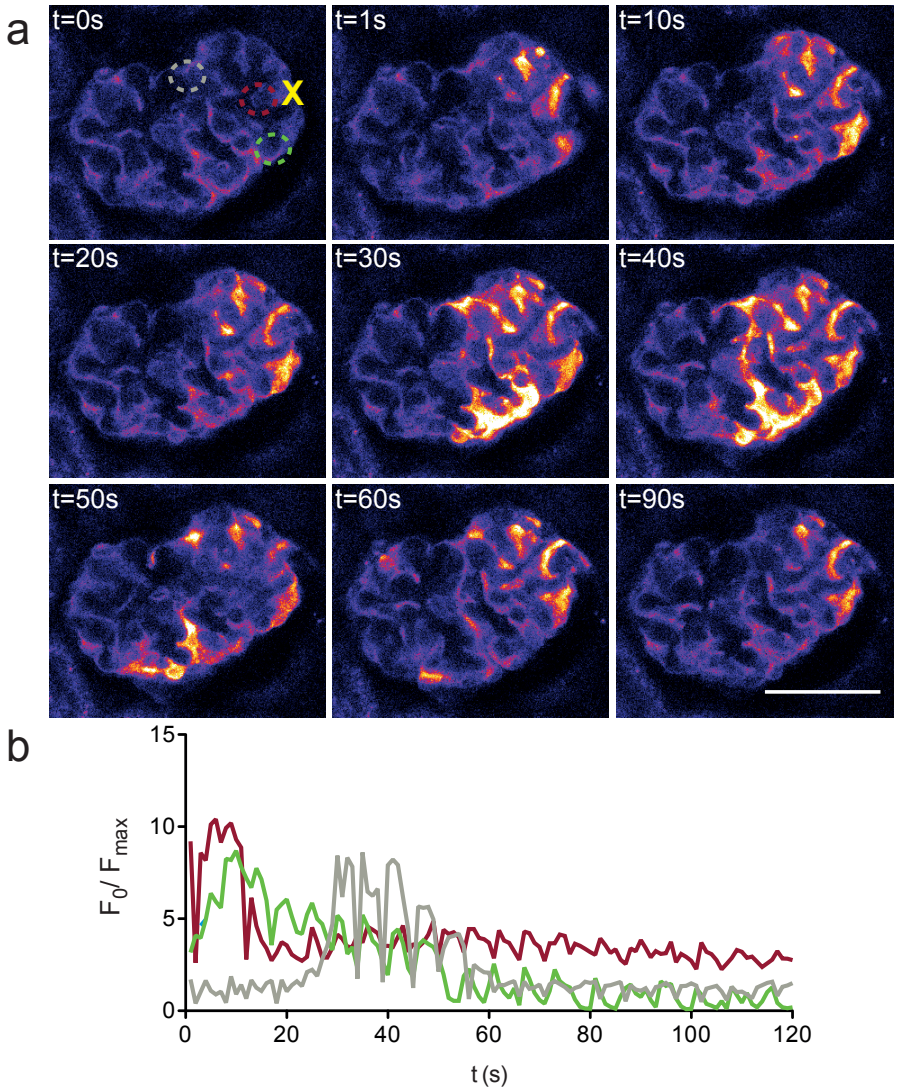

Figure 30: Calcium wave in podocytes triggered by laser induced injury *in vivo*. **a**, Representative images of a glomerulus over time (t=0 s to t=90 s) after laser induced injury. In t=0 s the yellow X marks the point of injury. The colored circles define different regions of interest (ROIs) in which the fluorescent changes over time were analyzed (b). **b**, Relative fluorescence changes (F_{max}/F_0) of the calcium indicator GCaMP3 over time for the ROIs indicated in (a). Green channel is shown in false color code. Scale bar: 40 μm.

6.2.7 ATP plays a role in propagating calcium transients observed upon laser injury

Since Burford et al. used ATP receptor inhibitors to identify ATP as a mediator of the observed calcium wave we wanted to confirm this finding. Therefore we used Suramin, a broad spectrum antagonist of purinergic receptors (P2X and P2Y), to block ATP-mediated calcium signaling [75]. Additionally, we used Lanthanumchloride ($LaCl_3$), an inhibitor of the transient receptor potential channel 6 (Trpc6), to inhibit calcium influx from the extracellular space. The number of glomeruli showing a calcium wave upon laser-induced injury, depicted as percentage, does not differ in control mice treated with NaCl (vehicle), Suramin or $LaCl_3$ as shown in Figure 31a. Furthermore, we measured the relative fluorescence increase of GCaMP3 in single podocytes and the number of podocytes showing a calcium signal in the different groups. No difference in the relative fluorescence (F_{max}/F_0) of GCaMP3 in single podocytes and in the number of podocytes showing a calcium signal could be detected (Figure31 b, c). However, measurement of the time between the laser-induced injury and the start of the calcium wave, meaning the first podocyte showing a calcium signal after injury, is significantly different between the groups. In control mice (vehicle) the mean time was 19 s, which increased by two-fold to a mean of 41 s in Suramin and to 51 s in $LaCl_3$ treated animals (Figure 31 d). Consequently, purinergic receptors could play a role in signal transmission between podocytes. Furthermore, even though $LaCl_3$ was able to delay the propagation of the calcium wave, it did not inhibit it completely suggesting that either more calcium permeable channels are involved or intracellular calcium stores are opened.

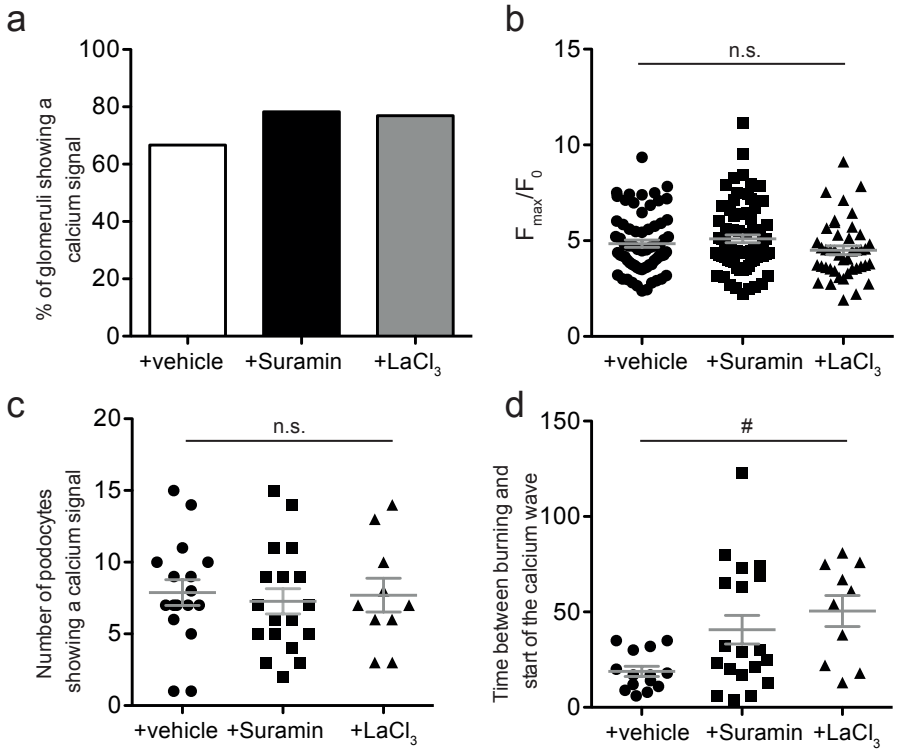

Figure 31: Inhibition of calcium influx and ATP receptors delays a calcium wave spreading over the glomeruli. a, percentage of glomeruli showing a calcium signal upon laser-induced injury in animals treated with NaCl (control, n=27), Suramin (1 mg, n=23) or $LaCl_3$ (check dosis, n=13). n=number of glomeruli analyzed. **b**, Changes in the relative fluorescence (F_{max}/F_0). NaCl (n=67, mean=4.8±0.2), Suramin (n=72, mean=5.1±0.2) and $LaCl_3$ (n=42, mean=4.5±0.2). **c**, Number of podocytes showing a calcium signal upon laser-induced injury. NaCl (n=17, mean=7.8±0.9), Suramin (n=18, mean=7.2±0.9), $LaCl_3$ (n=10, mean=7.7±1.2). **d**, Analysis of the time between injury initiation and the start of the calcium wave. NaCl (n=14, mean=18.8±2.7 s), Suramin (n=19, mean=40.6±7.4 s) and $LaCl_3$ (n=10, mean=50.5±8.1 s). n=number of podocytes analyzed. mean=SEM, #p=0.0115 One-way ANOVA Tukey's multiple comparison Test.

6.2.8 ATP is not able to trigger a calcium signal in podocytes *in vivo*

Since ATP seems to be involved in signaling between podocytes upon laser-induced injury we aimed at inducing calcium signals by directly stimulating purinergic receptors with ATP as shown for endothelial and proximal tubular cells (0.5 to 1 μg ATP). To this end we administered doses between 2 and 10 μg of ATP as bolus injections and flushed the catheter afterwards. Unfortunately, we were not able to trigger any calcium signal in healthy podocytes at any dose, instead injection of ATP resulted in strong effects on the blood flow by causing vasoconstriction [67].

Figure 32 shows representative images of a glomerulus of a mouse injected with 2 μg ATP and its effects on glomerular hemodynamics but no calcium signal can be observed. The white dashed line indicates a capillary region before (t=0s) and just after (t=15s) injection of ATP. At t=0s the capillary shows normal blood flow, indicated by the black lines caused by blood cells passing through the capillary. Due to their high velocity and lack of fluorescence the cells appear as black lines. At t=15s the black lines in the same capillary region are absent, instead the round shape of blood cells is visible indicating a severe decrease of blood flow. It should be noted that the blood flow normalizes quickly after the initial injection (t=20s). Furthermore, the injection of ATP results in unstable image acquisition. This change becomes obvious when comparing the glomerular size indicated by the grey dashed line at t=0s, t=25s and t=50s. The grey dashed line highlights the edges of the glomerulus at t=0s (before injection) in this particular image plane. The glomerular area is smaller at t=25s and t=50s since the glomerulus shifted upwards or downwards, respectively, resulting in a smaller portion of the glomerulus to be visible. At t=25s GCaMP3 fluorescence in podocytes seems to be increased but it should not be interpreted as a calcium signal since the fluorescence intensity is the same in the Z-Stack (not shown) acquired prior to injection. Taken together,

injection of ATP produced strong physiological effects on blood flow resulting in unstable imaging acquisition but no detectable calcium signaling in podocytes.

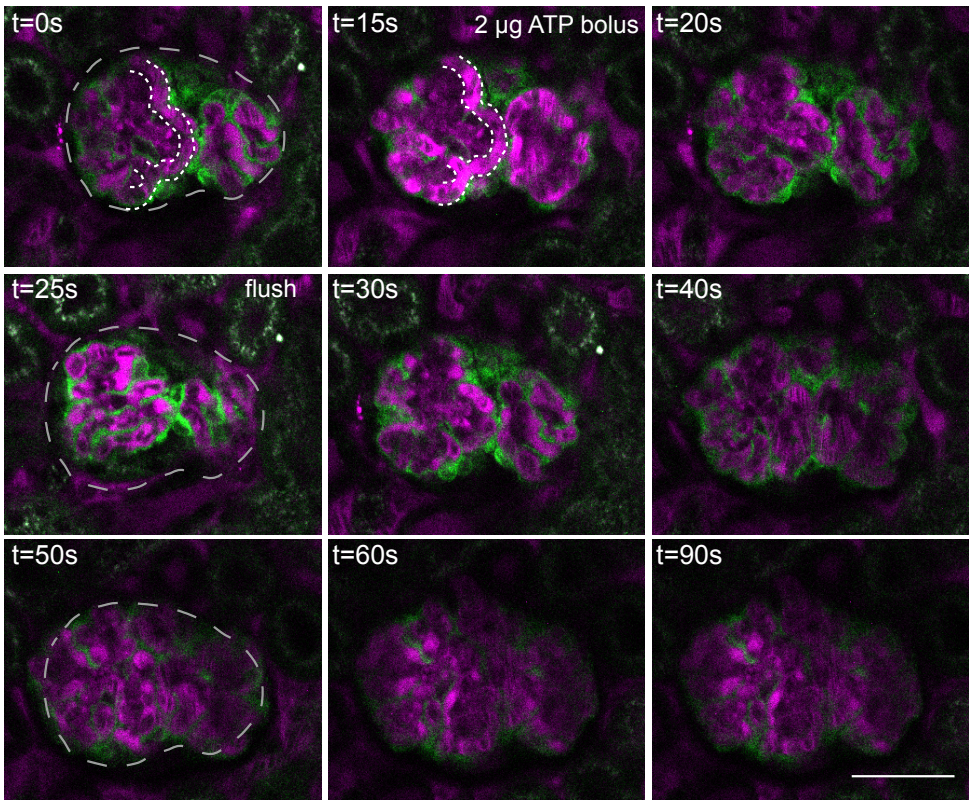

Figure 32: Bolus injection of ATP does not result in a calcium signal in podocytes but has a strong effects on blood flow. Representative images of a glomerulus of a healthy animal injected with ATP. A bolus of ATP (2 μg) was injected just before t=15 s. The dashed white line in the first image (t=0 s) and the second (t=15 s) mark the same capillary regions. The grey dashed line in t=0 s, t=25 s and t=50 s represent the size of the glomerulus at t=0 s and its changes during the course of imaging. At t=25 s the line was flushed, resulting in a second application of ATP. Scale bar: 40 μm.

Considering the fact that ATP is rapidly degraded or consumed we used a non-hydrolyzed ATP analogue called ATP-γ-S. We administered doses between 1 and 2 μg with no effect on calcium levels in podocytes but with comparable effects on the animal's physiology (not shown). Furthermore, repetitive bolus injections of ATP or ATP-γ-S resulted in complete loss of blood flow in the entire kidney and

ultimately in death of the animal. Table 16 gives and overview of the number of experiments performed using ATP or ATP-γ-S and the respective doses. In total a number of 30 mice and 56 individual glomeruli were imaged. Taken together ATP, or its non-hydrolyzable analogue were not able to induce calcium transients in podocytes while lower doses of 0.5 μg and 1 μg of ATP was sufficient to induce calcium signaling in endothelial and proximal tubular cells.

Table 16: Overview of ATP experiments *in vivo*

Substance	Dose	Number of glomeruli
ATP	1μg	6
ATP	2μg	56
ATP	>2μg	9
ATPγ–S	2μg	11

6.2.9 ATP mediates calcium transients in isolated glomeruli

Considering the fact that we were not able to induce calcium signaling in podocytes *in vivo* by injecting ATP we decided to isolate glomeruli from mouse kidneys and stimulate these with ATP. As discussed before, we could not use our transgenic mice expressing GCaMP3 selectively in podocytes (Pod:cre GCaMP3$^{fl/fl}$) due to instability of the calcium indicator. Therefore we isolated glomeruli from C57Bl6 mice and loaded them with Fluo4 for calcium imaging. Similar experiments using isolated glomeruli from rat have already been performed by Ilatovskaya et al. (2013) [73]. Representative images of a glomerulus are shown in Figure 33a. When we superfused the isolated glomeruli with solutions containing either 50, 100 or 200 μM ATP we were able to induce a strong and transient calcium signal as shown by the relative fluorescence increase of Fluo4 over time, thereby 200 μM ATP induced the most pronounced signal (Figure 33 b).

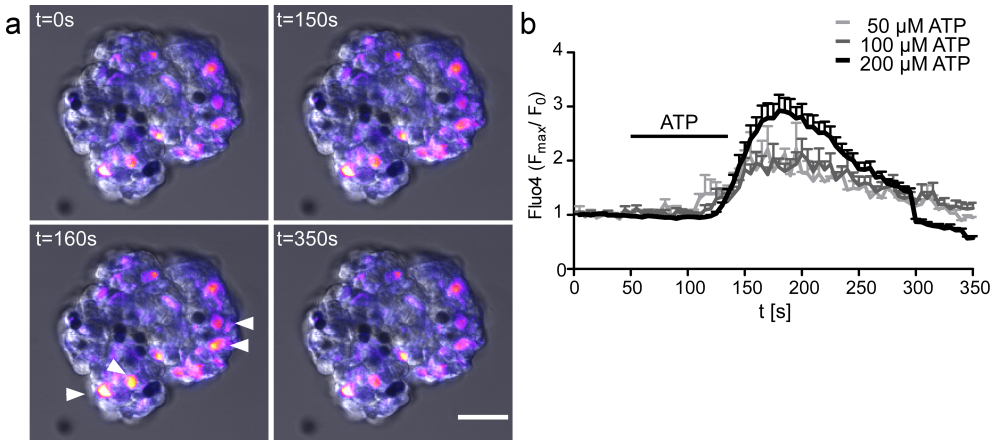

Figure 33: ATP induces dose dependent calcium transients in isolated glomeruli. a, Representative images of a glomerulus loaded with Fluo4 (5 μM) and stimulated with 200 μM ATP using a perfusion system (1 ml/min). Arrow heads indicate cell showing increased calcium levels. The green channel is shown in false color code. **b**, Relative fluorescence changes (F_{Max}/ F_0) over time for 50 μM ATP (n=2), 100 μM ATP (n=13) and 200 μM ATP (n=48). Black bar indicates the time period of ATP infusion. n=number of cells analyzed, mean=SEM, scale bar: 20 μm.

Taken together, we were able to show a strong and reproducible dose dependent calcium signals upon stimulation with ATP in cells which we identified as podocytes by their structure and position in the *ex vivo* setting.

7 Discussion

7.1 AngII signaling and calcium are involved in podocyte injury

In the present study we set out to understand the role of Angiotensin II (AngII) mediated calcium signaling in podocytes. AngII is a small peptide hormone playing an important role in electrolyte homeostasis and blood pressure regulation. Measurements of physiological AngII concentrations has revealed an increase in AngII concentration (340 fmol/g) as compared to plasma concentrations (50 fmol/g). However, its concentration in the glomerulus is not known, as studies mainly focus on intratubular fluid concentrations and local AngII metabolism can alters its concentration rapidly [101]. In the kidney, AngII regulates glomerular perfusion pressure on a single nephron level. Excessive activation of the Renin-Angiotensin-Aldosterone-Sytem (RAAS) is associated with disease and numerous studies using cell culture models, isolated glomeruli and *in vivo* models using transgenic animals have shown a connection between over-activation of this pathway and disease initiation and progression. Furthermore, studies in patients show beneficial effects of RAAS inhibition beyond blood pressure control for renal outcome in patients with proteinuria [102, 103]. AngII receptors (ATRs) belong to the family of G-protein coupled receptors (GPCRs) which are able to activate transient receptor potential cation channel (Trpc6). Activation of Trpc6 in a dysregulated manner has been shown to cause kidney disease in humans [16]. We wanted to understand the connection between AngII signaling and elevated calcium levels in the *in vivo* setting. To this end we applied intravital imaging of healthy and diseased animals expressing the calcium indicator GCaMP3 selectively in podocytes.

7.1.1 Podocytes maintain low intracellular calcium levels

At baseline, podocytes did not show any spontaneous calcium signals but a stable GCaMP3 fluorescence. Furthermore, we measured the GCaMP3 fluorescence over time and did not oberserve effects of bleaching in our imaging settings. The low baseline fluorescence observed in podocytes *in vivo* has previously been described [75]. The importance of low intracellular calcium levels is even more emphasized by the observation that, AngII mediated calcium transients in healthy and injured podocytes drop back to baseline within a few seconds represented by a fast decrease in GCaMP3 fluorescence. The same holds true for a laser-induced calcium wave. Therefore it can be concluded that regulation of intracellular calcium levels is crucial for podocytes. Nevertheless, one should keep in mind that this animal model includes overexpression of a calmodulin based calcium sensor. Calmodulin is an ubiquitously expressed calcium binding molecule and therefore it can not be excluded that its expression may interfere with calcium and calmodulin signaling [104]. Nevertheless, GCaMP3 has been successfully used in previous studies to monitor action potentials in mouse brain thereby proving its sensitivity and fast signaling [105].

7.1.2 Healthy podocytes show a low responsiveness to AngII

Using *in vivo* stimulation with a dose of 100 ng/g/min AngII we could induce calcium signaling in a minor fraction of healthy podocytes. The observed low responsiveness of healthy podocytes to AngII stimulation is in contrast to published data using podocyte cell culture, isolated glomeruli loaded with calcium sensitive dyes and patch-clamp experiments. In these experiments robust calcium transients could be observed and depolarization of podocyte cell membrane upon AngII stimulation was measured [93, 56, 95, 57]. Our effort to use isolated glomeruli of mice expressing GCaMP3 failed since the fluorescence signal was completely

diminished after isolation. Loading of isolated glomeruli with Fluo4 was successful but we could not observe calcium signals in a reproducible manner as published by others [59]. Furthermore, after isolation a lot of cells per glomerulus stained positive with propidium iodide (PI), indicating a high degree of cell death. In contrast, in healthy control mice no uptake of PI could be observed in any glomerular cell during *in vivo* imaging. While, proximal tubular cells showed a time-dependent unspecific uptake within 30 to 60 minutes.

Based on our observations using isolated glomeruli and our results we obtained from intravital microscopy of AngII-mediated calcium transients in podocytes we concluded that *ex vivo* and *in vitro* models have severe shortcomings in modeling the *in vivo* situation. On the one hand, glomerular isolation protocols result in damage to the glomerular integrity as indicated by PI positive nuclei. In our approach we used a short collagenase digestion and gentle purification and minimized mechanical strain on the tissue. In contrast, isolation of glomeruli from rats uses sequential sieving steps thereby applying more physical pressure on the tissue which likely causes more damage.

On the other hand, cell culture models cannot recapitulate the complex architecture of a glomerulus consisting of different cell types and its subjection to capillary and filtration pressure. The aforementioned limitations of *ex vivo* models might explain the contradiction of their results to the *in vivo* situation of the low responsiveness of podocytes to AngII stimulation. Minimal changes in cell membrane depolarization could be missed by our approach. Additionally, use of isolated glomeruli represents a state of damage to the glomeruli, which we do not observe in healthy animals.

7.1.3 Podocyte injury increases AngII-mediated calcium signals *in vivo*

To further elucidate the role of AngII-mediated calcium transients in disease we applied two different disease models both based on podocyte injury. Considering the fact that we need relatively young mice of age (3 to 4 weeks) for intravital imaging of glomeruli we chose an acute chemically induced podocyte injury model and a genetic model with an early onset. Chemically induced podocyte injury was achieved by injection of 25 mg/kg of Adriamycin (ADR) in Pod:Cre GCaMP3 mice in C57Bl6 background. Adriamycin is a chemotherapeutic agent and is a well-established model for focal segmental glomerulusclerosis (FSGS) in mice [106]. In this model, a single dose of the agent is sufficient to induce weight loss (not shown), proteinuria and histological abnormalities in 4 week old mice within five days after injection. As a second disease model we chose a genetic model, where the slit diaphgram component podocin is specifically deleted in podocytes. Mice with a homozygous deletion of podocin developed severe proteinuria and glomerulusclerosis by the age of 4 weeks [107].

We subjected mice of both models to *in vivo* imaging and AngII stimulation to monitor calcium levels. Without intervention injured podocytes did not show any spontaneous calcium signals, however in both models, but predominantly in the podocin knockout model (Pod^{pKO}) single podocytes showed an increase GCaMP3 fluorescence compared to neighboring cells. This could be reflective of injury as cells could have lost their ability to maintain a stable low intracellular calcium concentration as observed during laser-induced injury at the site of heat damage [75].

When ADR or Pod^{pKO} animals were subjected to acute AngII infusion we could measure an ∼2- to 3-fold increase in the AngII responsiveness in both models represented by the number of glomeruli showing a calcium signal in at least one podocyte. From this we concluded that injury rendered podocytes sensitive to

AngII-mediated calcium signals. Since podocyte specific overexpression of AngII type 1 receptor (AT1R) has been shown to be sufficient to induce proteinuria and FSGS lesions [108] we hypothesize that AngII signaling could aggravate a already present podocyte injury. This in turn could explain why patients suffering from proteinuric kidney disease profit the most from RAAS inhibition in regard to kidney function [102, 103].

7.1.4 Heterozygous loss of podocin effects AngII signaling in podocytes

As a control for Pod^{pKO} animals we used mice with loss of one allele of podocin (Pod^{pHet}) in our experimental set up. These mice were healthy and did not show any proteinuria or histological changes in kidney biopsies. Interestingly, Pod^{pHet} mice also showed an increased responsiveness to AngII compared to healthy control animals. Currently we can only hypothesize that loss of one podocin allele rendered cells more susceptible to AngII than control mice. Therefore, podocin might have gene-dose dependent functions. Since podocin is highly expressed in podocytes, loss of one allele might reduce the amount of protein at the slit diaphragm to a degree which makes it susceptible to AngII-mediated signaling. To answer this question Pod^{pHet} mice could be subjected to stress models such as Adriamycin, continuous low dose AngII infusion with osmotic mini pumps or a hypertension model.

7.1.5 Loss of Trpc6 does not block AngII-mediated calcium transients

The cation channel Trpc6 has been implicated to play a crucial role in podocyte calcium handling and there is experimental evidence that signaling via AngII receptors is able to acitivate Trpc6 channels [109, 57]. Therefore, we used a Trpc6 whole body knock out mouse model ($Trpc6^{KO}$) to verify if we lose AngII-mediated calcium signaling [82]. Our experiments show that AngII can still induce calcium

signaling in Trpc6 deficient podocytes in healthy and disease state, but to a lesser extent than in control mice. Given that we use a whole-body knock out mouse model it might very well be that other cation channels compensate for the loss of Trpc6, one candidate could be Trpc5. Trpc5 belongs to same family of cation channels even though its role as a protective or harmful agent in context of kidney injury remains a matter of debate [110, 111]. To verify if and which other calcium conductive channels are involved in AngII calcium signaling one could use channel specific inhibitors or a genetic approach by deleting Trpc5.

7.1.6 A common mechanism of podocytes in handling increased calcium levels

Further analysis of AngII-mediated calcium signaling showed that signal duration on a single podocyte level was the same in all groups treated with AngII and there was no difference between healthy and injured cells. Additionally we compared the relative fluorescence increases (F_{max}/ F_0) between all groups and could not find a significant difference. From this we concluded that the observed signal is an all-or-nothing response. This could be based on intrinsic molecular properties of the calcium indicator GCaMP3 which define its maximum intensity [105]. Molecular aspects also include the route of calcium entry into the cell, like activation of cell membrane cation channels by G-protein couples receptors (GPCRs) and calcium release from the endoplasmatic reticulum (ER). AngII receptors belong to the class of GPCRs. Activation of GPCRs results in generation of diacylglyerol (DAG) and inositol-1,4,5-triphosphate (IP_3) which can activate cation channels by DAG in the cell membrane and IP_3 regulated calcium channels on the ER membrane. Opening of any calcium channel will result in calcium entry along its concentration gradient. We hypothesize that during this signaling cascade a threshold is exceeded, opening further cation channels and thereby triggering the maximum fluorescence of GCaMP3. Small local elevations of calcium levels which do not activate release of

calcium from the ER might therefore not be represented in our measurements, since GCaMP3 is expressed in the cytosol and not specifically targeted to the cytoplasmic membrane. Visualization of calcium signaling at the membrane, especially in the foot processes, could be achieved by targeting GCaMP3 to the membrane.

7.1.7 Direct or indirect effects of AngII on calcium levels in podocytes

For podocytes it has been proposed that mechanical strain effects intracellular calcium levels [33, 79]. Considering the fact that the physiological function of AngII is regulation of glomerular perfusion pressure by inducing vasoconstriction of the efferent arteriole and subsequent swelling of the capillary loops can be observed, therefore AngII signaling involves a mechanical stimulus. We cannot exclude this mechanical component as an indirect effect on calcium levels in podocytes from our current hypothesis. However, using Angiotensin II receptor (ATRs) inhibitors we could show, that Angiotensin II type 1 receptor (AT1R) is responsible for the observed calcium transients in podocytes upon AngII stimulation. Application of Losartan completely inhibited AngII-mediated calcium signal. Losartan is a specific AT1 receptor blocker which is widely used in clinics to lower blood pressure and manage kidney disease [102]. In contrast, use of PD123319 which is a specific AT2 receptor blocker, did not show any consistent effect. These observations go well in hand with published data [93, 95, 96]. Since our model only allows global inhibition of ATRs we cannot distinguish between direct effects of AngII on podocytes or other cell types. In order to solve this question we would need to use a genetic approach by using cell specific AT1R knockout animals. Thereby we could delete AT1R specifically from podocytes and endothelial cells and demonstrate cell-specific effects which are responsible for the observed glomerular heamodynamic effects. Podocyte specific AT1R knockout animals should still show a vasoactive response to AngII, which should be lost in endothelial specific knockout. Thereby we could

distinguish between indirect heamodynamic and direct non-heamodynamic effects. Still, one should keep in mind that mice harbour two subtypes of the AT1 receptor encoded by two different genes [42]. Current research is not clear on which subtype is more relevant in the context of podocyte biology. Since there are no subtype specific inhibitors available, a genetic approach with deletion of either AT_{1A} or AT_{1B} is required to understand which receptor subtype is responsible for the observed calcium transients in podocytes.

7.1.8 Proteomic analysis identifies calcium related proteins upregulated in ADR

Finally, we conducted proteomic analysis of ADR treated glomeruli to understand changes in the proteome associated with the observed increased responsiveness to AngII. Unfortunately, we were not able to identify any AngII receptor or the Trpc6 channel in our dataset due to their low abundance abundance as previously published [112]. However, we could identify calcium-associated proteins upregulated in ADR treated groups compared to control, their function in AngII mediated calcium signaling is not understood. Furthermore, the data shows a significant down regulation of podocyte specific proteins such as podocin and neprhin indicating that the disease model is functional and that the slit diaphragm structure is destabilized during Adriamycin nephropathy. Nevertheless, one should keep in mind that our proteomics data was generated using whole glom lysates. Therefore, measurement of significantly upregulated proteins could be due to other cell types within the glomerulus. Thus, proteomic analysis of single podocytes after ADR would provide an even stronger data set. Additionally, validation of identified proteins and their localization within the glomerulus could be verified by performing immune fluorescence stainings.

The protein with the highest abundance found in ADR treated compared to control glomeruli was the gluthathione S-transerase omega 1 (Gsto1). Gsto1 has

been associated with stress responses, such as reactive oxygen species, and drug metabolism. Hence, the observed upregulation is mostly likely directly induced by Adriamycin treatment [113].

7.2 Podocytes show no response to ATP stimulation *in vivo*

In the present study we have used three different mouse models expressing GCaMP3 in either endothelial cells, proximal tubular cells or podocytes to delineate differences in adenosine-triphosphate (ATP) mediated calcium transients in different cell types of the nephron. We could show that endothelial cells and proximal tubular cells show a strong and immediate response to stimulation with ATP, while this response is absent in podocytes *in vivo* with the same dose.

7.2.1 Podocytes show a dose-dependent ATP response *ex vivo*

For podocyte cell culture it has been shown that podoctyes can release ATP upon mechanical strain which could then act in an autocrine and paracrine manner and activate purinergic receptors resulting in cation transients. Local increases of cytosolic calcium levels effects the elaborate cytoskeleton of podocytes [35]. The interplay between calcium and actin organization has been shown to be a common mechanism in many different cell types [24]. Since calcium channels are found in foot processes of podocytes, influx of calcium could directly alter the cytoskeleton which is crucial for podocyte structure and function. Thereby, ATP signaling could have a direct detrimental effect on filtration barrier function, if circulating ATP which is filtered reaches podocytes.

Patch-clamp experiments on podocytes of isolated glomeruli and use of podocyte cell culture have shown that podocytes are depolarized by ATP and increases in intracellular calcium levels can be observed [55, 74, 66]. We and others could show, using isolated glomeruli loaded with calcium sensitive dyes, that podocytes

show a strong calcium response to ATP *ex vivo*. In our experiments, we identified podocytes loaded with Fluo4 based on their localization within the glomerular structure and morphology as we could not use glomeruli isolated from our transgenic mouse model due to unstable fluorescence of GCaMP3 after isolation. In our *ex vivo* experiments we applied different ATP doses ranging from 50 to 200 μM ATP and measured transient calcium signals in a dose-dependent manner. Our findings go well in hand with published data using glomeruli isolated from rats and stimulated with 10 μM ATP [73]. Data obtained from cultured endothelial cells indicate that 20 μM ATP is sufficient to induce calcium transients [114].

7.2.2 Laser-induced injury and calcium signaling in podocytes involves ATP as a messenger of injury

In vivo imaging studies in mice indicate that ATP signaling is involved in propagation of a calcium wave upon laser-induced podocyte injury [75], which spreads between neighboring podo-cytes. We could recapitulate these findings by inducing the same podocyte injury. Furthermore, as published, we could interfere with signal transmission by using the unspecific ATP receptor inhibitor suramin. Application of suramin delayed the signal propagation, similar to what has been described [75] but did not block it completely. Therefore, unknown factors are additionally released into Bowman's space upon laser-induced injury and play a role in the observed calcium wave together with ATP. To address, which additionally factors play a role in propagation of the calcium wave one could use different receptor inhibitors to block other purinergic receptors specific to adenosine-diphosphate (ADP) for example. Even though the model of laser-induced injury is a rather artifical model for podocyte injury, but underlines the role of ATP signaling in podocyte biology to spread a damage signal *in vivo*.

7.2.3 Podocytes do not show a calcium signal upon ATP stimulation *in vivo*

In order to understand the role of ATP-mediated calcium transients in podocyte biology we injected different doses of ATP into mice expressing GCaMP3 in podocytes and monitored calcium transients. To this end, we used ATP doses between 1 to 10 μg of ATP but could not detect any ATP-mediated calcium transients in podocytes. Since ATP is very quickly degraded by so-called ectonucleosidases or consumed by cells we wanted to control if the injected doses actually reached the glomeruli in the kidney. Therefore, we generated mice with expression of GCaMP3 under the endothelial cell specific promoter Tie2. Endothelial cells have been shown to react to ATP with an intracellular calcium transient [99]. Upon stimulation of Tie2: GCaMP3 mice with ATP (0.5 μg) we could observe a pronounced and fast calcium signal in all glomerular endothelial cells including endothelial cells lining the afferent arteriole. Furthermore, we could show that injection of higher doses of ATP (2 μg) resulted in a calcium signal in post-glomerular endothelial cells. We concluded, that the injected dose is sufficient to potentially reach glomeruli.

Since the glomerular basement membrane (GBM) is located between a layer of endothelial cells and podocytes we wanted to confirm whether the injected ATP is actually filtered and is therefore present in the Bowman's space where it could activate receptors on podocytes cell membrane. Therefore, we generated a transgenic mouse line expressing GCaMP3 in proximal tubulur cells (Pax:cre). We could observe that injection of 1 μg ATP was sufficient to induce a calcium signal in proximal tubular cells indicating filtration of ATP. A similar experiment has been conducted in transgenic rats expressing GCaMP2 in proximal tubular cells [100]. Still, one should keep in mind that proximal tubular cells are also connected to pertibular capillaries on their basolateral site where they express ATP receptors as well as on the luminal site [98, 115, 116]. Therefore, the observed calcium transients in proximal tubular cells might originate from vascular ATP receptor populations.

To this point, we could demonstrate that our method of ATP injection *in vivo* is functional as we could induce calcium transients in endothelial cells of glomeruli and in cells of the proximal tubulus but not in podocytes.

7.2.4 Differences between *in vivo* and *ex vivo* results

Data acquired from *in vivo* experiments applying laser-induced injury as a model of podocyte injury clearly point towards a role of ATP in podocyte biology. Results obtained using isolated glomeruli and podocyte cell culture data additionally emphasize its relevance. In our *ex vivo* experiments we applied doses between 50 and 200 μM ATP to induce calcium transients. While, in the *in vivo* system we injected between 0.5 and in most cases 2 μg of ATP. A dose of 2 μg ATP would calculate to $\sim$ 3.6 μM when diluted in $\sim$ 1 ml of blood volume of a 3-4 week old mouse (6-8 % of a mouse body weight). Since we injected ATP as a bolus in a volume of 30 μl we injected ATP at a molarity of $\sim$ 120 μM. As 20 % of the heart injection volume directly goes to the kidney we would expect that $\sim$ around 25 μM ATP would directly arrive in the kidney. This dose is less than the minimal dose of 50 μM we used on isolated glomeruli. And in contrast to the *ex vivo* situation, blood and endothelial cells will consume ATP partially, therefore podocytes will encounter only a fraction of ATP which was injected. We therefore hypothesize, that we were unable to reach a sufficiently high concentration at the podocyte cell membrane and therefore could not recapitulate results from our experiments with isolated glomeruli. Since, ATP is a vasoactive compound and has a strong effect on the mouse's physiology we could not increase the dose to a sufficient degree without severely affecting the blood pressure of the animal in the process. Furthermore, we conclude that podocytes are less sensitive to ATP signaling compared to endothelial cells and proximal tubular cells since we were able to induce strong calcium signals while using less ATP. In order to achieve a higher concentration of ATP at the

podocyte cell membrane we could use a different route of injection to deliver a higher dose directly to the kidney. Furthermore, it would be of interest whether podocytes show an increased sensitivity to ATP after an initial injury had occurred, for instance after induction of Adriamycin nephropathy.

7.3 Concluding and perspectives

The focus of this thesis was to understand calcium signaling in podocytes using 2-photon intravital microscopy. Our approach puts experimental data obtained from podocyte cell culture model and experiments with isolated glomeruli compared to the *in vivo* situation into question. We focused on AngII- and ATP-mediated calcium transients in podocytes.

Our results suggest that podocytes maintain low intracellular calcium levels during a healthy state and dysregulation occurs during disease. High dose of AngII elicted a calcium signal in only a minor fraction of glomeruli and podocytes in healthy animals but significantly increased during disease. Our data might answer why patients suffering from kidney disease presenting with proteinuria show the biggest benefit from treatment with RAAS inhibitors beyond blood pressure control [102]. Therefore, inhibition of RAAS might protect podocytes from direct effects of AngII on calcium signaling in and thereby maintain its integrity. For ATP stimulation we found that podocytes are less sensitive to ATP than endothelial and proximal tubular cells. We therefore conclude, that a high local concentration at the podocyte cell membrane is necessary to induce ATP-mediated calcium signaling.

In summary, the observed low responsiveness to AngII and ATP suggests that maintenance of low intracellular calcium levels is crucial for podocytes.

8 Publications

8.1 Publications in academic journals

1. Binz J, Jüngst C, Rinschen MM, Koehler S, Zentis P, Schauss A, Schermer, B Benzing, T Hackl M.J.: Injured podocytes are sensitized to Angiotensin II induced calcium signaling. *In Revision at the Journal of the American Society of Nephrology (JASN).* Submission date: 4th February 2019, Manuscript ID: JASN-2019-02-0109.R1

2. Hohne M, Frese CK, Grahammer F, Dafinger C, Ciarimboli G, Butt L, Binz J, Hackl MJ, Rahmatollahi M, Kann M, Schneider S, Altintas MM, Schermer B, Reinheckel T, Gobel H, Reiser J, Huber TB, Kramann R, Seeger-Nukpezah T, Liebau MC, Beck BB, Benzing T, Beyer A, and Rinschen MM (2018) Single nephron proteomes connect morphology and function in proteinuric kidney disease. Kidney Int, 93(6):1308-1319.

3. Rinschen MM, Hoppe AK, Grahammer F, Kann M, Volker LA, Schurek EM, Binz J, Hohne M, Demir F, Malisic M, Huber TB, Kurschat C, Kizhakkedathu JN, Schermer B, Huesgen PF, and Benzing T (2017) N-Degradomic Analysis Reveals a Proteolytic Network Processing the Podocyte Cytoskeleton. JASN, 28(19): 2867-2878.

4. Koehler S, Brähler S, Kuczkowski A, Binz J, Hackl MJ, Hagmann H, Höhne M, Vogt MC, Wunderlich CM, Wunderlich FT, Schweda F, Schermer B, Benzing T, Brinkkoetter PT (2016) Single and Transient Ca^{2+} Peaks in Podocytes do not induce Changes in Glomerular Filtration and Perfusion. Sci Rep, 2016 Oct 19;6:35400.

8.2 Presentations on international academic conferences

1. Binz J, Jüngst C, Schermer B, Benzing T, Hackl MJ: Responsiveness to Angiotensin II is increased in Diseased Podocytes. International Podocyte Conference 2018. *(poster presentation)*

2. Binz J, Jüngst C, Zentis P, Schauss A, Schermer B, Benzing T, Hackl MJ: Intravital Imaging of the Kidney – Modelling Calcium Signaling. Day of Mouse Intravital Microscopy 2018. *(poster presentation)*

3. Binz J, Khalili H, Schermer B, Benzing T, Hackl MJ: Acute Kidney Slices as a tool to dissect Calcium Signals in Podocytes. American Society of Nephrology 2017. *(poster presentation)*

4. Binz J, Schermer B, Benzing T, Hackl MJ: Eine Glomeruläre Schädigung induziert Calciumsignale in proximalen Tubuluszellen. Deutsche Gesellschaft für Nephrologie 2016. *(poster presentation)*

5. Binz J, Hackl MJ, Schermer B, Benzing T: Glomeruläre Endothelzellen bilden ein funktionelles Synzytium für Calciumsignale nach Verletzung – Eine Multiphotonen *in-vivo* Studie. Deutsche Gesellschaft für Nephrologie 2015. *(poster presentation)*

6. Binz J, Hackl MJ, Schermer B, Benzing T: Glomerular endothelial cells form a functional syncytium for calcium signals upon injury – A multiphoton *in-vivo*. Annual Meeting of the American Society of Nephrology 2014. *(oral presentation)*

9 References

[1] Karen A Munger, David A Maddox, Barry M Brenner, and Curtis K Kost. *The Renal Circulations and Glomerular Ultrafiltration*. Elsevier Inc., tenth edit edition, 2017.

[2] Jan Willem Leeuwis, Tri Q Nguyen, Amélie Dendooven, Robbert J Kok, and Roel Goldschmeding. Targeting podocyte-associated diseases. *Advanced drug delivery reviews*, 62(14):1325–36, nov 2010.

[3] Hermann Pavenstädt, Wilhelm Kriz, and Matthias Kretzler. Cell biology of the glomerular podocyte. *Physiological reviews*, 83:253–307, 2003.

[4] C Schell, N Wanner, and T B Huber. Glomerular development–Shaping the multi-cellular filtration unit. *Seminars in cell & developmental biology*, 36:39–49, dec 2014.

[5] W Kriz. Progressive renal failure - inability of podocytes to replicate and the consequences for development of glomerulosclerosis. *Nephrology Dialysis Transplantation*, 11(9):1738–1742, 1996.

[6] Anna Greka and Peter Mundel. Cell Biology and Pathology of Podocytes. *Annual Review of Physiology*, 74:299–323, 2013.

[7] Florian Grahammer, Christoph Wigge, Christoph Schell, Oliver Kretz, Jaakko Patrakka, Simon Schneider, Martin Klose, Sebastian J. Arnold, Anja Habermann, Ricarda Bräuniger, Markus M. Rinschen, Linus Völker, Andreas Bregenzer, Dennis Rubbenstroth, Melanie Boerries, Dontscho Kerjaschki, Jeffrey H. Miner, Gerd Walz, Thomas Benzing, Alessia Fornoni, Achilleas S. Frangakis, and Tobias B. Huber. A flexible, multilayered protein scaffold

maintains the slit in between glomerular podocytes. *JCI Insight*, 1(9), jun 2016.

[8] Marjo Kestilä, Ulla Lenkkeri, Minna Ma, Jane Lamerdin, Paula Mccready, Heli Putaala, Vesa Ruotsalainen, Takako Morita, Marja Nissinen, Riitta Herva, Clifford E Kashtan, Leena Peltonen, Christer Holmberg, Anne Olsen, and Karl Tryggvason. Positionally cloned gene for novel glomerular protein-nephrin-is mutated in congenital nephrotic syndrome. *Molecular Cell*, 1:575–582, 1998.

[9] H Putaala, R Soininen, P Kilpeläinen, J Wartiovaara, and K Tryggvason. The murine nephrin gene is specifically expressed in kidney, brain and pancreas: inactivation of the gene leads to massive proteinuria and neonatal death. *Human molecular genetics*, 10(1):1–8, jan 2001.

[10] Lorenz Sellin, Tobias B. Huber, Peter Gerke, Ivo Quack, Hermann Pavenstädt, and Gerd Walz. NEPH1 defines a novel family of podocin interacting proteins. *The FASEB Journal*, 17(1):115–117, jan 2003.

[11] Jeong H. Kim, Hui Wu, Gopa Green, Cheryl A Winkler, Jeffrey B Kopp, Jeffrey H Miner, Emil R Unanue, and Andrey S. Shawl. CD2-associated protein haploinsufficiency is linked to glomerular disease susceptibility. *Science*, 300(5623):1298–1300, may 2003.

[12] Tobias B Huber, Björn Hartleben, Jeong Kim, Miriam Schmidts, Bernhard Schermer, Alexander Keil, Lotti Egger, Rachel L Lecha, Christoph Borner, Hermann Pavenstädt, Andrey S Shaw, Gerd Walz, and Thomas Benzing. Nephrin and CD2AP associate with phosphoinositide 3-OH kinase and stimulate AKT-dependent signaling. *Molecular and cellular biology*, 23(14):4917–28, 2003.

[13] Claire E. Martin and Nina Jones. Nephrin signaling in the podocyte: An updated view of signal regulation at the slit diaphragm and beyond. *Frontiers in Endocrinology*, 9(JUN):1–12, 2018.

[14] Tobias B Huber and Thomas Benzing. The slit diaphragm: a signaling platform to regulate podocyte function. *Current opinion in nephrology and hypertension*, 14(3):211–6, may 2005.

[15] Joshua M. Kaplan, Sung Han Kim, Kathryn N. North, Helmut Rennke, Lori Ann Correia, Hui Qi Tong, Beverly J. Mathis, José Carlos Rodríguez-Pérez, Philip G. Allen, Alan H. Beggs, and Martin R. Pollak. Mutations in ACTN4, encoding α-actinin-4, cause familial focal segmental glomerulosclerosis. *Nature Genetics*, 24(3):251–256, 2000.

[16] Michelle P Winn, Peter J Conlon, Kelvin L Lynn, Merry Kay Farrington, Tony Creazzo, April F Hawkins, Nikki Daskalakis, Shu Ying Kwan, Seth Ebersviller, James L Burchette, Margaret A Pericak-Vance, David N Howell, Jeffery M Vance, and Paul B Rosenberg. A mutation in the TRPC6 cation channel causes familial focal segmental glomerulosclerosis. *Science*, 308(5729):1801–1804, jun 2005.

[17] Jochen Reiser, Krishna R Polu, Clemens C Möller, Peter Kenlan, Mehmet M Altintas, Changli Wei, Christian Faul, Stephanie Herbert, Ivan Villegas, Carmen Avila-casado, Mary Mcgee, Hikaru Sugimoto, Dennis Brown, Raghu Kalluri, Peter Mundel, L Paula, David E Clapham, Martin R Pollak, Renal Unit, and Riñon-fresenius Medical Care. TRPC6 is a glomerular diaphram-associated channel required for normal renal f1unction. *Nature Genetics*, 37(7):739–744, 2006.

[18] G. Mollet, Julien Ratelade, Olivia Boyer, Andrea Onetti Muda, Ludivine Morisset, Tiphaine Aguirre Lavin, David Kitzis, Margaret J. Dallman, Laurence Bugeon, Norbert Hubner, M.-C. Gubler, Corinne Antignac, and Ernie L. Esquivel. Podocin Inactivation in Mature Kidneys Causes Focal Segmental Glomerulosclerosis and Nephrotic Syndrome. *Journal of the American Society of Nephrology*, 20(10):2181–2189, oct 2009.

[19] S J Shankland. The podocyte's response to injury: Role in proteinuria and glomerulosclerosis. *Kidney International*, 69(12):2131–2147, 2006.

[20] Angela C. Webster, Evi V. Nagler, Rachael L. Morton, and Philip Masson. Chronic Kidney Disease. *The Lancet*, 389(10075):1238–1252, 2017.

[21] Avi Z. Rosenberg and Jeffrey B. Kopp. Focal segmental glomerulosclerosis. *Clinical Journal of the American Society of Nephrology*, 12(3):502–517, 2017.

[22] David E Clapham. Calcium signaling. *Celll*, 131:1047–1058, 2007.

[23] Ernesto Carafoli and Joachim Krebs. Why calcium? How calcium became the best communicator. *Journal of Biological Chemistry*, 291(40):20849–20857, 2016.

[24] Pauline Wales, Christian E. Schuberth, Roland Aufschnaiter, Johannes Fels, Ireth García-Aguilar, Annette Janning, Christopher P. Dlugos, Marco Schäfer-Herte, Christoph Klingner, Mike Wälte, Julian Kuhlmann, Ekaterina Menis, Laura Hockaday Kang, Kerstin C. Maier, Wenya Hou, Antonella Russo, Henry N. Higgs, Hermann Pavenstädt, Thomas Vogl, Johannes Roth, Britta Qualmann, Michael M. Kessels, Dietmar E. Martin, Bela Mulder, and Roland Wedlich-Söldner. Calcium-mediated actin reset (CaAR) mediates acute cell adaptations. *eLife*, 5(DECEMBER2016), 2016.

[25] Paola Krall, Cesar P. Canales, Pamela Kairath, Paulina Carmona-Mora, Jessica Molina, J. Daniel Carpio, Phillip Ruiz, Sergio A. Mezzano, Jing Li, Changli Wei, Jochen Reiser, Juan I. Young, and Katherina Walz. Podocyte-specific overexpression of wild type or mutant Trpc6 in mice is sufficient to cause glomerular disease. *PLoS ONE*, 5(9):1–11, 2010.

[26] Marc Riehle, Anja K. Büscher, Björn-Oliver Gohlke, Mario Kaßmann, Maria Kolatsi-Joannou, Jan H. Bräsen, Mato Nagel, Jan U. Becker, Paul Winyard, Peter F. Hoyer, Robert Preissner, Dietmar Krautwurst, Maik Gollasch, Stefanie Weber, and Christian Harteneck. TRPC6 G757D Loss-of-Function Mutation Associates with FSGS . *Journal of the American Society of Nephrology*, 27(9):2771–2783, 2016.

[27] Daria V. Ilatovskaya and Alexander Staruschenko. TRPC6 channel as an emerging determinant of the podocyte injury susceptibility in kidney diseases. *American Journal of Physiology - Renal Physiology*, 309(5):F393–F397, 2015.

[28] Caleigh M. Azumaya, Francisco Sierra-Valdez, Julio F. Cordero-Morales, and Terunaga Nakagawa. Cryo-EM structure of the cytoplasmic domain of murine transient receptor potential cation channel subfamily C member 6 (TRPC6). *Journal of Biological Chemistry*, 293(26):10381–10391, 2018.

[29] Nirvan Mukerji, Tirupapuliyur V Damodaran, and Michelle P Winn. TRPC6 and FSGS: the latest TRP channelopathy. *Biochimica et biophysica acta*, 1772(8):859–68, aug 2007.

[30] Stuart E. Dryer and Jochen Reiser. TRPC6 channels and their binding partners in podocytes: role in glomerular filtration and pathophysiology. *American Journal of Physiology-Renal Physiology*, 299(4):F689–F701, 2010.

[31] Murali Prakriya and Richard S Lewis. Store-Operated Calcium Channels. *Physiology Reviews*, 24(4):1383–1436, 2013.

[32] David E Clapham, Loren W Runnels, and Carsten Strübing. The Trp ion channel family. *Nature Reviews Neuroscience*, 2(June):387–396, 2001.

[33] Tobias B Huber, Bernhard Schermer, Roman Ulrich Müller, Martin Höhne, Malte Bartram, Andrea Calixto, Henning Hagmann, Christian Reinhardt, Fabienne Koos, Karl Kunzelmann, Elena Shirokova, Dietmar Krautwurst, Christian Harteneck, Matias Simons, Hermann Pavenstädt, Dontscho Kerjaschki, Christoph Thiele, Gerd Walz, Martin Chalfie, and Thomas Benzing. Podocin and MEC-2 bind cholesterol to regulate the activity of associated ion channels. *Proceedings of the National Academy of Sciences of the United States of America*, 103(46):17079–86, nov 2006.

[34] Cory Wilson and Stuart E Dryer. A mutation in TRPC6 channels abolishes their activation by hypoosmotic stretch but does not affect activation by diacylglycerol or G protein signaling cascades. *American journal of physiology. Renal physiology*, 306(9):F1018–25, may 2014.

[35] Anna-Lena Forst, Vlad Sorin Olteanu, Géraldine Mollet, Tanja Wlodkowski, Franz Schaefer, Alexander Dietrich, Jochen Reiser, Thomas Gudermann, Michael Mederos Y Schnitzler, and Ursula Storch. Podocyte Purinergic P2X4 Channels Are Mechanotransducers That Mediate Cytoskeletal Disorganization. *Journal of the American Society of Nephrology*, 27(3):848–862, 2015.

[36] Karlhans Endlich, Felix Kliewe, and Nicole Endlich. Stressed podocytes—mechanical forces, sensors, signaling and response. *Pflugers Archiv European Journal of Physiology*, 469(7-8):937–949, 2017.

[37] Anna Greka and Peter Mundel. Regulation of podocyte actin dynamics by calcium. *Seminars in nephrology*, 32(4):319–326, 2013.

[38] Dequan Tian, Sarah M P Jacobo, David Billing, Anete Rozkalne, Steven D Gage, Theodora Anagnostou, Hermann Pavenstädt, Hsiang-hao Hsu, Johannes Schlondorff, Arnolt Ramos, and Anna Greka. Anatgonistic Regulation of Acting Dynamics and Cell Motility by TRPC5 and TRPC6 Channels. *Sci Signal Signal*, 3(145):1–25, 2011.

[39] Sebastian Brähler, Haiyang Yu, Hani Suleiman, Gokul M Krishnan, Brian T Saunders, Jeffrey B Kopp, Jeffrey H Miner, Bernd H Zinselmeyer, and Andrey S Shaw. Intravital and Kidney Slice Imaging of Podocyte Membrane Dynamics. *Journal of the American Society of Nephrology : JASN*, 27(11):3285–3290, nov 2016.

[40] Anne D.M. Riquier-Brison, Arnold Sipos, Agnes Prókai, Sahra L. Vargas, Ildiko Toma, Elliot J. Meer, Karie G. Villanueva, Jennifer C.M. Chen, Georgina Gyarmati, Christopher Yih, Elaine Tang, Braham Nadim, Sujith Pendekanti, Ingrid M. Garrelds, Genevieve Nguyen, A.H. Jan Danser, and János Peti-Peterdi. The macula densa prorenin receptor is essential in renin release and blood pressure control. *American Journal of Physiology-Renal Physiology*, 315(3):F521–F534, 2018.

[41] Helmy M. Siragy and Robert M. Carey. Role of the intrarenal renin-angiotensin-aldosterone system in chronic kidney disease, 2010.

[42] Michael I Oliverio, Hyung-Suk Kim, Masaki Ito, Thu Le, Laurent Audoly, Christopher F Best, Sylvia Hiller, Kimberly Kluckman, Nobuyo Maeda, Oliver Smithies, and Thomas M Coffman. Reduced growth, abnormal kidney structure, and type 2 (AT2) angiotensin receptor-mediated blood pressure

regulation in mice lacking both AT1A and AT1B receptors for angiotensin II. *Proceedings of the National Academy of Sciences*, 95(26):15496–15501, 1998.

[43] X Chen, W Li, S Tsuchida, F Takemoto, A Fogo, H Nishimura, T Matsusaka, S Okubo, H Yoshida, and I Ichikawa. Targeting deletion of angiotensin type 1B receptor gene in the mouse. *American Journal of Physiology-Renal Physiology*, 272(3):F299–F304, mar 2017.

[44] M Ito, M I Oliverio, P J Mannon, C F Best, N Maeda, O Smithies, and T M Coffman. Regulation of blood pressure by the type 1A angiotensin II receptor gene. *Proceedings of the National Academy of Sciences of the United States of America*, 92(8):3521–5, 1995.

[45] Mukut Sharma, Andrew. S. Greene, Ellen T. McCarthy, Virginia J. Savin, and Ram Sharma. Documentation of angiotensin II receptors in glomerular epithelial cells. *American Journal of Physiology-Renal Physiology*, 274(3):F623–F627, 1998.

[46] Steven D. Crowley, Matthew P. Vasievich, Phillip Ruiz, Samantha K. Gould, Kelly K. Parsons, A. Kathy Pazmino, Carie Facemire, Benny J. Chen, Hyung Suk Kim, Trinh T. Tran, David S. Pisetsky, Laura Barisoni, Minolfa C. Prieto-Carrasquero, Marie Jeansson, Mary H. Foster, and Thomas M. Coffman. Glomerular type 1 angiotensin receptors augment kidney injury and inflammation in murine autoimmune nephritis. *Journal of Clinical Investigation*, 119(4):943–953, 2009.

[47] Steven D. Crowley, Susan B. Gurley, Michael I. Oliverio, A. Kathy Pazmino, Robert Griffiths, Patrick J. Flannery, Robert F. Spurney, Hyung Suk Kim, Oliver Smithies, Thu H. Le, and Thomas M. Coffman. Distinct roles for the kidney and systemic tissues in blood pressure regulation by the renin-

angiotensin system. *Journal of Clinical Investigation*, 115(4):1092–1099, 2005.

[48] Nicole Endlich and Karlhans Endlich. The challenge and response of podocytes to glomerular hypertension. *Seminars in nephrology*, 32(4):327–41, jul 2012.

[49] Eva Márquez, Marta Riera, Julio Pascual, and María José Soler. Renin-angiotensin system within the diabetic podocyte. *American journal of physiology. Renal physiology*, 308(1):F1–10, jan 2015.

[50] Lance D Dworkin, Thomas H Hostetter, Helmut G Rennke, and Barry M Brenner. Hemodynamic Basis for Glomerular Injury in Rats with Desoxycorticosterone- Salt Hypertension. *Journal of Clinical Investigation1*, 73(7):1448–1461, 1984.

[51] A Griffin and M Picken. Method of Renal Mass Reduction Is a Critical Modulator of Subsequent Hypertension and Glomerular Injury. *Journal of the American Society of Nephrology*, pages 2023–2031, 1994.

[52] Agata L Gava, Flavia P S Freitas, Camille M Balarini, Elisardo C Vasquez, and Silvana S Meyrelles. Effects of 5/6 nephrectomy on renal function and blood pressure in mice. *Int J Physiol Pathophysiol Pharmacol*, 4(3):167–173, 2012.

[53] Kerstin Amann, Tomasz Irzyniec, Gerhard Mall, and Eberhard Ritz. The effect of enalapril on glomerular growth and glomerular lesions after subtotal nephrectomy in the rat: a stereological analysis, 1993.

[54] Virginia Chamorro, Rosemary Wangensteen, Juan Sainz, Juan Duarte, Francisco O'valle, Antonio Osuna, and Félix Vargas. Protective effects of the

angiotensin II type I (AT I) receptor blockade in low-renin deoxycorticosterone acetate (DOCA)-treated spontaneously hypertensive rats. *Clinical Science*, 106(3):251–259, 2004.

[55] Anna Henger, Tob1as Huber, Karl-Georg Fischer, Roland Nitschke, Peter Mundel, Peter Schollmeyer, Rainer Greger, and Hermann Pavenstadt. Angiotensin II increases the cytosolic calcium activity in rat podocytes in culture. *Kidney International*, 52:687–693, 1997.

[56] Roland Nitschke, Anna Henger, Sigrid Ricken, Joachim Gloy, Victoria Müller, Rainer Greger, and Hermann Pavenstädt. Angiotensin II increases the intracellular calcium activity in podocytes of the intact glomerulus. *Kidney International*, 57(1):41–49, jan 2000.

[57] Daria V Ilatovskaya, Oleg Palygin, Vladislav Chubinskiy-Nadezhdin, Yuri a Negulyaev, Rong Ma, Lutz Birnbaumer, and Alexander Staruschenko. Angiotensin II has acute effects on TRPC6 channels in podocytes of freshly isolated glomeruli. *Kidney international*, 86(3):506–514, mar 2014.

[58] Ying Yu, Lihong Zhang, Guang Xu, Zhenghong Wu, Qian Li, Yong Gu, and Jianying Niu. Angiotensin II Type i receptor agonistic autoantibody induces podocyte injury via activation of the TRPC6-Calcium/calcineurin pathway in pre-eclampsia. *Kidney and Blood Pressure Research*, 43(5):1666–1676, 2018.

[59] Daria V. Ilatovskaya, Vladislav Levchenko, Andrea Lowing, Leonid S. Shuyskiy, Oleg Palygin, and Alexander Staruschenko. Podocyte injury in diabetic nephropathy: implications of angiotensin II – dependent activation of TRPC channels. *Scientific Reports*, 5(November):17637, 2015.

[60] F. Bonnet, M. E. Cooper, G Kawachi, H.Boner, T. J. Allen, and Z. Cao. Irbesartan normalises the deficiency in glomerular nephrin expression in a model of diabetes and hypertension. *Diabetologia*, 44(7):874–877, 2001.

[61] R.G. Langham, D.J. Kelly, A.J. Cox, N.M. Thomson, H. Holthöfer, P. Zaoui, N. Pinel, D.J. Cordonnier, and R.E. Gilbert. Proteinuria and the expression of the podocyte slit diaphragm protein, nephrin, in diabetic nephropathy: effects of angiotensin converting enzyme inhibition. *Diabetologia*, 45(11):1572–1576, 2002.

[62] Belinda J. Davis, Zemin Cao, Marc De Gasparo, Hiroshi Kawachi, Mark E. Cooper, and Terri J. Allen. Disparate effects of angiotensin II antagonists and calcium channel blockers on albuminuria in experimental diabetes and hypertension: Potential role of nephrin. *Journal of Hypertension*, 21(1):209–216, 2003.

[63] Anna Zimnol, Kerstin Amann, Philipp Mandel, Christina Hartmann, and Nicole Schupp. Angiotensin II type 1a receptor-deficient mice develop angiotensin II-induced oxidative stress and DNA damage without blood pressure increase. *American Journal of Physiology-Renal Physiology*, 313(6):F1264–F1273, dec 2017.

[64] Laura K Schenk, Annika Oller-Kerutt, Rafael Klosowski, Dirk Wolters, Elisabeth Schaffner-Reckinger, Thomas Weide, Hermann Pavenstädt, and Beate Vollenb. Angiotensin II regulates phosphorylation of actin-associated proteins in human podocytes. *the FASEB Journal*, 31(11):5019–5035, 2018.

[65] O Vonend, CM Turner, and CM Chan. Glomerular expression of the ATP-sensitive P2X7 receptor in diabetic and hypertensive rat models. *Kidney international*, 66:157–166, 2004.

[66] Hila Roshanravan and Stuart E. Dryer. ATP acting through P2Y receptors causes activation of podocyte TRPC6 channels: Role of podocin and reactive oxygen species. *American journal of physiology. Renal physiology*, 306(9):F1088–F1097, feb 2014.

[67] C.M. Chan, R.J. Unwin, and G. Burnstock. Potential Functional Roles of Extracellular ATP in Kidney and Urinary Tract. *Nephron Experimental Nephrology*, 6(3):200–207, 1998.

[68] Robert I Menzies, Amelia R Howarth, Robert J Unwin, Frederick W.K. Tam, John J Mullins, and Matthew A Bailey. P2X7 receptor antagonism improves renal blood flow and oxygenation in angiotensin-II infused rats. *Kidney International*, 88(5):1079–1087, 2015.

[69] R.I. Menzies, F.W. Tam, R.J. Unwin, and M.A. Bailey. Purinergic signaling in kidney disease. *Kidney International*, 91(2):315–323, 2017.

[70] David G. Shirley, Renu M. Vekaria, and Jean Sévigny. Ectonucleotidases in the kidney. *Purinergic Signalling*, 5(4):501–511, 2009.

[71] Bernd Hohenstein, Sindy Renk, Kathrin Lang, Christoph Daniel, Monique Freund, Catherine Léon, Kerstin U Amann, Christian Gachet, and Christian P M Hugo. P2Y1 gene deficiency protects from renal disease progression and capillary rarefaction during passive crescentic glomerulonephritis. *Journal of the American Society of Nephrology : JASN*, 18(2):494–505, mar 2007.

[72] S. R.J. Taylor, Clare M Turner, Elliot I. Elliot, John McDavid, Reiko Hewitt, Jennifer Smith, Matthew C. Pickering, Darren L. Whitehouse, H. Terence Cook, Geoffrey Burnstock, Charles D. Pusey, Robert J. Unwin, and Frederick W.K. Tam. P2X7 Deficiency Attenuates Renal Injury in Experi-

mental Glomerulonephritis. *Journal of the American Society of Nephrology*, 20(6):1275–1281, 2009.

[73] Daria V Ilatovskaya, Oleg Palygin, Vladislav Levchenko, and Alexander Staruschenko. Pharmacological characterization of the P2 receptors profile in the podocytes of the freshly isolated rat glomeruli. *American journal of physiology. Cell physiology*, 305(10):C1050–9, nov 2013.

[74] K G Fischer, U Saueressig, C Jacobshagen, a Wichelmann, and H Pavenstädt. Extracellular nucleotides regulate cellular functions of podocytes in culture. *American journal of physiology. Renal physiology*, 281(6):F1075–81, dec 2001.

[75] James L Burford, Karie Villanueva, Lisa Lam, Anne Riquier-Brison, Matthias J Hackl, Jeffrey Pippin, Stuart J Shankland, and János Peti-Peterdi. Intravital imaging of podocyte calcium in glomerular injury and disease. *Journal of Clinical Investigation*, 124(5):2050–2058, 2014.

[76] Kenneth W Dunn, Ruben M Sandoval, Katherine J Kelly, Pierre C Dagher, George a Tanner, Simon J Atkinson, Robert L Bacallao, and Bruce a Molitoris. Functional studies of the kidney of living animals using multicolor two-photon microscopy. *American journal of physiology. Cell physiology*, 283(3):C905–C916, sep 2002.

[77] Andrew M Hall, George J Rhodes, Ruben M Sandoval, Peter R Corridon, and Bruce a Molitoris. In vivo multiphoton imaging of mitochondrial structure and function during acute kidney injury. *Kidney international*, 83(1):72–83, jan 2013.

[78] Ina Maria Schießl, Sophia Bardehle, and Hayo Castrop. Superficial Nephrons in BALB/c and C57BL/6 Mice Facilitate In Vivo Multiphoton Microscopy of the Kidney. *PLoS ONE*, 8(1), 2013.

[79] Daria V. Ilatovskaya, Oleg Palygin, Vladislav Levchenko, Bradley T. Endres, and Alexander Staruschenko. The role of angiotensin II in glomerular volume dynamics and podocyte calcium handling. *Scientific Reports*, 2017.

[80] Hatim A Zariwala, Bart G Borghuis, Tycho M Hoogland, Linda Madisen, Lin Tian, Chris I De Zeeuw, Hongkui Zeng, Loren L Looger, Karel Svoboda, and Tsai-Wen Chen. A Cre-dependent GCaMP3 reporter mouse for neuronal imaging in vivo. *Journal of Neuroscience*, 32(9):3131–3141, 2012.

[81] Marcus J. Moeller, Silja K. Sanden, Abdulsalam Soofi, Roger C. Wiggins, and Lawrence B. Holzman. Podocyte-specific expression of cre recombinase in transgenic mice. *genesis*, 35(1):39–42, jan 2003.

[82] Alexander Dietrich, Michael Mederos Y Schnitzler, Maik Gollasch, Volkmar Gross, Ursula Storch, Galyna Dubrovska, Michael Obst, Eda Yildirim, Birgit Salanova, Hermann Kalwa, Kirill Essin, Olaf Pinkenburg, Friedrich C Luft, Thomas Gudermann, and Lutz Birnbaumer. Increased vascular smooth muscle contractility in TRPC6-/- mice. *Molecular and cellular biology*, 25(16):6980–6989, aug 2005.

[83] Yaz Y. Kisanuki, Robert E. Hammer, Jun ichi Miyazaki, S. Clay Williams, James A. Richardson, and Masashi Yanagisawa. Tie2-Cre transgenic mice: A new model for endothelial cell-lineage analysis in vivo. *Developmental Biology*, 230(2):230–242, 2001.

[84] Maxime Bouchard, Abdallah Souabni, and Meinrad Busslinger. Tissue-Specific Expression of Cre Recombinase from the Pax8 Locus. *Genesis*, 38(3):105–109, mar 2004.

[85] Gary E. Truett, P Heeger, R L Mynatt, A A Truett, J A Walker, and M L Warman. Preparation of PCR-quality mouse genomic dna with hot sodium hydroxide and tris (HotSHOT). *BioTechniques*, 29(1):52–54, jul 2000.

[86] Vincent WS Lee and David CH Harris. Adriamycin nephropathy: A model of focal segmental glomerulosclerosis. *Nephrology*, 16(1):30–38, jan 2011.

[87] Marie Jeansson, Karin Björck, Olav Tenstad, and Börje Haraldsson. Adriamycin alters glomerular endothelium to induce proteinuria. *Journal of the American Society of Nephrology : JASN*, 20(1):114–22, jan 2009.

[88] Markus M Rinschen, Caroline Pahmeyer, Trairak Pisitkun, Nicole Schnell, Xiongwu Wu, Martina Maaß, Malte P Bartram, Tobias Lamkemeyer, Bernhard Schermer, Thomas Benzing, and Paul T Brinkkoetter. Comparative phosphoproteomic analysis of mammalian glomeruli reveals conserved podocin C-terminal phosphorylation as a determinant of slit diaphragm complex architecture. *Proteomics*, 15(7):1326–31, apr 2015.

[89] Markus M Rinschen, Puneet Bharill, Xiongwu Wu, Priyanka Kohli, Matthäus J Reinert, Oliver Kretz, Isabel Saez, Bernhard Schermer, Martin Höhne, Malte P Bartram, Sriram Aravamudhan, Bernard R Brooks, David Vilchez, Tobias B Huber, Roman-Ulrich Müller, Marcus Krüger, and Thomas Benzing. The ubiquitin ligase Ubr4 controls stability of podocin/MEC-2 supercomplexes. *Human molecular genetics*, 25(7):1328–44, apr 2016.

[90] Malte P Bartram, Sandra Habbig, Caroline Pahmeyer, Martin Höhne, Lutz T Weber, Holger Thiele, Janine Altmüller, Nina Kottoor, Andrea Wenzel, Marcus Krueger, Bernhard Schermer, Thomas Benzing, Markus M Rinschen, and Bodo B Beck. Three-layered proteomic characterization of a novel ACTN4

mutation unravels its pathogenic potential in FSGS. *Human molecular genetics*, 25(6):1152–64, mar 2016.

[91] V. G. Tusher, R. Tibshirani, and G. Chu. Significance analysis of microarrays applied to the ionizing radiation response. *Proceedings of the National Academy of Sciences*, 98(9):5116–5121, apr 2001.

[92] Juan A Vizcaíno, Eric W Deutsch, Rui Wang, Attila Csordas, Florian Reisinger, Daniel Ríos, José A Dianes, Zhi Sun, Terry Farrah, Nuno Bandeira, Pierre-Alain Binz, Ioannis Xenarios, Martin Eisenacher, Gerhard Mayer, Laurent Gatto, Alex Campos, Robert J Chalkley, Hans-Joachim Kraus, Juan Pablo Albar, Salvador Martinez-Bartolomé, Rolf Apweiler, Gilbert S Omenn, Lennart Martens, Andrew R Jones, and Henning Hermjakob. ProteomeXchange provides globally coordinated proteomics data submission and dissemination. *Nature Biotechnology*, 32(3):223–226, mar 2014.

[93] Joachim Gloy, Anna Henger, Karl-Georg Fischer, Roland Nitschke, Peter Mundel, Markus Bleich, Peter Schollmeyer, Rainer Greger, and Hermann Pavenstädt. Angiotensin II Depolarizes Podocytes in the Intact Glomerulus of the Rat. *J. Clin. Invest*, 99(11):2772–2781, 1997.

[94] Michel Hir, Cornelia Keller, Valérie Eschmann, Brunhilde Hahnel, Hiltraude Hosser, and Wilhelm Kriz. Podocyte Bridges between the Tuft and Bowman's Capsule: An Early Event in Experimental Crescentic Glomerulonephritis. *J. Am. Soc. Nephrol.*, 9(11):2013–2026, oct 2001.

[95] Max C. Liebau, Hermann Pavenstädt, N. Endlich, Peter W. Mathieson, J. Böhm, Martin J. Bek, D. Lang, Moin A. Saleem, Karl-Georg Fischer, and Ian Witherden. Functional expression of the renin-angiotensin system

in human podocytes. *American Journal of Physiology-Renal Physiology*, 290(3):F710–F719, 2005.

[96] Ina Maria Schießl and Hayo Castrop. Angiotensin II AT2 receptor activation attenuates AT1 receptor-induced increases in the glomerular filtration of albumin: a multiphoton microscopy study. *American journal of physiology. Renal physiology*, 305(8):F1189–200, oct 2013.

[97] Sybille Koehler, Sebastian Brähler, Alexander Kuczkowski, Julia Binz, Matthias J Hackl, Henning Hagmann, Martin Höhne, Merly C Vogt, Claudia M. Wunderlich, F Thomas Wunderlich, Frank Schweda, Bernhard Schermer, Thomas Benzing, and Paul T Brinkkoetter. Single and Transient Ca2+ Peaks in Podocytes do not induce Changes in Glomerular Filtration and Perfusion. *Scientific Reports*, 6(1):35400, oct 2016.

[98] Matthew A. Bailey, Kate A. Hillman, and Robert J. Unwin. P2 receptors in the kidney. *Journal of the Autonomic Nervous System*, 81(1-3):264–270, 2000.

[99] Marcial Sanchez-Tecuatl, Ajelet Vargaz-Guadarrama, Juan Manuel Ramirez-Cortes, Pilar Gomez-Gil, Francesco Moccia, and Roberto Berra-Romani. Automated intracellular calcium profiles extraction from endothelial cells using digital fluorescence images. *International Journal of Molecular Sciences*, 19(11):1–17, 2018.

[100] Kornélia Szebényi, András Füredi, Orsolya Kolacsek, Rózsa Csohány, Ágnes Prókai, Katalin Kis-Petik, Attila Szabó, Zsuzsanna Bősze, Balázs Bender, József Tóvári, Ágnes Enyedi, Tamás I. Orbán, Ágota Apáti, and Balázs Sarkadi. Visualization of Calcium Dynamics in Kidney Proximal Tubules. *Journal of the American Society of Nephrology*, 26(11):2731–2740, 2015.

[101] L Gabriel Navar, Kenneth D Mitchell, Lisa M Harrison-Bernard, Hiroyuki Kobori, and Akira Nishiyama. Review: Intrarenal angiotensin II levels in normal and hypertensive states. *Journal of the Renin-Angiotensin-Aldosterone System*, 2(1_suppl):S176–S184, 2001.

[102] Jackson T Wright, George Bakris, Tom Greene, Lawrence J Appel, Deanna Cheek, Janice G Douglas-baltimore, Richard Glassock, Kenneth Jamerson, Robert a Phillips, John P Middleton, and Stephen G Rostand. Effect of Blood Pressure Lowering and Antihypertensive Drug Class on Progression of Hypertensive Kidney Disease. *Jama*, 288(19):2421–2432, 2002.

[103] Sheldon W. Tobe, Catherine M. Clase, Peggy Gao, Matthew McQueen, Anja Grosshennig, Xingyu Wang, Koon K. Teo, Salim Yusuf, and Johannes F.E. Mann. Cardiovascular and renal outcomes with telmisartan, ramipril, or both in people at high renal risk: Results from the ONTARGET and TRANSCEND studies. *Circulation*, 123(10):1098–1107, mar 2011.

[104] Michael Whitaker. *Genetically encoded probes for measurement of intracellular calcium*, volume 99. 2010.

[105] Lin Tian, Andrew Hires, Mao, Tianyi, Daniel Huber, M. Eugenia Chiappe, Sreekanth H. Chalasani, Leopoldo Petreanu, Jasper Akerboom, Sean A. McKinney, Eric R Schreiter, Cornelia I Bargmann, Vivek Jayaraman, Karel Svoboda, and Loren L Looger. Imaging neural activity in worms, flies and mice with improved GCaMP calcium indicators. *Nature Methods*, 6(12):875, 2009.

[106] Ann Chen, Lai Fa Sheu, Yat Sen Ho, Yu Fen Lin, Wei Yuan Chou, Tz Chong Chou, and Wei Hwa Lee. Experimental focal segmental glomerulosclerosis in mice. *Nephron*, 78(4):440–452, 1998.

[107] Séverine Roselli, Laurence Heidet, Mireille Sich, Anna Henger, Matthias Kretzler, M.-C. Marie-Claire Gubler, and Corinne Antignac. Early glomerular filtration defect and severe renal disease in podocin-deficient mice. *Molecular and cellular biology*, 24(2):550–560, jan 2004.

[108] S. Hoffmann. Angiotensin II Type 1 Receptor Overexpression in Podocytes Induces Glomerulosclerosis in Transgenic Rats. *Journal of the American Society of Nephrology*, 15(6):1475–1487, jun 2004.

[109] Marc Anderson, Hila Roshanravan, Justin Khine, and Stuart E Dryer. Angiotensin II activation of TRPC6 channels in rat podocytes requires generation of reactive oxygen species. *Journal of cellular physiology*, 229(4):434–42, apr 2014.

[110] Xuexiang Wang, Ranadheer R Dande, Hao Yu, Beata Samelko, Rachel E Miller, Mehmet M Altintas, and Jochen Reiser. TRPC5 Does Not Cause or Aggravate Glomerular Disease. *J Am Soc Nephrol*, 29:409–415, 2018.

[111] Anna Greka and Peter Mundel. Balancing calcium signals through TRPC5 and TRPC6 in podocytes. *Journal of the American Society of Nephrology : JASN*, 22(11):1969–80, nov 2011.

[112] Markus M Rinschen, Christina B Schroeter, Sybille Koehler, Christina Ising, Bernhard Schermer, Martin Kann, Thomas Benzing, and Paul T Brinkkoetter. Quantitative deep mapping of the cultured podocyte proteome uncovers shifts in proteostatic mechanisms during differentiation. *American Journal of Physiology - Cell Physiology*, 311(3):C404–C417, sep 2016.

[113] John D. Hayes and David J. Pulford. The glut athione s-transferase supergene family: Regulation of GST and the contribution of the lsoenzymes to cancer

chemoprotection and drug resistance part i. *Critical Reviews in Biochemistry and Molecular Biology*, 30(6):445–520, 1995.

[114] Trevor J. Hallam and Jeremy D. Pearson. Exogenous ATP raises cytoplasmic free calcium in fura-2 loaded piglet aortic endothelial cells. *FEBS Letters*, 207(1):95–99, 1986.

[115] C.M. Turner, O. Vonend, C. Chan, G. Burnstock, and R.J. Unwin. The Pattern of Distribution of Selected ATP-Sensitive P2 Receptor Subtypes in Normal Rat Kidney: An Immunohistological Study. *Cells Tissues Organs*, 175(2):105–117, 2003.

[116] M. A. Bailey. Inhibition of bicarbonate reabsorption in the rat proximal tubule by activation of luminal P2Y1 receptors. *AJP: Renal Physiology*, 287(4):F789–F796, 2004.

10 Aknowledgements

An aller erster Stelle möchte ich Prof. Dr. Thomas Benzing und Prof. Dr. Bernhard Schermer danken, dass ich meine PhD Arbeit in ihrer Arbeitsgruppe absolvieren durfte. Durch ihre Unterstützung über die letzten Jahre konnte ich meine Doktorarbeit mit einem positiven Ergebnis abschließen und freue mic, auch weiterhin hier arbeiten zu können.

Als nächstes möchte ich mich ganz herzlich bei Dr. Matthias Hackl bedanken. Er gab mir die Möglichkeit an diesem außergewöhnlichen Projekt zu arbeiten und hat mir immer sein vollstes Vertrauen geschenkt. Es ist mir eine Ehre von einem solche brillianten Menschen gelernt zu haben. Mit viel Ruhe und Geduld hat er mich in dieses Feld, welches für mich ganz neu war, eingeführt und mich in all meinen Ideen unterstützt und vor allem auch verstanden, wenn es mal gar nicht weiter ging. Ich freue mich schon auf zukünftige gemeinsame Projekte.

Ich möchte auch Dr. Christian Jüngst ganz herzlich danken. Ohne seinen kontinuierlichen Support am Mikroskop wäre dieses Projekt nicht möglich gewesen. Er war immer da und stand mir mit Rat und Tat zu Seite. An dieser Stelle möchte ich auch Dr. Peter Zentis danken für seine Unterstützung bei der Bildanalyse und dafür, dass er sich all meinen Fragen immer gestellt hat und auch (fast) immer eine bioinformatische Lösung zur Hand hatte.

Als nächstes möchte ich dem ganzen Team im Nephrolab danken. Die letzten Jahre hier waren geprägt von vielen schönen Momenten, an die ich immer gerne zurück denken werde und ich freue mich auf die Zukunft mit euch allen hier! Ein paar Personen möchte ich besonders hervor heben: Manaswita, danke das es dich hier gab. Du warst mein Fels in der Brandung über viele Jahre und ich vermisse dich jeden Tag! Danke an Claudia, dass du bei meinen vielen Mausfragen immer Geduld mit mir hattest. Danke an Lena, das du mir in Sachen Crispr geholfen hast. Danke an Lisa, Johanna, Micha und Linus für unsere Telko's und ganz viel

mehr... Danke an Myna, ohne dich würde ich immernoch nicht wissen, wie ich eine IF mache und sie auch funktioniert. Ich vergesse bestimmt ganz viele an dieser Stelle...daher: Danke einfach das ich ein Teil von allem sein durfte.

Als vorletztes möchte ich mich bei meiner Familie bedanken. Meinen Eltern danken, denn sie haben mich während meines Studiums immer unterstützt und motiviert. Ich verdanke euch mein wissenschaftliches Interesse, denn beim Abendessen ging es ja nur um Krankheiten und deren Entstehen - da musste ich mich ja mit Biologie auseinandersetzen. Danke für alles. Und meinem kleinen Bruder, der mir bei der Formatierung meiner Doktorarbeit geholfen hat.

Als letztes möchte ich meinem Mann Steve danken. Du hast mich durch den ganzen PhD begleitet und mit mir gelitten und dich mit mir gefreut. Ohne deinen Rückhalt hätte ich es nicht geschafft. Danke.

11 Erklärung

Ich versichere, dass ich die von mir vorgelegte Dissertation selbständig angefertigt, die benutzten Quellen und Hilfsmittel vollständig angegeben und die Stellen der Arbeit - einschließlich Tabellen, Karten und Abbildungen -, die anderen Werken im Wortlaut oder dem Sinn nach entnommen sind, in jedem Einzelfall als Entlehnung kenntlich gemacht habe; dass diese Dissertation noch keiner anderen Fakultät oder Universität zur Prüfung vorgelegen hat; dass sie - abgesehen von unten angegebenen Teilpublikationen - noch nicht veröffentlicht worden ist, sowie, dass ich eine solche Veröffentlichung vor Abschluss des Promotionsverfahrens nicht vornehmen werde. Die Bestimmungen der Promotionsordnung sind mir bekannt. Die von mir vorgelegte Dissertation ist von Prof. Thomas Benzing und Prof. Peter Kloppenburg betreut worden.

Teilpublikation:

Binz J, Jüngst C, Rinschen MM, Koehler S, Zentis P, Schauss A, Schermer B, Benzing T, Hackl M.J.: Injured podocytes are sensitized to Angiotensin II induced calcium signaling. *In Revision at the Journal of the American Society of Nephrology (JASN). Submission date: 4th February 2019, Manuscript ID: JASN-2019-02-0109.R1*

Datum

Julia Binz-Lotter